



Dissertations and Theses

2013

Dynamics and Control of Higher-order Nonholonomic Systems

Jaime Rubio Hervás

Embry-Riddle Aeronautical University - Daytona Beach

Follow this and additional works at: <https://commons.erau.edu/edt>



Part of the [Navigation, Guidance, Control and Dynamics Commons](#), and the [Robotics Commons](#)

Scholarly Commons Citation

Hervás, Jaime Rubio, "Dynamics and Control of Higher-order Nonholonomic Systems" (2013).
Dissertations and Theses. 154.

<https://commons.erau.edu/edt/154>

This Dissertation - Open Access is brought to you for free and open access by Scholarly Commons. It has been accepted for inclusion in Dissertations and Theses by an authorized administrator of Scholarly Commons. For more information, please contact commons@erau.edu.

**DYNAMICS AND CONTROL OF HIGHER-ORDER
NONHOLONOMIC SYSTEMS**

by

Jaime Rubio Hervás

A Dissertation Submitted in Partial Fulfillment of the Requirements
for the Degree of

**DOCTOR OF PHILOSOPHY
(Engineering Physics)
Embry-Riddle Aeronautical University**

2013

DYNAMICS AND CONTROL OF HIGHER-ORDER NONHOLONOMIC SYSTEMS

by

Jaime Rubio Hervás

This Dissertation was prepared under the direction of the candidate's Dissertation Committee Chair, Dr. Mahmut Reyhanoglu, Professor; and Dissertation Committee Members Dr. Yechiel Crispin, Professor; Dr. Taeyoung Lee, Assistant Professor, George Washington University; Dr. William MacKunis, Assistant Professor; Dr. Anthony Reynolds, Associate Professor; and has been approved by the Dissertation Committee. It was submitted to the College of Arts and Sciences in partial fulfillment of the requirements for the degree of Doctor of Philosophy in Engineering Physics

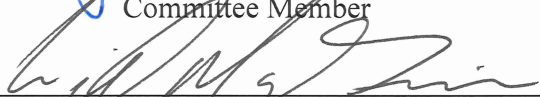
Dissertation Committee:



Mahmut Reyhanoglu, Ph.D.
Committee Chair



Yechiel Crispin, Ph.D.
Committee Member



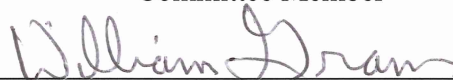
William MacKunis, Ph.D.
Committee Member



Anthony Reynolds, Ph.D.
Committee Member



Taeyoung Lee, Ph.D.
Committee Member



William Grams, Ph.D.
Dean, College of Arts and Sciences



Michael Hickey, Ph.D.
Dean of Research and Graduate Studies

2nd July 2013
Date

Abstract

A theoretical framework is established for the control of higher-order nonholonomic systems, defined as systems that satisfy higher-order nonintegrable constraints. A model for such systems is developed in terms of differential-algebraic equations defined on a higher-order tangent bundle. A number of control-theoretic properties such as nonintegrability, controllability, and stabilizability are presented. Higher-order nonholonomic systems are shown to be strongly accessible and, under certain conditions, small time locally controllable at any equilibrium. There are important examples of higher-order nonholonomic systems that are asymptotically stabilizable via smooth feedback, including space vehicles with multiple slosh modes and Prismatic-Prismatic-Revolute (PPR) robots moving open liquid containers, as well as an interesting class of systems that do not admit asymptotically stabilizing continuous static or dynamic state feedback. Specific assumptions are introduced to define this class, which includes important examples of robotic systems. A discontinuous nonlinear feedback control algorithm is developed to steer any initial state to the equilibrium at the origin. The applicability of the theoretical development is illustrated through two examples: control of a planar PPR robot manipulator subject to a jerk constraint and control of a point mass moving on a constant torsion curve in a three dimensional space.

To my family with love

Acknowledgements

First and foremost, I would like to express my sincere gratitude to my advisor Dr. Mahmut Reyhanoglu for the continuous support of my study and research, for his patience, motivation, enthusiasm, and immense knowledge. His guidance helped me throughout the research and writing of this dissertation. I could not have imagined having a better advisor and mentor.

I thank all my friends at Embry-Riddle Aeronautical University, especially Athul Radhakrishnan, Adrien Mikaeloff, Alfonso Garrido, Jason McMahon, Jorge Pantoja, and Peter Azizi for the nice atmosphere they created around me during these years. Thanks to Daniela Zúñiga Ballesteros for her moral support. Also I thank my Ph.D. fellows and my colleagues from Polytechnic University of Madrid, in a especial way to Niloofar N Kamran, Miguel Rey Alonso, Diego Represa Martín, and Zeli Xu Li for giving me their advise for the important personal decisions. Finally, I would like to express my gratitude to the faculty of the Physical Sciences Department at Embry-Riddle Aeronautical University, especially to Dr. Sergey Drakunov and Dr. Anthony Reynolds, for their patience and constant advice.

Last but not least, I would like to thank my family: my parents Agustín Rubio Requena and Remedios Hervás Gil, for giving birth to me at the first place and supporting me in such a brilliant way throughout my life; my brother Carlos Rubio Hervás, for supporting me spiritually and providing me with the best advices I could expect; to my uncle Jacinto Hervás Gil in his role as a second father, my cousin Carmen Pérez Rubio, for her wise advise, my grandparents Jacinto Hervás Muñoz and Candida Gil Muñoz, my uncles Antonio Rubio Requena and Eladio Rubio Requena, my aunt Carmen Rubio Requena, and a long list of familiars, for having the proud of fueling their own proud.

Contents

List of Figures	vi
List of Tables	viii
1 INTRODUCTION	1
2 MATHEMATICAL BACKGROUND	4
2.1 Overview of Differential Geometry	4
2.2 Higher-Order Tangent Bundles	8
2.3 Controllability of Nonlinear Systems	9
2.4 Stabilizability of Nonlinear Systems	12
3 NONLINEAR MODELING OF HIGHER-ORDER NONHOLONOMIC SYSTEMS	14
3.1 Mathematical Formulation	14
3.1.1 Universal D'Alembert's Principle	14
3.1.2 Mićević Dušan-Rusov Lazar's Form	15
3.1.3 Generalized Lagrange's Equations	15
3.1.4 Higher-Order Nonholonomic Constraints	16
3.2 Nonlinear Control System Formulation	18
4 CONTROLLABILITY AND STABILIZABILITY RESULTS	20
5 FEEDBACK CONTROL OF A CLASS OF HIGHER-ORDER NON-HOLONOMIC SYSTEMS	28
5.1 Mathematical Model	28
5.2 Feedback Control Law	29

6	EXAMPLES: SECOND-ORDER NONHOLONOMIC SYSTEMS	32
6.1	Control of Space Vehicles with Fuel Slosh Dynamics	32
6.1.1	Planar Thrust Vector Control of an Upper-Stage Rocket with Time-Invariant Slosh Parameters	35
6.1.1.1	Model Formulation	35
6.1.1.2	Controllability and Stabilizability Analysis	43
6.1.1.3	Feedback Control Laws	46
6.1.1.4	Simulations	48
6.1.2	Planar Thrust Vector Control of an Upper-Stage Rocket with Time-Varying Slosh Parameters	53
6.1.2.1	Model Formulation	54
6.1.2.2	Feedback Control Laws	56
6.1.2.3	Simulations	60
6.1.3	Thrust-Vector Control of a Three-Axis Stabilized Spacecraft with Fuel Slosh Dynamics	65
6.1.3.1	Model Formulation	65
6.1.3.2	Feedback Control Laws	70
6.1.3.3	Simulations	73
6.2	Liquid Container Transfer via a PPR Robot	78
6.2.1	Model Formulation	79
6.2.2	Controllability and Stabilizability Analysis	84
6.2.3	Feedback Control Laws	87
6.2.3.1	Partial-State Feedback	87
6.2.3.2	Full-State Feedback	88
6.2.4	Simulations	91
7	EXAMPLES: THIRD-ORDER NONHOLONOMIC SYSTEMS	96
7.1	Control of a Manipulator with a Jerk Constraint	96
7.1.1	Model Formulation	97
7.1.2	Controllability and Stabilizability Analysis	98
7.1.3	Feedback Control Laws	100
7.1.4	Simulations	101
7.2	A Point Mass Moving on a Constant-Torsion Curve	103
8	CONCLUSIONS AND FUTURE RESEARCH	106

CONTENTS

APPENDIX	108
Bibliography	111

List of Figures

6.1	A multiple slosh mass-spring model for a spacecraft.	37
6.2	A multiple slosh pendula model for a spacecraft.	41
6.3	Time responses of v_x , v_z and θ (Multi-mass-spring case).	50
6.4	Time responses of s_1 and s_2 (Multi-mass-spring case).	51
6.5	Gimbal deflection angle δ and pitching moment M (Multi-mass-spring case).	51
6.6	Time responses of v_x , v_z and θ (Multi-pendulum case).	52
6.7	Time responses of ψ_1 and ψ_2 (Multi-pendulum case).	52
6.8	Gimbal deflection angle δ and pitching moment M (Multi-pendulum case).	53
6.9	Time responses of v_x , v_z and θ	62
6.10	Time responses of s_1 and s_2	62
6.11	Gimbal deflection angle δ and pitching moment M	63
6.12	Time responses of v_x , v_z and θ (zero control case).	63
6.13	Time responses of s_1 and s_2 (zero control case).	64
6.14	Gimbal deflection angle δ and pitching moment M (zero control case).	64
6.15	A spacecraft with a liquid propellant tank.	66
6.16	A multi mass-spring model of sloshing.	67
6.17	Time responses of v_x , v_y and v_z	75
6.18	Time responses of θ_1 , θ_2 and θ_3	75
6.19	Time responses of ξ_1 and ξ_2	76
6.20	Time responses of η_1 and η_2	76
6.21	Gimbal deflection angles δ_1 and δ_2	77
6.22	Control moments M_x , M_y and M_z	77
6.23	A PPR robot moving a liquid filled container.	80
6.24	A multi-mass-spring model of liquid slosh.	80
6.25	Time responses of x , y and θ (Partial-state feedback).	92

LIST OF FIGURES

6.26	Time responses of s_1 and s_2 (Partial-state feedback).	93
6.27	Time responses of F_x , F_y and τ_θ (Partial-state feedback).	93
6.28	Time responses of x , y and θ (Full-state feedback).	94
6.29	Time responses of s_1 and s_2 (Full-state feedback).	94
6.30	Time responses of F_x , F_y and τ_θ (Full-state feedback).	95
7.1	Simplified model of a PPR manipulator.	97
7.2	Time responses of x , y and θ	102
7.3	Time responses of u_1 and u_2	102
7.4	Time responses of F_x , F_y and T	103

List of Tables

6.1	Physical parameters for a spacecraft (multi-mass-spring analogy). . .	49
6.2	Physical parameters for a spacecraft (multi-pendulum analogy). . . .	50
6.3	Physical parameters for a spacecraft (time-varying slosh parameters). .	61
6.4	Physical parameters for a spacecraft (three-dimensional case).	74
6.5	Physical parameters for a PPR robot and liquid container.	91
7.1	Physical parameters for a PPR robot manipulator.	101

1

INTRODUCTION

Dynamic systems can be classified as either holonomic or nonholonomic. The term “holonomic” comes from the Greek words “integral” (or “whole”) and “law” (Hertz, 1894), and refers to mechanical systems subject to constraints that limit their possible configurations. If the constraints given in terms of the velocity, acceleration or higher-order time derivatives can be integrated to constraints on the configuration variables, they are called holonomic constraints. A typical example is the length constraint for a simple pendulum. On the other hand, if the constraints cannot be integrated to the configuration variables, they are called nonintegrable or nonholonomic. The rolling disk and ball are classical examples of systems with first-order nonholonomic constraints (Bloch, 2003).

The problem of controlling dynamical systems that satisfy nonintegrable relations has attracted considerable attention in the recent past. These studies were primarily limited to systems satisfying nonintegrable kinematic relations, also known as systems with first-order (classical) nonholonomic constraints. Examples of systems with nonintegrable first-order constraints include systems subject to rolling constraints as well as mechanical systems that involve symmetries, which result in nonintegrable conserved quantities such as angular momentum. Several examples of systems with first-order nonholonomic constraints have been studied in the context of robot manipulation, mobile robots, wheeled vehicles, and space robotics. A few representative control works include the study of controllability and stabilizability (Bloch et al., 1992; Laumond, 1993; Reyhanoglu and McClamroch, 1991), motion planning (Murphy and Sastry, 1993; Nakamura and Mukherjee, 1991; Reyhanoglu and Al-Regib, 1994), and feedback stabilization and tracking (Aneke et al., 2003; Aneke, 2003; Astolfi, 1996; Godhavn and Egeland, 1997; Jiang and Nijmeijer, 1997, 1999; Jiang et al.,

2001; Kolmanovsky et al., 1996; Lefeber, 2000; Samson, 1995; Sordalen and Egeland, 1995; Walsh et al., 1994; Walsh and Bushnell, 1995).

In Reyhanoglu et al. (1999), the ideas in Bloch et al. (1992) have been extended to dynamical systems that satisfy nonintegrable acceleration relations. It has been shown that such systems can arise not only by imposition of certain design constraints on the allowable motions of redundant robot manipulators but also as models of underactuated mechanical systems, defined as systems with fewer inputs than degrees of freedom. Examples of such systems include underactuated space vehicles (Cho et al., 2000b; Krishnan et al., 1992; Reyhanoglu and Rubio Hervas, 2012a; Rubio Hervas and Reyhanoglu, 2012a) and underactuated manipulators (Baillieul, 1993; Mahindrakar et al., 2005; Reyhanoglu and Rubio Hervas, 2012b).

Since the beginning of last century, there has been considerable work on the dynamics formulation of systems with higher-order nonholonomic constraints. Most notable developments in this field include the works of Nielsen, Tzenoff, Mangeron, Deleanu, Appell, and Gibbs (see e.g., Jarzebowska (2006) and references therein). More recently, new forms of the differential equations of systems with higher-order nonholonomic constraints have been derived (Jarzebowska, 2002; Ze-chun and Feng-xiang, 1987). In Jarzebowska (2002), the concept of program constraint is introduced as a demand imposed by design on a system whose sources are not necessarily in other bodies, which can be formulated as differential equations of any order. Material and program constraints are subsequently incorporated into a unified formulation to model nonholonomic systems of any order. To the best of our knowledge, little has been done in generalizing the control and stabilization ideas developed in Bloch et al. (1992) and Reyhanoglu et al. (1999) to higher-order nonholonomic dynamic systems, except for tracking control problems (Jarzebowska, 2005, 2006).

There are important examples of second-order nonholonomic systems that are asymptotically stabilizable via smooth feedback, including space vehicles with multiple slosh modes and Prismatic-Prismatic-Revolute (PPR) robots moving open liquid containers, as well as an interesting class of systems that do not admit asymptotically stabilizing continuous static or dynamic state feedback. It has been demonstrated that pendulum and mass-spring models can approximate complicated fluid and structural dynamics; such models have formed the basis for many studies on dynamics and control of space vehicles with fuel slosh (Bandyopadhyay et al., 2009a,b; Peterson et al., 1989; Shekhawat et al., 2006). There is an extensive body of literature on the interaction of vehicle dynamics and slosh dynamics and their control, but this literature treats only the case of small perturbations to the vehicle dynamics.

The control approaches developed for accelerating space vehicles have commonly employed methods of linear control design (Sidi, 1997; Wie, 1998) and adaptive control (Adler et al., 1991). A number of related papers following a similar approach are motivated by robotic systems moving liquid filled containers (Feddemma et al., 1997; Grundelius and Bernhardsson, 1999; Grundelius, 2000; Terashima and Schmidt, 1994; Yano et al., 2001a,b; Yano and Terashima, 2001, 2005). The linear control laws for the suppression of the slosh dynamics inevitably lead to excitation of the transverse vehicle motion through coupling effects. The complete nonlinear dynamics formulation in this dissertation allows simultaneous control of the transverse, pitch, and slosh dynamics (Reyhanoglu and Rubio Hervas, 2011a,b, 2012a,b,c,d, 2013; Rubio Hervas and Reyhanoglu, 2012a,b; Rubio Hervas et al., 2013; Rubio Hervas and Reyhanoglu, 2013f,g).

There is an interesting class of systems that do not admit asymptotically stabilizing continuous static or dynamic state feedback. Specific assumptions are introduced to define this class, which includes important examples of robotic systems. A discontinuous nonlinear feedback control algorithm is developed to steer any initial state to the equilibrium at the origin. The applicability of the theoretical development is illustrated through a third-order nonholonomic system example: control of a planar PPR robot manipulator subject to a jerk constraint (Rubio Hervas and Reyhanoglu, 2013d). Jerk is defined as the time derivative of the acceleration, and thus is an interesting example of third-order constraints. In the context of robot manipulators, it is associated with rapidly changing actuator forces. Excessive jerk leads to premature wear on the actuators, resonant vibrations in the robot's structure, and is difficult for a controller to track accurately; even some experiments indicate that our brain realizes a version of minimum-jerk in planning grasping motions for our arms (Freeman, 2012).

The organization of the dissertation is as follows: Chapter 2 summarizes some notions of differential calculus, differential geometry, controllability, and stabilizability. In Chapter 3 models of higher-order nonholonomic systems are presented and a nonlinear control system representation is developed. Theoretical results on controllability and stabilizability are presented in Chapter 4. Chapter 5 is devoted to the synthesis of feedback control algorithms for a class of higher-order nonholonomic systems. Physical examples illustrating the theoretical development of this dissertation are included in Chapters 6 and 7. Finally, Chapter 8 contains conclusions and remarks on future research directions.

2

MATHEMATICAL BACKGROUND

In this section, we review the general mathematical background from differential calculus and differential geometry on which our development in later chapters is based. This summary is borrowed from Reyhanoglu (1992). For full details, see Abraham et al. (1988); Crampin and Pirani (1986); Nijmeijer and van der Schaft (1990).

2.1 Overview of Differential Geometry

Let $h : A \rightarrow \mathbb{R}$ be a scalar function defined on an open subset A of \mathbb{R}^n . The value of h at $x = (x_1, \dots, x_n) \in A$ is denoted by $h(x) = h(x_1, \dots, x_n)$. The function h is called a C^k (k times continuously differentiable) function if it possesses continuous partial derivatives of all orders $\leq k$ on A . Here $k \in \mathbb{Z}^+$, i.e., k is a positive integer. If h is C^k for all k then h is said to be a smooth or C^∞ function. A mapping $H : A \rightarrow \mathbb{R}^m$ is a collection (H_1, \dots, H_m) of functions $H_i : A \rightarrow \mathbb{R}$. The mapping H is C^k if all H_i 's are C^k . A mapping $P : A \rightarrow \mathbb{R}^{m_1 \times m_2}$ is an $m_1 \times m_2$ matrix of functions $P_{ij} : A \rightarrow \mathbb{R}$. The mapping P is C^k if all P_{ij} 's are C^k . We use the notation P' to denote the transpose of P .

A *topological space* is a set S with a topology. Any open set containing a point p of a topological space is called a *neighborhood* of p . For a subset S_0 of a topological space S , there is a unique open set, denoted $\text{int}(S_0)$ and called the *interior* of S_0 , which is contained in S_0 and contains any other open set contained in S_0 . We say that S_0 has *empty interior* with respect to S if S_0 contains no open set of S other than

the empty set \emptyset . Consider a mapping $F : S_1 \rightarrow S_2$, where S_1 and S_2 are topological spaces. The mapping F is said to be *continuous* if the inverse image of every open set of S_2 is an open set of S_1 . The mapping F is *open* if the image of an open set of S_1 is an open set of S_2 . The mapping F is a *homeomorphism* if it is a bijection and both continuous and open.

A *locally Euclidean space* E of dimension n is a topological space such that for each $p \in E$ there exists a homeomorphism φ from some open neighborhood of p onto an open set in \mathbb{R}^n . A *manifold* \mathbf{M} of dimension n is a topological space which is a locally Euclidean space of dimension n , is Hausdorff (any two different points have disjoint neighborhoods) and has a countable basis. A *coordinate chart* on a manifold \mathbf{M} is a pair (U, ϕ) , where U is an open set of \mathbf{M} and ϕ a homeomorphism of U onto an open set of \mathbb{R}^n . Sometimes ϕ is represented as (ϕ_1, \dots, ϕ_n) , where $\phi_i : U \rightarrow \mathbb{R}$ is called the *i-th coordinate function*. If $p \in U$, the n -tuple of real numbers $(\phi_1(p), \dots, \phi_n(p))$ is called the set of *local coordinates* of p in the coordinate chart (U, ϕ) .

A C^∞ *atlas* on a manifold \mathbf{M} is a collection $\{(U_i, \phi_i)\}_{i \in I}$, where I is an index set, of pairwise C^∞ -compatible coordinate charts with the property that $\cup_{i \in I} U_i = \mathbf{M}$. An atlas is *complete* if it is not properly contained in any other atlas. A *smooth* (C^∞) *manifold* is a manifold equipped with a complete C^∞ atlas.

Let \mathbf{M}_1 and \mathbf{M}_2 denote two smooth manifolds of dimension n . Then a bijective mapping $F : \mathbf{M}_1 \rightarrow \mathbf{M}_2$ is a *diffeomorphism* if F is bijective and both F and F^{-1} are smooth mappings. The manifolds \mathbf{M}_1 and \mathbf{M}_2 are *diffeomorphic* if there exists a diffeomorphism $F : \mathbf{M}_1 \rightarrow \mathbf{M}_2$.

One may define the notion of analytic manifold, analytic mappings of manifolds and so on, by assuming that functions, mappings, etc. are analytic. We shall make this assumption explicit whenever needed.

Let \mathbf{M} be a smooth manifold of dimension n . The *tangent space* to \mathbf{M} at a point $x \in \mathbf{M}$ is denoted by $T_x \mathbf{M}$. The *tangent bundle* of \mathbf{M} is $T\mathbf{M} = \bigcup_{x \in \mathbf{M}} T_x \mathbf{M}$, the union of tangent spaces. A *vector field* τ on \mathbf{M} is a smooth map, which assigns to each point on $x \in \mathbf{M}$ a tangent vector $\tau(x) \in T_x \mathbf{M}$. In local coordinates, τ is represented as a column vector whose elements depends on x :

$$\tau(x) = (\tau_1(x), \dots, \tau_n(x))' .$$

Alternatively, considering τ as a differential operator, we write

$$\tau(x) = \tau_1(x) \frac{\partial}{\partial x_1} + \dots + \tau_n(x) \frac{\partial}{\partial x_n} .$$

The symbol $\frac{\partial}{\partial x_i}$ is to be thought of as a basis element for the tangent space with respect to a given set of local coordinates. A *distribution* assigns a subspace of the tangent space to each point in \mathbf{M} in a smooth way. A distribution can be defined by a set of smooth vector fields τ^1, \dots, τ^r . In this case we define the distribution as

$$\Delta = \text{span}\{\tau^1, \dots, \tau^r\},$$

where we take the span over the set of smooth real-valued functions on \mathbf{M} . At any point $x \in \mathbf{M}$ the distribution is a linear subspace of the tangent space, i.e.,

$$\Delta(x) = \text{span}\{\tau^1, \dots, \tau^r\}(x) \subset T_x \mathbf{M}.$$

Given two smooth vector fields $X = \sum_{i=1}^n X_i \frac{\partial}{\partial x_i}$ and $Y = \sum_{i=1}^n Y_i \frac{\partial}{\partial x_i}$ on \mathbf{M} , we define a new vector field, denoted as $[X, Y]$ and called the *Lie bracket* of X and Y , as

$$[X, Y] = \sum_{j=1}^n \left(\sum_{i=1}^n \frac{\partial Y_j}{\partial x_i} X_i - \frac{\partial X_j}{\partial x_i} Y_i \right) \frac{\partial}{\partial x_j}.$$

A distribution Δ is called *involutive* if $[X, Y] \in \Delta$ whenever X and Y are vector fields in Δ .

Denote by $V(\mathbf{M})$ the linear space of smooth vector fields defined on \mathbf{M} . Then $V(\mathbf{M})$ with the Lie bracket operation is a *Lie algebra*. In particular, it can be shown that the map $(X, Y) \mapsto [X, Y]$ is bilinear, skew-commutative and satisfies the *Jacobi identity*

$$[X, [Y, Z]] + [Y, [Z, X]] + [Z, [X, Y]] = 0, \quad \forall X, Y, Z \in V.$$

A linear subspace $L \subset V(\mathbf{M})$ is called a *Lie subalgebra* if

$$[X, Y] \in L, \quad \forall X, Y \in L.$$

Let $\{X^i \mid 1 \leq i \leq q\}$ be a finite set of vector fields and L_1, L_2 two subalgebras of $V(\mathbf{M})$ which contain the vector fields X^1, \dots, X^q . Clearly, the intersection $L_1 \cap L_2$ is again a subalgebra of $V(\mathbf{M})$ and contains X^1, \dots, X^q . Thus we conclude that there exists a unique subalgebra L of $V(\mathbf{M})$ which contains X^1, \dots, X^q , and has the property of being contained in all the subalgebras of $V(\mathbf{M})$ which contain the vector fields X^1, \dots, X^q . This subalgebra is referred to as the *smallest subalgebra* of $V(\mathbf{M})$ which contains the vector fields X^1, \dots, X^q . By an inductive argument using the Jacobi identity, it can be shown that every element of L is a linear combination of repeated Lie brackets of the form $[X^{i_k}, [\dots [X^{i_2}, X^{i_1}] \dots]]$, where $X^{i_j}, 1 \leq i_j \leq q$, is in

the set $\{X^i \mid 1 \leq i \leq q\}$ and $1 < j < \infty$. With the subalgebra L we may associate a distribution \mathcal{L} in a natural way:

$$\mathcal{L}(x) = \text{span}\{X(x) \mid X \in L\}, \quad x \in \mathbf{M}.$$

The *cotangent space* to \mathbf{M} at $x \in \mathbf{M}$ is denoted by $T_x^*\mathbf{M}$, which is identified as the dual space associated with the tangent space $T_x\mathbf{M}$. The *cotangent bundle* of \mathbf{M} is $T^*\mathbf{M} = \bigcup_{x \in \mathbf{M}} T_x^*\mathbf{M}$, the union of cotangent spaces. Just as we defined vector fields on $T_x\mathbf{M}$, on $T_x^*\mathbf{M}$ we can define a *covector field* (one-form) ω . In local coordinates, we represent ω as a row vector whose elements depends on x :

$$\omega(x) = (\omega_1(x), \dots, \omega_n(x)).$$

Alternatively, we write

$$\omega(x) = \omega_1(x)dx_1 + \dots + \omega_n(x)dx_n.$$

The symbols dx_i represent the basis dual to the basis $\frac{\partial}{\partial x_i}$ on $T_x\mathbf{M}$ and are defined as

$$dx_i \cdot \frac{\partial}{\partial x_j} = \delta_{ij},$$

where δ_{ij} is the Kronecker delta. A one-form acts on a vector field to give a real valued function on \mathbf{M} ,

$$\omega \cdot \tau = \left(\sum_{i=1}^n \omega_i dx_i \right) \cdot \left(\sum_{j=1}^n \tau_j \frac{\partial}{\partial x_j} \right) = \sum_{i=1}^n \tau_i \omega_i.$$

A *codistribution* assigns a subspace of the cotangent space to each point in \mathbf{M} in a smooth way. A codistribution can be defined by a set of smooth covector fields $\omega^1, \dots, \omega^s$. In this case we define the codistribution as

$$\Omega = \text{span}\{\omega^1, \dots, \omega^s\},$$

where we take the span over the set of smooth real-valued functions on \mathbf{M} . At any $x \in \mathbf{M}$ the codistribution is a linear subspace of the cotangent space, i.e.,

$$\Omega(x) = \text{span}\{\omega^1, \dots, \omega^s\}(x) \subset T_x^*\mathbf{M}.$$

It is possible to construct a codistribution starting from a given distribution, and conversely. The natural way to do this is the following: given a distribution Δ , for

each $x \in \mathbf{M}$ consider the *annihilator* of $\Delta(x)$, that is the set of all covectors which annihilate all vectors in $\Delta(x)$

$$\Delta^\perp(x) = \{\omega \in T_x^* \mathbf{M} \mid \omega \cdot v = 0, \forall v \in \Delta(x)\}.$$

Since $\Delta^\perp(x)$ is a subspace of $T_x^* \mathbf{M}$, this construction identifies exactly a codistribution Δ^\perp , called the *annihilator* of Δ . Conversely, given a codistribution Ω , we can construct a distribution, denoted Ω^\perp and called the annihilator of Ω , so that for each $x \in \mathbf{M}$

$$\Omega^\perp(x) = \{v \in T_x \mathbf{M} \mid \omega \cdot v = 0, \forall \omega \in \Omega(x)\}.$$

2.2 Higher-Order Tangent Bundles

Consider a system defined on a smooth (C^∞) configuration manifold \mathbf{Q} of dimension n with local coordinates $q = (q^1, \dots, q^n)$. We introduce higher-order tangent bundles in order to deal with higher-order constraints.

For the configuration manifold \mathbf{Q} , the usual tangent bundle is given by

$$T\mathbf{Q} = \bigcup_{q \in \mathbf{Q}} T_q \mathbf{Q} = \{(q, \dot{q}) \mid q \in \mathbf{Q}, \dot{q} \in T_q \mathbf{Q}\}.$$

The second-order tangent bundle is defined as

$$T^2\mathbf{Q} = T(T\mathbf{Q}) = \bigcup_{(q, \dot{q}) \in T\mathbf{Q}} T_{(q, \dot{q})} T\mathbf{Q} = \{(q, \dot{q}, \ddot{q}) \mid (q, \dot{q}) \in T\mathbf{Q}, \ddot{q} \in T_{(q, \dot{q})} T\mathbf{Q}\}.$$

The p -th order tangent bundle can be defined iteratively as

$$T^p\mathbf{Q} = T(T^{p-1}\mathbf{Q}).$$

The local coordinates for the p -th order tangent bundle are given by $(q, \dot{q}, \dots, q^{(p)})$.

First-order (classical) nonholonomic constraints (Bloch et al., 1992) and second-order nonholonomic constraints (Reyhanoglu et al., 1999), defined on $T\mathbf{Q}$ and $T^2\mathbf{Q}$ respectively, naturally appear in several physical examples. In this dissertation, we will extend the development in Bloch et al. (1992) and Reyhanoglu et al. (1999) to *higher-order nonholonomic constraints* of the form

$$G_\beta(t, q, \dot{q}, \dots, q^{(p)}) = 0, \quad \beta = 1, \dots, k < n, \quad p \in \mathbb{Z}^+. \quad (2.1)$$

Assume that there exists a non-constant smooth function

$$h(\cdot) : \mathbb{R} \times T^{p-1}\mathbf{Q} \rightarrow \mathbb{R}$$

such that $\frac{dh}{dt} = 0$ along the trajectories of (2.1), then h is called a *non-trivial first integral*.

Definition 2.1 : *The constraints (2.1) are (completely) p -th order nonholonomic if and only if there does not exist any non-trivial first integral.*

Remark 2.1 : *The p -th order jet prolongation of $\mathbb{R} \times \mathbf{Q}$ is denoted by $J^p(\mathbb{R} \times \mathbf{Q})$. If (t, q) are fibered coordinates on $\mathbb{R} \times \mathbf{Q}$, then $(t, q, \dot{q}, \dots, q^{(p)})$ are fibered coordinates on $J^p(\mathbb{R} \times \mathbf{Q})$. Clearly, one can identify $J^p(\mathbb{R} \times \mathbf{Q})$ with $\mathbb{R} \times T^p\mathbf{Q}$. Thus $h(t, q, \dot{q}, \dots, q^{(p)})$ can also be viewed as a scalar function defined on the p -th order jet prolongation.*

2.3 Controllability of Nonlinear Systems

Assume control-affine systems of the form

$$\dot{x} = f(x) + \sum_{i=1}^m g_i(x)u_i, \quad x \in \mathbf{M}, \quad u \in \mathbf{U}, \quad (2.2)$$

where \mathbf{M} is a smooth n dimensional manifold, $\mathbf{g} = (g_0, \dots, g_m)$, where $g_0 = f$, is an $(m+1)$ -tuple of smooth vector fields on \mathbf{M} , and \mathbf{U} is a subset of \mathbb{R}^m containing zero in its interior.

Referring to the triple $\Sigma = (\mathbf{M}, \mathbf{g}, \mathbf{U})$ as the control system, an admissible control for Σ is a Lebesgue integrable, \mathbf{U} -valued function defined on some interval $[0, T]$. An equilibrium solution of (2.2) is denoted by x^e corresponding to $u = 0$, i.e., $f(x^e) = 0$.

The simplest approach to studying the controllability of the nonlinear system (2.2) is to consider its linearization. Nevertheless, this approach, although easier, may lead to the loss of some information. This is the reason why we directly consider applying tools from nonlinear control theory. Some results from the nonlinear control literature (see e.g., Nijmeijer and van der Schaft (1990), Sussmann (1987a), Sussmann and Jurdjevic (1972)) are presented as follows:

Let $\mathcal{R}(p, t)$ denote the set of reachable states from the initial state p in time exactly t , for the nonlinear system (2.2).

Definition 2.2 (Nijmeijer and van der Schaft, 1990; Sussmann and Jurdjevic, 1972; Sussmann, 1987a): *Consider the nonlinear system (2.2) and let $p \in \mathbf{M}$. Then*

(1) The system is said to be accessible at p if for any $T > 0$, $\bigcup_{t \leq T} \mathcal{R}(p, t)$ has a nonvoid interior with respect to \mathbf{M} . If this holds for all $p \in \mathbf{M}$, then the system is said to be accessible.

(2) The system is said to be strongly accessible at p if for any $T > 0$, $\mathcal{R}(p, T)$ has a nonvoid interior with respect to \mathbf{M} . If this holds for all $p \in \mathbf{M}$, then the system is said to be strongly accessible.

(3) The system is said to be small time locally controllable (STLC) at p if for any $T > 0$, p is an interior point of $\bigcup_{t \leq T} \mathcal{R}(p, t)$.

Definition 2.3 (Nijmeijer and van der Schaft, 1990; Sussmann and Jurdjevic, 1972; Sussmann, 1987a): Consider the nonlinear system (2.2).

(1) Let L denote the smallest subalgebra of $V(\mathbf{M})$ which contains the vector fields f, g_1, \dots, g_m , and let \mathcal{L} denote the corresponding involutive distribution defined by

$$\mathcal{L}(x) = \text{span}\{X(x) \mid X \in L\}, \quad x \in \mathbf{M}.$$

Then L and \mathcal{L} are called the accessibility algebra and accessibility distribution, respectively.

(2) Let L_0 denote the smallest subalgebra of $V(\mathbf{M})$ which contains the vector fields g_1, \dots, g_m and satisfies $[f, X] \in L_0$ for all $X \in L_0$, and let \mathcal{L}_0 denote the corresponding involutive distribution defined by

$$\mathcal{L}_0(x) = \text{span}\{X(x) \mid X \in L_0\}, \quad x \in \mathbf{M}.$$

Then L_0 and \mathcal{L}_0 are called the strong accessibility algebra and strong accessibility distribution, respectively.

The accessibility distribution \mathcal{L} can be defined in a natural way as follows:

$$\mathcal{L}(p) = \text{span}\{X(p) : X \in \bigcup_{k \geq 0} \mathcal{S}^k\},$$

where

$$\begin{aligned} \mathcal{S}^0 &= \text{span}\{f, g_i, i \in I_m\}, \\ \mathcal{S}^k &= \mathcal{S}^{k-1} + \text{span}\{[f, X], [g_i, X], i \in I_m : X \in \mathcal{S}^{k-1}\}, k \geq 1. \end{aligned}$$

Similarly, the strong accessibility distribution \mathcal{L}_0 can be defined as

$$\begin{aligned}\mathcal{L}_0(p) &= \text{span}\{X(p) : X \in \bigcup_{k \geq 0} \mathcal{S}_0^k\}, \\ \mathcal{S}_0^0 &= \text{span}\{g_i, i \in I_m\}, \\ \mathcal{S}_0^k &= \mathcal{S}_0^{k-1} + \text{span}\{[f, X], [g_i, X], i \in I_m : X \in \mathcal{S}_0^{k-1}\}, k \geq 1.\end{aligned}$$

The following results are standard.

Theorem 2.1 (Nijmeijer and van der Schaft, 1990; Sussmann and Jurdjevic, 1972; Sussmann, 1987a): *Consider the system (2.2) and let $p \in \mathbf{M}$. Then*

(1) *A sufficient condition for the system to be accessible from p is that*

$$\dim \mathcal{L}(p) = n. \quad (2.3)$$

(2) *A sufficient condition for the system to be strongly accessible from p is that*

$$\dim \mathcal{L}_0(p) = n. \quad (2.4)$$

If the system is real analytic then the above conditions are also necessary.

Note that in the nonlinear control literature the conditions (2.3) and (2.4) are referred to as the accessibility and strong accessibility rank conditions, respectively.

In our analysis we also use the sufficient condition of Sussmann (1987a) for small time local controllability. The condition involves the notion of the degree of a bracket.

Let $Br(\mathbf{X})$ denote the smallest Lie algebra of vector fields containing f, g_1, \dots, g_m and let B denote any bracket in $Br(\mathbf{X})$. We define the degree of a bracket to be $\delta(B) = \sum_{i=0}^m \delta^i(B)$, where $\delta^0(B), \delta^1(B), \dots, \delta^m(B)$ denote the number of times X_0, \dots, X_m , respectively, occur in B . The bracket B is called “bad” if $\delta^0(B)$ is odd and $\delta^i(B)$ is even for each $i, i = 1, \dots, m$.

Theorem 2.2 (Sussmann, 1987a): *Let $x^e \in \mathbf{M}$. The system (2.2) is STLC at x^e if it satisfies the accessibility rank condition; and if B is “bad” there exist good brackets C_1, \dots, C_k of lower degree in $Br(\mathbf{X})$ such that B can be written as a linear combination of $C_i, i = 1, \dots, k$, at x^e .*

Theorem 2.2 can be generalized by introducing an admissible weight vector $\mathbf{l} = (l_0, l_1, \dots, l_m)$, $l_i \geq l_0 \geq 0$, $\forall i$. Then we define the \mathbf{l} -degree of B as the value of $\sum_{i=0}^m l_i \delta^i(B)$.

Theorem 2.3 (Bianchini and Stefani, 1993): *Let $x^e \in \mathbf{M}$. The system (2.2) is STLC at x^e if it satisfies the accessibility rank condition; and if B is a “bad” bracket, it must be \mathbf{l} -neutralized for an admissible weight vector \mathbf{l} , i.e., must be a linear combination of good (i.e., not of the bad type) brackets of lower \mathbf{l} -degree at the equilibrium.*

2.4 Stabilizability of Nonlinear Systems

Feedback stabilization of nonlinear systems is a problem of great importance in control theory. While tremendous progress has been made towards the understanding of controllability of control systems of the form (2.2), it has also become clear that the feedback stabilization problem is much more complicated (see e.g., Sontag, 1990).

From the many results on feedback stabilization which have been obtained in recent years here we only need to recall the two cornerstone results, which show most clearly where our work fits in. Under some controllability assumptions the first guarantees the existence of asymptotically stabilizing discontinuous state feedback controllers for real analytic systems, the other result gives very restrictive necessary conditions for the existence of stabilizing continuous state feedback laws. For details and the precise definitions of the employed notions we refer the reader to the original papers.

Theorem 2.4 (Sussmann, 1979) : *Consider the system (2.2) and let x^e denote an equilibrium solution. Assume that the system is real analytic. If the system is STLC at x^e , then there exists a piecewise analytic feedback controller which locally asymptotically stabilizes the system to x^e .*

Theorem 2.5 (Brockett, 1983) : *Consider the system (2.2) and let x^e denote an equilibrium solution. A necessary condition for the existence of a C^1 static state feedback law which asymptotically stabilizes the system to x^e is that the image of the*

map

$$(x, u) \mapsto f(x) + \sum_{i=1}^m g_i u_i$$

contains a neighborhood of zero.

It should be noted that the above condition is also necessary for the existence of a C^0 (continuous) asymptotically stabilizing static or dynamic state feedback which results in existence of unique trajectories (Coron, 1990; Sontag, 1990; Zabczyk, 1989).

3

NONLINEAR MODELING OF HIGHER-ORDER NONHOLONOMIC SYSTEMS

This chapter studies the nonlinear modeling problem for systems with higher-order nonholonomic constraints using tools from theoretical mechanics. A general control systems approach is developed for such systems. The applicability of the theoretical development is illustrated in the subsequent chapters.

3.1 Mathematical Formulation

In this section we introduce different concepts that allow us to derive the dynamic equations for systems with higher-order nonholonomic constraints.

3.1.1 Universal D'Alembert's Principle

Consider a mechanical system that consists of N mass points and let m_s and \vec{r}_s denote the mass and the radius vector of the s -th particle, respectively. Denote by \vec{F}_s the force acting on the s -th particle. Let \vec{p}_s be the linear momentum of the s -th

particle. Then the *Universal D'Alembert's Principle* can be written as:

$$\sum_{s=1}^N (-\dot{\vec{p}}_s + \vec{F}_s) \cdot \delta \vec{r}_s^{(p)} = 0, \quad p \in \mathbb{Z}^+,$$

$$\delta t = 0, \quad \delta \vec{r}_s = \dots = \delta \vec{r}_s^{(p-1)} = 0, \quad \delta \vec{r}_s^{(p)} \neq 0, \quad (3.1)$$

where p denotes the p -th order derivative.

3.1.2 Mićević Dušan-Rusov Lazar's Form

Let \mathbf{Q} denote the configuration manifold such that $\vec{r}_s = \vec{r}_s(q^1, \dots, q^n)$, $s = 1, \dots, N$, is a smooth transformation. Let $(q, \dot{q}, \dots, q^{(p)})$ for $q \in \mathbb{R}^n$ be the local coordinates on the p -th order tangent bundle $\mathbf{M} = T^{(p)}\mathbf{Q}$, where p refers to the order of the nonholonomic constraint. As shown in Ze-chun and Feng-xiang (1987), the Universal D'Alembert's Principle (3.1) can be changed into the *Mićević Dušan-Rusov Lazar's form*:

$$\sum_{i=1}^n \left(-\frac{\partial T^{(p)}}{\partial q^{i(p)}} + \frac{\partial T^{(p-1)}}{\partial q^{i(p-1)}} + \frac{\partial T}{\partial q^i} + \hat{Q}_i \right) \delta q^{i(p)} = 0, \quad p \in \mathbb{Z}^+, \quad (3.2)$$

where \hat{Q}_i denotes the i -th generalized force given by

$$\hat{Q}_i = \sum_{s=1}^N \vec{F}_s \cdot \frac{\partial \vec{r}_s^{(p)}}{\partial q^{i(p)}} = \sum_{s=1}^N \vec{F}_s \cdot \frac{\partial \vec{r}_s}{\partial q^i}, \quad p \in \mathbb{Z}^+. \quad (3.3)$$

3.1.3 Generalized Lagrange's Equations

Given the kinetic energy of the system

$$T = \frac{1}{2} \sum_{s=1}^N m_s \dot{\vec{r}}_s \cdot \dot{\vec{r}}_s, \quad (3.4)$$

and the relation

$$\frac{\partial \vec{r}_s^{(p+1)}}{\partial q^{i(p)}} = (p+1) \frac{\partial \dot{\vec{r}}_s}{\partial q^i}, \quad \forall p, \quad (3.5)$$

it is easy to prove that the following relation applies

$$\frac{\partial T^{(p-1)}}{\partial q^{i(p-1)}} = \frac{1}{p} [(p-1) \frac{\partial T^{(p)}}{\partial q^{i(p)}} + \frac{\partial T}{\partial q^i}]. \quad (3.6)$$

Substituting (3.6) into (3.2), we obtain the *Generalized Lagrange Equations* as

$$\sum_{i=1}^n \left\{ \frac{1}{p} \left[\frac{\partial T^{(p)}}{\partial q^{i(p)}} - (p+1) \frac{\partial T}{\partial q^i} \right] - \hat{Q}_i \right\} \delta q^{i(p)} = 0, \quad p \in \mathbb{Z}^+. \quad (3.7)$$

Note that if the system is holonomic, then the $\delta q^{i(p)}$ are independent of each other in (3.7), hence for $p = 1$ we have

$$\frac{\partial \dot{T}}{\partial \dot{q}^i} - 2 \frac{\partial T}{\partial q^i} = \hat{Q}_i,$$

which are commonly known as Nielsen equations (Nielsen, 1935). Similarly for $p = 2$, Tzenoff equations (Tzenoff, 1924) are obtained.

Given a kinetic energy of the form $T = T(q, \dot{q})$, the following result (Jarzebowska, 2002) can be applied: If the function T is regular enough, i.e., all derivatives up to certain order p can be computed, then the identity below holds

$$\frac{d}{dt} \frac{\partial T}{\partial \dot{q}^i} \equiv \frac{1}{p} \left[\frac{\partial T^{(p)}}{\partial q^{i(p)}} - \frac{\partial T}{\partial q^i} \right], \quad i = 1, \dots, n, \quad p \in \mathbb{Z}^+. \quad (3.8)$$

Therefore, equations (3.7) can be shown equivalent to

$$\sum_{i=1}^n \left\{ \frac{d}{dt} \frac{\partial T}{\partial \dot{q}^i} - \frac{\partial T}{\partial q^i} - \hat{Q}_i \right\} \delta q^{i(p)} = 0, \quad p \in \mathbb{Z}^+, \quad (3.9)$$

which is the commonly used *Lagrange's formulation*.

If we wish to formulate equations (3.7) in terms of a *Lagrangian* we have first to separate the generalized forces (\hat{Q}_i) into conservative forces (derivable from a potential V) and nonconservative forces (Q_i), i.e.,

$$\hat{Q}_i = -\frac{\partial V}{\partial q^i} + Q_i.$$

Defining the Lagrangian as $L = T - V$ together with the fact that for $V = V(q)$

$$\frac{\partial V^{(p)}}{\partial q^{i(p)}} = \frac{\partial V}{\partial q^i}$$

holds, the following equations can be easily obtained

$$\sum_{i=1}^n \left\{ \frac{1}{p} \left[\frac{\partial L^{(p)}}{\partial q^{i(p)}} - (p+1) \frac{\partial L}{\partial q^i} \right] - Q_i \right\} \delta q^{i(p)} = 0, \quad p \in \mathbb{Z}^+. \quad (3.10)$$

3.1.4 Higher-Order Nonholonomic Constraints

Assume that the system is subject to $n-m$, $1 \leq m < n$, nonholonomic *constraints* of p -th order

$$G_\beta(q, \dot{q}, \dots, q^{(p)}) = 0, \quad \beta = 1, \dots, n-m, \quad p \in \mathbb{Z}^+, \quad (3.11)$$

so that the generalized virtual displacements satisfy the condition

$$\sum_{i=1}^n \frac{\partial G_\beta}{\partial q^{i(p)}} \delta q^{i(p)} = 0, \quad \beta = 1, \dots, n-m. \quad (3.12)$$

From (3.7) and (3.12), using the method of *Lagrange's multipliers* yields

$$\frac{1}{p} \left[\frac{\partial T^{(p)}}{\partial q^{i(p)}} - (p+1) \frac{\partial T}{\partial q^i} \right] = \hat{Q}_i + \sum_{\beta=1}^{n-m} \lambda_\beta \frac{\partial G_\beta}{\partial q^{i(p)}}, \quad i = 1, \dots, n, \quad p \in \mathbb{Z}^+, \quad (3.13)$$

or

$$\frac{d}{dt} \nabla_{\dot{q}^i} T - \nabla_{q^i} T = \hat{Q}_i + \sum_{\beta=1}^{n-m} \lambda_\beta \frac{\partial G_\beta}{\partial q^{i(p)}}, \quad i = 1, \dots, n, \quad p \in \mathbb{Z}^+, \quad (3.14)$$

where λ_β 's are undetermined Lagrange's multipliers, $\nabla_{(\cdot)}$ refers to the gradient operator with respect to the variable (\cdot) , $T = T(q, \dot{q})$ is the kinetic energy of the system, and Q_i are the generalized forces. Note that a "prime" denotes transpose. Equation (3.14) can be written in matrix form as

$$\frac{d}{dt} \nabla_{\dot{q}} T - \nabla_q T = \hat{Q} + \left(\frac{\partial G}{\partial q^{(p)}} \right)' \lambda. \quad (3.15)$$

We now partition the set of generalized coordinates $q = (q^1, \dots, q^n)$ as $q = (q_1, q_2)$, $q_1 \in \mathbb{R}^m$, $q_2 \in \mathbb{R}^{n-m}$, where $1 \leq m < n$. For second order constraints, these forms appear naturally in systems under the action of $m < n$ independent control forces and/or torques, i.e., systems with fewer control inputs than degrees of freedom (see e.g., Reyhanoglu et al. (1999) and references therein). Examples of such systems include underactuated space vehicles (Krishnan et al., 1992; Reyhanoglu and Rubio Hervas, 2012b; Rubio Hervas and Reyhanoglu, 2012a) and underactuated manipulators (Mahindrakar et al., 2005; Reyhanoglu and Rubio Hervas, 2012a, 2013).

Without loss of generality, we assume that the actuated degrees of freedom are represented by the elements of q_1 and the unactuated degrees of freedom are represented by the elements of q_2 .

Suppose that $q_2^{(p)}$ are in a *linear form* with respect to $q_1^{(p)}$, i.e.,

$$q_2^{(p)} = J(q, \dot{q}, \dots, q^{(p-1)}) q_1^{(p)} + R(q, \dot{q}, \dots, q^{(p-1)}), \quad (3.16)$$

where $J \in \mathbb{R}^{(n-m) \times m}$ and $R \in \mathbb{R}^{n-m}$ are C^∞ (smooth) functions defined on appropriate subsets of $T^{p-1}\mathbf{Q}$. Then the condition imposed on the generalized virtual displacements by the constraints (3.16) is given by

$$\delta q_2^{(p)} = J(q, \dot{q}, \dots, q^{(p-1)}) \delta q_1^{(p)}$$

and equations (3.7) can be formulated, in a compact form, as

$$\frac{1}{p}\{[\nabla_{q_1^{(p)}}T^{(p)} - (p+1)\nabla_{q_1}T] + J'[\nabla_{q_2^{(p)}}T^{(p)} - (p+1)\nabla_{q_2}T]\} = \hat{Q}_1 + J'\hat{Q}_2, \quad (3.17)$$

or in terms of the Lagrangian

$$\frac{1}{p}\{[\nabla_{q_1^{(p)}}L^{(p)} - (p+1)\nabla_{q_1}L] + J'[\nabla_{q_2^{(p)}}L^{(p)} - (p+1)\nabla_{q_2}L]\} = Q_1 + J'Q_2. \quad (3.18)$$

These equations can be also written in the usual form as

$$[\frac{d}{dt}\nabla_{\dot{q}_1}T - \nabla_{q_1}T] + J'[\frac{d}{dt}\nabla_{\dot{q}_2}T - \nabla_{q_2}T] = \hat{Q}_1 + J'\hat{Q}_2, \quad (3.19)$$

or

$$[\frac{d}{dt}\nabla_{\dot{q}_1}L - \nabla_{q_1}L] + J'[\frac{d}{dt}\nabla_{\dot{q}_2}L - \nabla_{q_2}L] = Q_1 + J'Q_2, \quad (3.20)$$

Here $\hat{Q}_1, Q_1 \in \mathbb{R}^m$ and $\hat{Q}_2, Q_2 \in \mathbb{R}^{n-m}$ correspond to the partitioning of \hat{Q} and Q . All of these forms are equivalent. It must be pointed out that, although these equations remind us of the commonly used Lagrangian formulation, their novelty is given by the fact that they are proved to be valid for any order of the nonholonomic constraints (i.e., not necessarily first and second order as it would be expected from the usual analysis) and they give the minimum set of equations compatible with the constraints while embedding the constraint actions into the formulation.

3.2 Nonlinear Control System Formulation

In this section we define a general procedure to write the equations above in a nonlinear control system form.

Let $Q = B(q)u$, where $B(q) \in \mathbb{R}^{n \times r}$, $r \geq m$ is a full rank matrix, and let

$$C(q, \dots, q^{(p-1)}) = \begin{bmatrix} 1 \\ J(q, \dots, q^{(p-1)}) \end{bmatrix},$$

where 1 is the $m \times m$ identity matrix and $u \in \mathbb{R}^r$ denotes the control input vector.

Given $L = L(q, \dot{q})$, the expression (3.20) can be rewritten as

$$C'[M(q)\ddot{q} + F(q, \dot{q})] = C'B(q)u. \quad (3.21)$$

The constrained system defined by (3.16) and (3.21) can be expressed as

$$q_1^{(p)} = v, \quad (3.22)$$

$$q_2^{(p)} = J(q, \dot{q}, \dots, q^{(p-1)})v + R(q, \dot{q}, \dots, q^{(p-1)}), \quad (3.23)$$

where $v \in \mathbb{R}^m$ denotes the new control input vector.

The main idea can now be described as follows. We first design the new control input v and solve for the corresponding motion $q, \dot{q}, \dots, q^{(p-1)}$ based on the system given by (3.22) and (3.23). Then we compute the actual control input vector u using the expression (3.21). If $r = m$, the control input u can be found by using the inverse of $C'B$. When $r > m$, $C'B$ has full row rank and hence there are infinitely many solutions. In this case, $C'BB'C$ is not singular and one can use a right inverse of $C'B$ to solve for a control input vector u as

$$u = (C'B)^\dagger C' [M(q)\ddot{q} + F(q, \dot{q})], \quad (3.24)$$

where $(C'B)^\dagger = B'C(C'BB'C)^{-1}$ denotes the right inverse of $C'B$.

In the next chapter, a number of control-theoretic properties are studied for systems of the form above. A clear example illustrating this development is a point mass moving on a constant-torsion curve, which can be found in Chapter 7.

4

CONTROLLABILITY AND STABILIZABILITY RESULTS

Here we develop a number of control-theoretic results such as nonintegrability, controllability, and stabilizability for higher-order nonholonomic systems. This chapter is based on papers by Rubio Hervas and Reyhanoglu (2013a,b,e).

Let $(q, \dot{q}, \dots, q^{(p-1)})$ for $q \in \mathbb{R}^n$ denote local coordinates on the $(p-1)$ -th order tangent bundle $\mathbf{M} = T^{p-1}\mathbf{Q}$, where p refers to the order of the nonholonomic constraint. Generalizing the ideas introduced in Reyhanoglu et al. (1999), we define the $n-m$ -covector fields

$$\omega = Jdq_1^{(p-1)} - dq_2^{(p-1)} + Rdt, \quad (4.1)$$

on $\mathbf{M} \times \mathbb{R}$ so that the $n-m$ relations given by the equation (3.16) can be rewritten as $\omega = 0$. Augment the covector fields (4.1) with the contact forms

$$\tilde{\omega}^1 = dq_1 - \dot{q}_1 dt, \quad \tilde{\omega}^2 = dq_2 - \dot{q}_2 dt, \quad (4.2)$$

\vdots

$$\tilde{\omega}^{2(p-1)-1} = dq_1^{(p-2)} - q_1^{(p-1)} dt, \quad \tilde{\omega}^{2(p-1)} = dq_2^{(p-2)} - q_2^{(p-1)} dt, \quad (4.3)$$

and let $\Omega \subset T^*(\mathbf{M} \times \mathbb{R})$ denote the codistribution

$$\Omega = \text{span}\{\omega, \tilde{\omega}^i, i \in I_{2(p-1)}\}, \quad (4.4)$$

where $I_{2(p-1)}$ denotes the set $\{1, \dots, 2(p-1)\}$. The annihilator of Ω , denoted Ω^\perp , is

spanned by $m + 1$ linearly independent smooth vector fields

$$\tau_0 = \sum_{j=1}^{p-1} q^{(j)'} \nabla_{q^{(j-1)}} + R' \nabla_{q_2^{(p-1)}} + \frac{\partial}{\partial t}, \quad (4.5)$$

$$\tau_j = \frac{\partial}{\partial q_1^{j(p-1)}} + J_j' \nabla_{q_2^{(p-1)}}, \quad j \in I_m. \quad (4.6)$$

We present the following result.

Definition 4.1 : Consider the distribution Ω^\perp and let $\tilde{\mathcal{C}}$ denote its accessibility algebra; i.e., the smallest subalgebra of $V^\infty(\mathbf{M} \times \mathbb{R})$ that contains $\tau_0, \tau_1, \dots, \tau_m$. Let \tilde{C} denote the accessibility distribution generated by the accessibility algebra $\tilde{\mathcal{C}}$. Then the constraints defined by equation (3.16) are completely nonholonomic (nonintegrable) if

$$\dim \tilde{C}(\eta, t) = pn + 1, \quad \forall (\eta, t) \in \mathbf{M} \times \mathbb{R}.$$

Note that the sufficient condition in Definition 4.1 gives a coordinate-free characterization of nonintegrability for any set of constraints of the form (3.16). This result is analogous of those given in Bloch et al. (1992) and Reyhanoglu et al. (1999) for the nonintegrability of velocity and acceleration constraints. In the real analytic case, this condition is also a necessary condition for the nonintegrability. In what follows, we will consider the real analytic case.

Equations (3.22) and (3.23) can be expressed in the usual nonlinear control system form by defining the following state variables

$$\eta_1 = q_1, \quad \eta_2 = q_2, \dots, \eta_{2p-1} = q_1^{(p-1)}, \quad \eta_{2p} = q_2^{(p-1)}.$$

The state equations are given by

$$\dot{\eta}_i = \eta_{i+2}, \quad i \in I_{2p-2}, \quad (4.7)$$

$$\dot{\eta}_{2p-1} = v, \quad (4.8)$$

$$\dot{\eta}_{2p} = J(\eta_1, \dots, \eta_{2p})v + R(\eta_1, \dots, \eta_{2p}), \quad (4.9)$$

which can be identified with the usual normal form (Reyhanoglu et al., 1999). Equations (4.7)-(4.9) define a drift vector field $f(\eta) = (\eta_3, \dots, \eta_{2p-1}, \eta_{2p}, 0, R)$ and control vector fields $g_i(\eta) = (0, \dots, 0, e_i, J_i)$, where e_i denotes the i 'th standard basis vector

in \mathbb{R}^m and J_i denotes the i -th column of the matrix function J , $i \in I_m$, according to the standard control system form

$$\dot{\eta} = f(\eta) + \sum_{i=1}^m g_i(\eta)v_i. \quad (4.10)$$

Note that an equilibrium solution η^e , corresponding to $v = 0$, of equation (4.10) has the form $\eta_1^e \in \mathbb{R}^m$, $\eta_2^e \in \mathbb{R}^{n-m}$, where $R(\eta_1^e, \eta_2^e, 0, \dots, 0) = 0$, and $\eta_3^e = \eta_4^e = \dots = \eta_{2p}^e = 0$; i.e., an equilibrium solution corresponds to a motion of the system for which all the configuration variables remain constant. The controllability and stabilizability properties of a system subject to the constraints (3.16) near an equilibrium configuration q^e can be obtained by studying local properties of the system (4.7)-(4.9) near the corresponding equilibrium solution $\eta_3^e = \dots = \eta_{2p}^e = 0$.

Following the development in Reyhanoglu et al. (1999), it can be shown that a higher-order nonholonomic system, which satisfies the sufficient condition of Definition 4.1, is strongly accessible. This nonlinear controllability property is equivalent to Definition 2.1 and it guarantees that a necessary condition for small time local controllability (STLC) of the system at the equilibrium is satisfied.

Theorem 4.1 : *Assume that the constraints (3.16) are (completely) p -th order non-holonomic. Then the system (4.10) is strongly accessible.*

Proof : Since relations (3.23) are assumed to be completely nonintegrable

$$\dim \tilde{C}(\eta, t) = pn + 1, \quad \forall (\eta, t) \in \mathbf{M} \times \mathbb{R},$$

i.e., the distribution Ω^\perp spanned by $\tau_0, \tau_1, \dots, \tau_m$ satisfies the accessibility Lie algebra rank condition at any $(q, \dots, q^{(p-1)}, t) \in \mathbf{M} \times \mathbb{R}$.

Let $\pi_M : \mathbf{M} \times \mathbb{R} \rightarrow \mathbf{M}$ denote the projection onto \mathbf{M} . Then, $\pi_{M^*}\tau_0 = f$ and $\pi_{M^*}\tau_i = g_i$, $i \in I_m$. Let \mathcal{C}_0 denote the strong accessibility algebra associated with f, g_i , $i \in I_m$, i.e., the smallest subalgebra which contains g_1, \dots, g_m and satisfies $[f, X] \in \mathcal{C}_0, \forall X \in \mathcal{C}_0$, and let C_0 denote the strong accessibility distribution generated by the strong accessibility algebra \mathcal{C}_0 . Since

$$\dim \tilde{C}(\eta, t) = \dim C_0(\eta) + 1$$

it follows that

$$\dim C_0(\eta) = pn, \quad \forall \eta \in \mathbf{M}.$$

Hence the system (4.7)-(4.9) is strongly accessible. Consequently, the system with higher-order nonholonomic constraints, defined by (3.22) and (3.23), is strongly accessible.

The following result illustrates the fact that for certain higher-order nonholonomic systems a given equilibrium configuration cannot be asymptotically stabilized using time-invariant continuous (static or dynamic) state feedback. This property has been previously recognized for a class of second-order nonholonomic (or underactuated) systems in Reyhanoglu et al. (1999).

Theorem 4.2 : *Assume that $R_i(q, 0, \dots, 0) = 0$, $\forall q \in \mathbf{Q}$, for some $i \in I_{n-m}$. Let $n - m \geq 1$ and let $(q^e, 0, \dots, 0)$ denote an equilibrium solution. Then the higher-order nonholonomic system, defined by equations (4.7)-(4.9) (or equivalently by equation (4.10)), is not asymptotically stabilizable to $(q^e, 0, \dots, 0)$ using time-invariant continuous (static or dynamic) state feedback law.*

Proof : A necessary condition for the existence of a time-invariant continuous asymptotically stabilizing state feedback law for system (4.7)-(4.9) is that the image of the mapping

$$(\eta_1, \eta_2, \dots, \eta_{2p-1}, \eta_{2p}, v) \mapsto (\eta_3, \eta_4, \dots, v, J(\eta_1, \eta_2, \dots, \eta_{2p-1}, \eta_{2p})v + R(\eta_1, \eta_2, \dots, \eta_{2p-1}, \eta_{2p}))$$

contains some neighborhood of zero (see Brockett (1983)). This necessary condition is not satisfied since no points of the form

$$(0, \dots, 0, \epsilon), \quad \epsilon_i \neq 0,$$

are in its image. Hence system (4.7)-(4.9) cannot be asymptotically stabilized to an equilibrium $(\eta_1^e, \eta_2^e, 0, \dots, 0)$ by a time-invariant continuous (static or dynamic) state feedback law and the system with higher-order nonholonomic constraints, defined by (3.22) and (3.23), is not asymptotically stabilizable to $(q^e, 0, \dots, 0)$ using time-invariant continuous (static or dynamic) state feedback law.

Strong accessibility is not sufficient to guarantee the existence of a piecewise analytic feedback law for asymptotic stabilization of the higher-order nonholonomic system at an equilibrium solution in the real analytic case. In certain cases a stronger controllability property such as small time local controllability (STLC) can be proved to guarantee that existence (Sussmann, 1979).

The first test for controllability is related to the system linearization about an equilibrium $q = q^e$ and $v = 0$. If the linearization of the system is controllable then so is the system itself. The converse is not true and, in this case, this first order test is inconclusive and a nonlinear analysis is required. Since Kalman rank condition is the commonly used test for linear controllability, small time local controllability can be extended for nonlinear systems as follows (Sussmann, 1987a):

Consider the system (3.22) and (3.23) together with the drift and control vector fields

$$\begin{aligned} f &= (q, \dot{q}, \dots, q^{(p-1)}, 0, R(q, \dot{q}, \dots, q^{(p-1)})), \\ g_i &= (0, \dots, 0, e_i, J_i(q, \dot{q}, \dots, q^{(p-1)})) , \quad i \in I_m. \end{aligned}$$

The following Lie brackets can be easily obtained:

$$\begin{aligned} ad_f g_i &= (0, \dots, 0, -e_i, -J_i, 0, *) , \quad i \in I_m , \\ ad_{f^2} g_i &= (0, \dots, 0, e_i, J_i, 0, *, 0, *) , \quad i \in I_m , \\ &\vdots \\ ad_{f^{p-1}} g_i &= ((-1)^{p-1} e_i, (-1)^{p-1} J_i, 0, *, \dots, 0, *) , \quad i \in I_m , \\ [g_i, g_j] &= (0, \dots, 0, H_{ji} - H_{ij}) , \quad i, j \in I_m , \\ [g_j, [f, g_i]] &= (0, \dots, 0, -H_{ij}, 0, *) , \quad i, j \in I_m , \\ ad_f [g_j, [f, g_i]] &= (0, \dots, 0, H_{ij}, 0, *, 0, *) , \quad i, j \in I_m , \\ ad_{f^2} [g_j, [f, g_i]] &= (0, \dots, 0, -H_{ij}, 0, *, 0, *, 0, *) , \quad i, j \in I_m , \\ &\vdots \\ ad_{f^{p-2}} [g_j, [f, g_i]] &= (0, (-1)^{p-1} H_{ij}, 0, *, \dots, 0, *) , \quad i, j \in I_m , \end{aligned}$$

where

$$H_{ij}(q, \dots, q^{(p-1)}) = \frac{\partial J_i(q, \dots, q^{(p-1)})}{\partial q^{(p-1)}} b_j(q, \dots, q^{(p-1)}) , \quad i, j \in I_m, \quad (4.11)$$

$$b_i(q, \dots, q^{(p-1)}) = \begin{pmatrix} e_i \\ J_i(q, \dots, q^{(p-1)}) \end{pmatrix} , \quad i \in I_m . \quad (4.12)$$

Note that b_i is a projection of g_i .

Theorem 4.3 : *Let $n - m \geq 1$ and let $(q^e, 0, \dots, 0)$ denote an equilibrium solution. The system with higher-order nonholonomic constraints, defined by (3.22) and (3.23), is small time locally controllable at $(q^e, 0, \dots, 0)$ if*

$$\dim \text{span}\{ad_{f^\alpha} g_i(q^e), \alpha = p, \dots, p^*, i \in I_m\} = p(n - m) \quad (4.13)$$

for a sufficiently large p^* .

Proof : Consider the system (3.22) and (3.23). By condition (4.13), the space spanned by the vectors

$$ad_{f^\alpha} g_i, \alpha = 0, \dots, p-1, i \in I_m, \quad (4.14)$$

$$ad_{f^\alpha} g_i, \alpha = p, \dots, p^*, i \in I_m. \quad (4.15)$$

has dimension pn at $(q^e, 0, \dots, 0)$, and hence the system is strongly accessible at $(q^e, 0, \dots, 0)$. Let $l_0 = l$ and $l_i = p^*l$, $i \in I_m$. The only bad bracket with $\delta(B) = 1$ is f which vanishes at the equilibrium. Any bad bracket with $\delta(B) \geq 3$ will have an \mathbf{l} -degree greater or equal to $(2p^* + 1)l$. Since the spanning good brackets (4.15) have \mathbf{l} -degree less than $(2p^* + 1)l$, any bad bracket with $\delta(B) \geq 3$ can be written as linear combinations of the good brackets which have lesser \mathbf{l} -degree. It follows that the Bianchini and Stefani condition is satisfied at $(q^e, 0, \dots, 0)$. Hence, under the stated assumptions, the system (3.22) and (3.23) is small time locally controllable at $(q^e, 0, \dots, 0)$.

Theorem 4.3 can be expressed in terms of $R(\eta_1, \eta_2, \dots, \eta_{2p-1}, \eta_{2p})$ and $J_i(\eta_1, \eta_2, \dots, \eta_{2p-1}, \eta_{2p})$, $i \in I_m$, as follows:

Corollary 4.1 : *Let $n - m \geq 1$ and let $(q^e, 0, \dots, 0)$ denote an equilibrium solution. The system with higher-order nonholonomic constraints, defined by (3.22) and (3.23), is small time locally controllable at $(q^e, 0, \dots, 0)$ if $\text{rank} [A_1 \dots A_m]$ is $p(n - m)$, where $A_i \in \mathbb{R}^{p(n-m) \times p}$, $i \in I_m$, is the matrix*

$$A_i = \begin{bmatrix} (a_1)_i & \cdots & (a_p)_i \\ \vdots & \ddots & \vdots \\ (a_p)_i & \cdots & (a_{2p-1})_i \end{bmatrix}, i \in I_m,$$

and

$$(a_j)_i = \left[\left(\sum_{k=0}^{j-1} \beta_k \frac{\partial R}{\partial q^{(p-j+k)}} \right) b_i \right]_{(q^e, 0, \dots, 0)}, i \in I_m, j \in I_{2p-1}, (p - j + k) \geq 0,$$

$$\beta_k = \left[\sum_{l=0}^{k-1} \frac{\partial R}{\partial q_2^{(p-k+l)}} \beta_l \right]_{(q^e, 0, \dots, 0)}, k \in I_{j-1}, \beta_0 = 1 \in \mathbb{R}^{(n-m) \times (n-m)}, (p - k + l) \geq 0,$$

$$b_i(q, \dots, q^{(p-1)}) = \begin{pmatrix} e_i \\ J_i(q, \dots, q^{(p-1)}) \end{pmatrix}, i \in I_m,$$

where 1 is the $(n - m) \times (n - m)$ identity matrix.

Proof : The expressions for $ad_{f^\alpha} g_i(q^e)$, $\alpha = p, \dots, 2p-1$, $i \in I_m$, result in a set of matrices A_i , $i \in I_m$, multiplied by a matrix $C = \text{diag}\{(-1)^p, \dots, (-1)^{2p-1}\}$. The rank of the matrices $A_i C$, $i \in I_m$, is the same as that for A_i , $i \in I_m$. Since dimension of the span $\{ad_{f^\alpha} g_i(q^e), \alpha = 0, \dots, 2p-1, i \in I_m\}$ is pn , we have a set of good brackets $ad_{f^\alpha} g_i(q^e)$, $\alpha = 0, \dots, 2p-1$, $i \in I_m$, which spans a space with a dimension of pn . It follows that the conditions of Theorem 4.3 are satisfied with $p^* = 2p-1$ at $(q^e, 0, \dots, 0)$. Hence, under the stated assumptions, the system (3.22) and (3.23) is small time locally controllable at $(q^e, 0, \dots, 0)$.

Other sufficient conditions for small time local controllability can be obtained as a generalization of that in Reyhanoglu et al. (1999).

Theorem 4.4: *Let $n - m \geq 1$ and let $(q^e, 0, \dots, 0)$ denote an equilibrium solution. The system with higher-order nonholonomic constraints, defined by (3.22) and (3.23), is small time locally controllable at $(q^e, 0, \dots, 0)$ if there exists a set of $n - m$ pairs of indices $(i_k, j_k) \in I_m^2$, $i_k \neq j_k$, $k \in I_{n-m}$,*

$$\dim \text{span}\{H_{i_k j_k}(q^e), k \in I_{n-m}\} = n - m, \quad (4.16)$$

$$H_{i_k j_k}(q^e) \neq H_{j_k i_k}(q^e), k \in I_{n-m}, \quad (4.17)$$

and

$$H_{i_k i_k}(q^e) = 0, \forall k \in I_{n-m}. \quad (4.18)$$

Proof : Consider the system (3.22) and (3.23) and assume that conditions (4.16)-(4.18) hold. By condition (4.16) and (4.17), the space spanned by the vectors

$$\begin{aligned} & ad_{f^\alpha} g_i, \alpha = 0, \dots, p-1, i \in I_m, \\ & [g_{i_k}, g_{j_k}], ad_{f^\beta} [g_{j_k}, [f, g_{i_k}]], \beta = 0, \dots, p-2, k \in I_{n-m}, \end{aligned} \quad (4.19)$$

has dimension pn at $(q^e, 0, \dots, 0)$, and hence, the system is strongly accessible at $(q^e, 0, \dots, 0)$. Let $l_0 = l_{i_k} = l$ and $l_i = 2l$, $i \neq i_k$, $i \in I_m$, $k \in I_{n-m}$. The degree $\delta(B) = \sum_{i=0}^m \delta^i(B)$ of a bad bracket must necessarily be odd. Any bad bracket with $\delta(B) \geq p+2$ has **I**-degree greater than or equal to $l(p+2)$. Clearly, these brackets are **I**-neutralized since the spanning good brackets (4.19) have **I**-degree less than $l(p+2)$. Hence, it suffices to show that bad brackets with $\delta(B) = 1, \delta(B) = 3, \dots, \delta(B) < p+2$ are **I**-neutralized. The only bad bracket with $\delta(B) = 1$ is f which vanishes at the equilibrium. By conditions (4.16)-(4.18), the bad brackets with repeating

indexes i_k , $k \in I_{n-m}$ can be written as linear combinations of good brackets of lower \mathbf{l} -degree; and by condition (4.16), the bad brackets with repeating indexes i , $i \neq i_k$, $i \in I_m$, $k \in I_{n-m}$, can be written as linear combinations of the good brackets which have lesser \mathbf{l} -degree. It follows that the Bianchini and Stefani condition is satisfied at $(q^e, 0, \dots, 0)$. Hence, under the stated assumptions, the system (3.22) and (3.23) is small time locally controllable at $(q^e, 0, \dots, 0)$.

In the next chapter, a control algorithm is presented for a particular class of systems with higher-order nonholonomic constraints. The results of this chapter are illustrated in Chapters 6 and 7.

5

FEEDBACK CONTROL OF A CLASS OF HIGHER-ORDER NONHOLONOMIC SYSTEMS

This chapter studies the control problem for a special class of systems with higher-order nonholonomic constraints. Specific assumptions are introduced that define this class, which includes important models of robotic system examples. The main result of the chapter is the construction of a discontinuous nonlinear feedback control algorithm for which the closed loop equilibrium at the origin is made globally attractive. The control construction approach is introduced in detail, and a proof of attractiveness is presented. This chapter is based on papers by Rubio Hervas and Reyhanoglu (2013b,g).

5.1 Mathematical Model

In the previous chapter we have shown that after suitable nonlinear state and control transformations, many examples of higher-order nonholonomic systems can be described by nonlinear control equations of the form

$$q_1^{(p)} = v, \tag{5.1}$$

$$q_2^{(p)} = J(q, \dot{q}, \dots, q^{(p-1)})v + R(q, \dot{q}, \dots, q^{(p-1)}), \tag{5.2}$$

where $q_1 \in \mathbb{R}^m$ denotes the configuration variables for the $m \geq 2$ directly actuated degrees of freedom, $v \in \mathbb{R}^m$ denotes the transformed control variables for the directly

actuated degrees of freedom, and $q_2 \in \mathbb{R}^{n-m}$ denotes the configuration variables the control of which must be achieved through the system coupling characterized by the functions $J(q, \dot{q}, \dots, q^{(p-1)}) \in \mathbb{R}^{(n-m) \times m}$ and $R(q, \dot{q}, \dots, q^{(p-1)}) \in \mathbb{R}^{n-m}$. Here $q = (q_1, q_2)$. In this chapter, we will restrict the subsequent development to $R \equiv 0$ so that any rest configuration is an equilibrium configuration q^e for $v = 0$. Our objective is to construct a controller which makes a given equilibrium configuration globally attractive.

Assume now that (5.2) can be arranged as

$$q_2^{(p)} = N_1(q_{12}, \dot{q}_{12}, \dots, q_{12}^{(p-1)})q_{11}^{(p)} + N_2(q, \dot{q}, \dots, q^{(p-1)})q_{12}^{(p)}, \quad (5.3)$$

where $q_1 = (q_{11}, q_{12})$, $q_{11} \in \mathbb{R}^l$, $q_{12} \in \mathbb{R}^{m-l}$, and $1 \leq n-m \leq l \leq m$. Then (5.1) and (5.2) can be rewritten as

$$q_{11}^{(p)} = v_1, \quad (5.4)$$

$$q_{12}^{(p)} = v_2, \quad (5.5)$$

$$q_2^{(p)} = N_1(q_{12}, \dot{q}_{12}, \dots, q_{12}^{(p-1)})v_1 + N_2(q_1, q_2, \dots, q_1^{(p-1)}, q_2^{(p-1)})v_2. \quad (5.6)$$

5.2 Feedback Control Law

This section develops a control strategy for systems with higher-order nonholonomic constraints of the form (5.3). Given its structure, a four-step feedback control algorithm can be designed to drive the system from any initial state to the origin. The idea here is based on the finite-time stabilization results developed in the literature for linear control systems (Bhat and Bernstein, 2005; Hon, 2002; Kryachkov et al., 2010; Levant, 2001).

Following Bhat and Bernstein (2005), consider the p -integrator system

$$z^{(p)} = v. \quad (5.7)$$

There exists $\epsilon \in (0, 1)$ such that, for every $\alpha \in (1 - \epsilon, 1)$, the origin is a globally finite-time-stable equilibrium for the system (5.7) under the feedback

$$v = - \sum_{i=1}^p k_i |z^{(i-1)}|^{\alpha_i} \text{sign} z^{(i-1)}, \quad (5.8)$$

where $z^{(0)} = z$ and $k_i > 0$, $i = 1, \dots, p$, are chosen such that the polynomial $s^p + k_p s^{p-1} + \dots + k_2 s + k_1$ is Hurwitz and $\alpha_1, \dots, \alpha_p$ satisfy

$$\alpha_{i-1} = \frac{\alpha_i \alpha_{i+1}}{2\alpha_{i+1} - \alpha_i}, \quad i = 2, \dots, p,$$

with $\alpha_{p+1} = 1$ and $\alpha_p = \alpha$.

Based on the controller (5.8), an algorithm can be generated to control any initial state to the origin of (5.4)-(5.6) in finite time.

Assume that there exists a nonzero equilibrium configuration q_{12}^e such that $N_1(q_{12}^e, 0, \dots, 0)$ has full row rank $n-m$. Also assume that $N_1(0, \dots, 0) = 0$, $N_2(q_1, 0, \dots, q_1^{(p-1)}, 0) = 0$. Then, a control strategy for the system (5.4)-(5.6) can be proposed to drive any initial state to the origin in four steps as follows:

Step 1) Drive the system to a nonzero equilibrium q_{12}^e such that $N_1(q_{12}^e, 0, \dots, 0)$ has full row rank $n-m$ in finite time using

$$\begin{aligned} v_1 &= 0, \\ v_2 &= -L_1 |q_{12} - q_{12}^e|^{\beta_1} \text{sign}(q_{12} - q_{12}^e) - \sum_{i=2}^p L_i |q_{12}^{(i-1)}|^{\beta_i} \text{sign} q_{12}^{(i-1)}; \end{aligned}$$

Step 2) Drive the q_2 variables to zero while keeping the $q_{12} = q_{12}^e$ using

$$\begin{aligned} v_1 &= -N_1^\dagger(q_{12}^e, 0, \dots, 0) \sum_{i=1}^p K_i |q_2^{(i-1)}|^{\alpha_i} \text{sign} q_2^{(i-1)}, \\ v_2 &= -L_1 |q_{12} - q_{12}^e|^{\beta_1} \text{sign}(q_{12} - q_{12}^e) - \sum_{i=2}^p L_i |q_{12}^{(i-1)}|^{\beta_i} \text{sign} q_{12}^{(i-1)}; \end{aligned}$$

where $N_1^\dagger = N_1^T (N_1 N_1^T)^{-1}$ denotes the right inverse of $N_1(q_{12}^e, 0, \dots, 0)$;

Step 3) Drive the q_{12} variables to zero while keeping the $q_2 \equiv 0$ using

$$\begin{aligned} v_1 &= -\sum_{i=1}^p K'_i |q_2^{(i-1)}|^{\alpha'_i} \text{sign} q_2^{(i-1)}, \\ v_2 &= -\sum_{i=1}^p L'_i |q_{12}^{(i-1)}|^{\beta'_i} \text{sign} q_{12}^{(i-1)}; \end{aligned}$$

Step 4) Drive the q_{11} variables to zero while keeping the $q_{12} \equiv 0$ using

$$\begin{aligned} v_1 &= -\sum_{i=1}^p K''_i |q_{11}^{(i-1)}|^{\alpha''_i} \text{sign} q_{11}^{(i-1)}, \\ v_2 &= -\sum_{i=1}^p L''_i |q_{12}^{(i-1)}|^{\beta''_i} \text{sign} q_{12}^{(i-1)}. \end{aligned}$$

Here $K_i, L_i, K'_i, L'_i, K''_i, L''_i, \alpha_i, \beta_i, \alpha'_i, \beta'_i, \alpha''_i, \beta''_i$ satisfy the sufficient conditions of Bhat and Bernstein (2005) for the finite-time stability of the p -integrator system (5.7).

In Chapter 7, this theoretical framework is illustrated through an example. In particular, we introduce a manipulator with a jerk constraint and apply the results of this chapter.

6

EXAMPLES: SECOND-ORDER NONHOLONOMIC SYSTEMS

This chapter is based on papers by Rubio Hervas and Reyhanoglu (Reyhanoglu and Rubio Hervas, 2011a,b, 2012a,b,c,d, 2013; Rubio Hervas and Reyhanoglu, 2012a,b; Rubio Hervas et al., 2013; Rubio Hervas and Reyhanoglu, 2013f,g). We consider two important examples of second-order nonholonomic systems that are asymptotically stabilizable via smooth feedback: space vehicles with multiple slosh modes and Prismatic-Prismatic-Revolute (PPR) robots moving open liquid containers.

6.1 Control of Space Vehicles with Fuel Slosh Dynamics

In fluid mechanics, liquid slosh refers to the movement of liquid inside an accelerating tank or container. Important examples include propellant slosh in spacecraft tanks and rockets (especially upper stages), cargo slosh in ships and trucks transporting liquids, and liquid slosh in robotically controlled moving containers.

Propellant slosh has been a problem studied in spacecraft design since the early days of large, liquid-fuel rockets. In launch vehicles or spacecraft, sloshing can be induced by propellant tank motions resulting from guidance and control system commands or from changes in vehicle acceleration. When the fuel tanks are only partially filled, large quantities of fuel move inside the tanks under translational and rotational

accelerations and generate the slosh dynamics. The slosh dynamics interacts with the rigid body dynamics of the spacecraft.

The traditional treatment of liquid slosh control began with the inclusion of physical barriers, such as baffles and complete compartmentalization, meant to limit the movement of liquid fuel to small amplitudes of high, negligible frequencies. Later, bladders were added to the list of ways to limit these motions. These techniques, although helpful in some cases, do not completely succeed in canceling the sloshing effects. Moreover, these suppression methods involve adding to the spacecraft structural mass, thereby increasing mission cost. Hence the control system must both assure stability during the thrusting phase and achieve good attitude control while suppressing the slosh dynamics.

The effects of baffle positions (and quantities) on sloshing frequency have been studied in the literature (Biswal et al., 2003). The mathematical techniques used in these studies are based on the velocity potential function solved using finite-element analysis. Results show that baffles are more effective when near the free-surface of the fluid. In Venugopal and Bernstein (1996), surface pressure control and surface flap actuators have been proposed for controlling slosh in rectangular tanks. The feedback controllers are designed using a Linear-Quadratic-Gaussian (LQG) synthesis. Fluid is assumed to be incompressible, inviscid, and irrotational. Results show a steady-state slosh amplitude lower than the no-actuator case.

The effect of liquid fuel slosh on spinning spacecraft has also been explored in the literature (Hubert, 2003, 2004). Different slosh motion types - surface waves, bulk fluid motion, and vortices - as well as fluid configurations during spinning are defined (Hubert, 2003). The design of control strategies for a launch vehicle with propellant sloshing has also been studied in several works (Blackburn and Vaughan, 1971; Freudenberg and Morton, 1992; Hubert, 2004; Kim and Choi, 2000; Qi et al., 2009). In Blackburn and Vaughan (1971), an advanced linear model of the Saturn V launch vehicle is developed and a linear optimal control law is proposed to control the vehicle. The work in Freudenberg and Morton (1992) studies the problem of robust control of a launch vehicle subject to aerodynamic, flexible, and slosh mode instabilities.

It has been demonstrated that pendulum and mass-spring models can approximate complicated fluid and structural dynamics; such models have formed the basis for many studies on dynamics and control of space vehicles with fuel slosh (Bandyopadhyay et al., 2009a,b; Peterson et al., 1989; Shekhawat et al., 2006). These models are obtained using computational fluid dynamic techniques (Dodge, 2000). There

is an extensive body of literature on the interaction of vehicle dynamics and slosh dynamics and their control, but this literature treats only the case of small perturbations to the vehicle dynamics. The control approaches developed for accelerating space vehicles have commonly employed methods of linear control design (Sidi, 1997; Wie, 1998) and adaptive control (Adler et al., 1991). A number of related papers following a similar approach are motivated by robotic systems moving liquid filled containers (Feddemma et al., 1997; Grundelius and Bernhardsson, 1999; Grundelius, 2000; Terashima and Schmidt, 1994; Yano et al., 2001a,b; Yano and Terashima, 2001, 2005). The linear control laws for the suppression of the slosh dynamics inevitably lead to excitation of the transverse vehicle motion through coupling effects. The complete nonlinear dynamics formulation in this section allows simultaneous control of the transverse, pitch, and slosh dynamics.

The previous work in Cho et al. (2000b) and Reyhanoglu (2003) considered a spacecraft with a partially filled spherical fuel tank and included only the lowest frequency slosh mode in the dynamic model using pendulum and mass-spring analogies. In this section, the previous results are extended by using multi-mass-spring and multi-pendulum models for the characterization of the most prominent sloshing modes. First, the modeling and control problem for planar maneuvering of space vehicles is considered. Models with time-invariant and time-varying slosh parameters are developed and studied in detail. The control inputs are defined by the gimbal deflection angle of a non-throttleable thrust engine and a pitching moment about the center of mass of the spacecraft. Later, the development is extended to a three-dimensional case. In this case, the control inputs are the two gimbal deflection angles of a main engine and three independent torques, generated by either gas jet pairs or control moment gyros, about the center of mass of the spacecraft. It is assumed that the rocket acceleration due to the main engine thrust is large enough so that surface tension forces do not significantly affect the propellant motion during main engine burns. The control objective is to control the translational velocity vector and the attitude of the spacecraft, while attenuating the sloshing modes characterizing the internal dynamics. The results are applied to the AVUM upper stage—the fourth stage of the European launcher Vega (Perez, 2006). The main contributions in this section are (i) the development of full nonlinear mathematical models for maneuvering of the spacecraft and (ii) the design of Lyapunov-based nonlinear feedback control laws. Simulation examples are included to illustrate the effectiveness of the controllers.

6.1.1 Planar Thrust Vector Control of an Upper-Stage Rocket with Time-Invariant Slosh Parameters

This section considers the modeling and control problem for planar maneuvering of space vehicles with fuel slosh dynamics. Slosh parameters are considered to be time-invariant.

6.1.1.1 Model Formulation

We now formulate the dynamics of a spacecraft with a single propellant tank including the prominent fuel slosh modes. The spacecraft is represented as a rigid body (base body) and the sloshing fuel masses as internal bodies. The main ideas in Cho et al. (2000a) are employed to express the equations of motion in terms of the spacecraft translational velocity vector, the angular velocity, and the internal (shape) coordinates representing the slosh modes.

To summarize the formulation in Cho et al. (2000a), let $v \in \mathbb{R}^3$, $\omega \in \mathbb{R}^3$, and $\eta \in \mathbb{R}^N$ denote the base body translational velocity vector, the base body angular velocity vector, and the vector of internal coordinates, respectively. In these coordinates, the Lagrangian has the form $L = L(v, \omega, \eta, \dot{\eta})$, which is $SE(3)$ -invariant ($SE(2)$ in the planar case) in the sense that it does not depend on the base body position and attitude. The generalized forces and moments on the spacecraft are assumed to consist of control inputs which can be partitioned into two parts: $\tau_t \in \mathbb{R}^3$ (typically from thrusters) is the vector of generalized control forces that act on the base body and $\tau_r \in \mathbb{R}^3$ (typically from symmetric rotors, reaction wheels, control moment gyros, and thruster pairs) is the vector of generalized control torques that act on the base body. It is also assumed that the internal dissipative forces are derivable from a Rayleigh dissipation function R . Then, the equations of motion of the spacecraft with internal dynamics are shown to be given by (Cho et al., 2000a):

$$\frac{d}{dt} \frac{\partial L}{\partial v} + \hat{\omega} \frac{\partial L}{\partial v} = \tau_t, \quad (6.1)$$

$$\frac{d}{dt} \frac{\partial L}{\partial \omega} + \hat{\omega} \frac{\partial L}{\partial \omega} + \hat{v} \frac{\partial L}{\partial v} = \tau_r, \quad (6.2)$$

$$\frac{d}{dt} \frac{\partial L}{\partial \dot{\eta}} - \frac{\partial L}{\partial \eta} + \frac{\partial R}{\partial \dot{\eta}} = 0, \quad (6.3)$$

where \hat{a} denotes a 3×3 skew-symmetric matrix formed from $a = [a_1, a_2, a_3]' \in \mathbb{R}^3$:

$$\hat{a} = \begin{bmatrix} 0 & -a_3 & a_2 \\ a_3 & 0 & -a_1 \\ -a_2 & a_1 & 0 \end{bmatrix}.$$

It must be pointed out that in the above formulation it is assumed that no control forces or torques exist that directly control the internal dynamics. The objective is to simultaneously control the rigid body dynamics and the internal dynamics using only control effectors that act on the rigid body; the control of internal dynamics must be achieved through the system coupling. In this regard, equations (6.1)-(6.3) model interesting examples of underactuated mechanical systems. The published literature on the dynamics and control of such systems includes the development of theoretical controllability and stabilizability results for a large class of systems using tools from nonlinear control theory (Reyhanoglu et al., 1996, 1999) and the development of effective nonlinear control design methodologies (Reyhanoglu et al., 2000) that are applied to several practical examples, including underactuated space vehicles (Cho et al., 2000b; Reyhanoglu, 2003).

In the subsequent sections, mechanical-analogy models are developed to characterize the propellant sloshing during a typical thrust vector control maneuver. The spacecraft acceleration due to the main engine thrust is assumed to be large enough so that surface tension forces do not significantly affect the propellant motion during main engine burns. This situation corresponds to a “high-acceleration” regime that can be characterized by using the Bond number Bo —the ratio of acceleration related forces to the liquid propellant’s surface tension forces, which is given by

$$Bo = \frac{\rho a \mathcal{R}^2}{\sigma},$$

where ρ and σ denote the liquid propellants density and surface tension, respectively; a is the spacecraft acceleration, and \mathcal{R} is a characteristic dimension (e.g., propellant tank radius). During the steady-state high-acceleration situation the propellant settles at the “bottom” of the tank with a flat free surface. When the main engine operation for thrust vector control introduces lateral accelerations, the propellant begins sloshing. As discussed in Enright and Wong (1994), Bond numbers as low as 100 would indicate that low-gravity (i.e., low-acceleration) effects may be of some significance. A detailed discussion of low-gravity fluid mechanics is given in Dodge (2000).

Multi-mass-spring analogy

We now derive a multi-mass-spring model of the sloshing fuel where the oscillation frequencies of the mass-spring elements represent the prominent sloshing modes (Sidi, 1997).

Consider a rigid spacecraft moving on a plane as indicated in Fig. 6.1, where v_x , v_z are the axial and transverse components, respectively, of the velocity of the center of

the fuel tank, and θ denotes the attitude angle of the spacecraft with respect to a fixed reference. The fluid is modeled by moment of inertia I_0 assigned to a rigidly attached mass m_0 and point masses m_i , $i = 1, \dots, N$, which are restricted to move along the spacecraft fixed z -axis. The relative positions of m_i are denoted by s_i . Moments of inertia of these masses are taken as zero. The locations h_0 and h_i are referenced to the center of the tank. A restoring force $-k_i s_i$ acts on the mass m_i whenever the mass is displaced from its neutral position $s_i = 0$. A thrust F is produced by a gimbaled thrust engine as shown in Fig. 6.1, where δ denotes the gimbal deflection angle, which is considered as one of the control inputs. A pitching moment M is also available for control purposes. The constants in the problem are the spacecraft mass m and moment of inertia I ; the fuel masses m_0, m_i ; the distance b between the body z -axis and the spacecraft center of mass location along the longitudinal axis, and the distance d from the gimbal pivot to the spacecraft center of mass. If the tank center is in front of the spacecraft center of mass then $b > 0$. The parameters m_i, h_i, k_i and b depend on the shape of the fuel tank, the characteristics of the fuel and the fill ratio of the fuel tank.

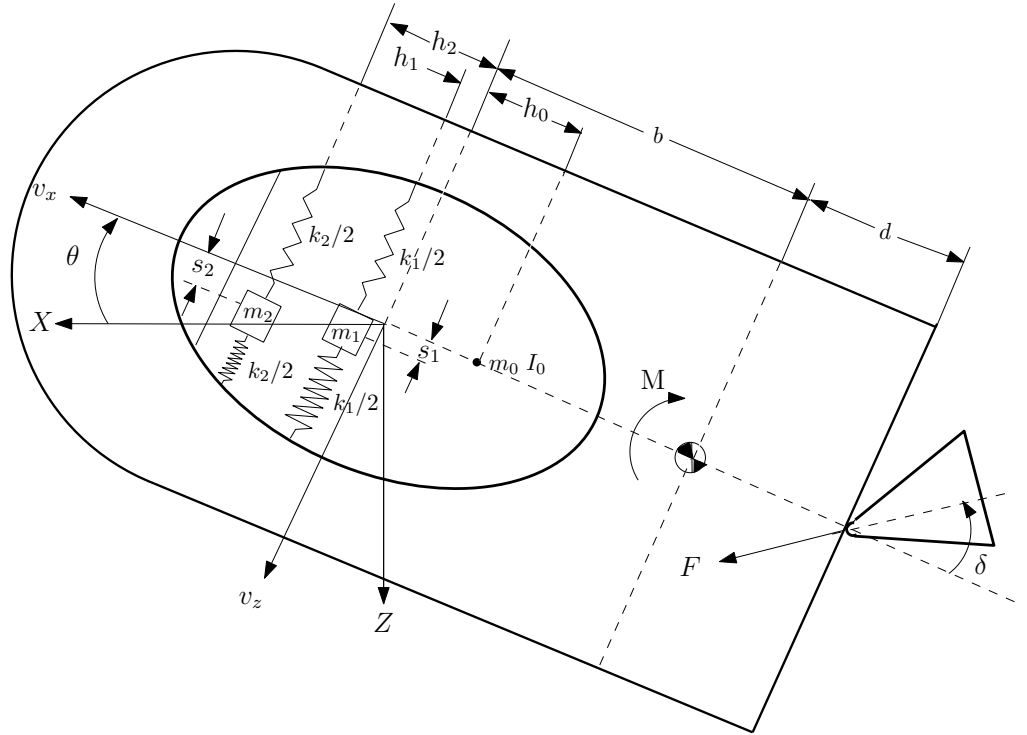


Figure 6.1: A multiple slosh mass-spring model for a spacecraft.

6.1 Control of Space Vehicles with Fuel Slosh Dynamics

To preserve the static properties of the liquid, the sum of all the masses must be the same as the fuel mass m_f , and the center of mass of the model must be at the same elevation as that of the fuel, i.e.,

$$m_0 + \sum_{i=1}^N m_i = m_f, \quad (6.4)$$

$$m_0 h_0 + \sum_{i=1}^N m_i h_i = 0. \quad (6.5)$$

Let \hat{i} and \hat{k} be the unit vectors along the spacecraft-fixed longitudinal and transverse axes, respectively, and denote by (x, z) the inertial position of the center of the fuel tank. The position vector of the center of mass of the vehicle can then be expressed in the spacecraft-fixed coordinate frame as

$$\vec{r} = (x - b)\hat{i} + z\hat{k}. \quad (6.6)$$

Clearly, the inertial velocity of the vehicle can be computed as

$$\dot{\vec{r}} = v_x \hat{i} + (v_z + b\dot{\theta})\hat{k}, \quad (6.7)$$

where $v_x = \dot{x} + z\dot{\theta}$ and $v_z = \dot{z} - x\dot{\theta}$.

Similarly, the position vectors of the fuel masses $m_0, m_i, \forall i$, in the spacecraft-fixed coordinate frame are given, respectively, by

$$\begin{aligned} \vec{r}_0 &= (x + h_0)\hat{i} + z\hat{k}, \\ \vec{r}_i &= (x + h_i)\hat{i} + (z + s_i)\hat{k}, \quad \forall i. \end{aligned}$$

Assuming h_i are constants, the inertial velocities can be computed as

$$\begin{aligned} \dot{\vec{r}}_0 &= v_x \hat{i} + (v_z - h_0\dot{\theta})\hat{k}, \\ \dot{\vec{r}}_i &= (v_x + s_i\dot{\theta})\hat{i} + (v_z - h_i\dot{\theta} + \dot{s}_i)\hat{k}, \quad \forall i. \end{aligned}$$

The total kinetic energy can now be expressed as

$$T = \frac{1}{2}m\dot{\vec{r}}^2 + \frac{1}{2}m_0\dot{\vec{r}}_0^2 + \frac{1}{2}\sum_{i=1}^N m_i\dot{\vec{r}}_i^2 + \frac{1}{2}(I + I_0)\dot{\theta}^2.$$

Since gravitational effects are ignored, there is no gravitational potential energy. The acceleration of the rocket gives rise to the elastic potential energy given by

$$U = \frac{1}{2}\sum_{i=1}^N k_i s_i^2.$$

Typically, k_i would be a function of the axial acceleration. However, in this section it is assumed that the axial acceleration is not significantly affected by small gimbal deflections, pitch changes and fuel motion so that k_i remain constant.

Thus, under the indicated assumptions, the Lagrangian ($L = T - U$) can be computed as

$$L = \frac{1}{2}m \left[v_x^2 + (v_z + b\dot{\theta})^2 \right] + \frac{1}{2}m_0 \left[v_x^2 + (v_z - h_0\dot{\theta})^2 \right] + \frac{1}{2}(I + I_0)\dot{\theta}^2 \\ + \frac{1}{2} \sum_{i=1}^N m_i \left[(v_x + s_i\dot{\theta})^2 + (v_z - h_i\dot{\theta} + \dot{s}_i)^2 \right] - \frac{1}{2} \sum_{i=1}^N k_i s_i^2.$$

Dissipative effects due to fuel slosh are included via damping constants c_i . The damping coefficients for the sloshing masses are usually determined by experimental measurements with partially filled tanks (Dodge, 2000). A fraction of kinetic energy of sloshing fuel is dissipated during each cycle of the motion. When the damping is small, it can be represented accurately by equivalent linear viscous damping. Even with baffles, the damping ratio is seldom greater than about 0.05. It is customary to include the damping via a Rayleigh dissipation function R given by

$$R = \frac{1}{2} \sum_{i=1}^N c_i \dot{s}_i^2.$$

Applying equations (6.1)-(6.3) with

$$\eta = \begin{bmatrix} s_1 \\ \vdots \\ s_N \end{bmatrix}, \quad v = \begin{bmatrix} v_x \\ 0 \\ v_z \end{bmatrix}, \quad \omega = \begin{bmatrix} 0 \\ \dot{\theta} \\ 0 \end{bmatrix}, \\ \tau_t = \begin{bmatrix} F \cos \delta \\ 0 \\ F \sin \delta \end{bmatrix}, \quad \tau_r = \begin{bmatrix} 0 \\ M + Fp \sin \delta \\ 0 \end{bmatrix},$$

where $p = b + d$, the equations of motion can be obtained as

$$(m + m_f)a_x + mb\ddot{\theta} + \sum_{i=1}^N m_i(s_i\ddot{\theta} + 2\dot{s}_i\dot{\theta}) = F \cos \delta, \quad (6.8)$$

$$(m + m_f)a_z + mb\ddot{\theta} + \sum_{i=1}^N m_i(\ddot{s}_i - s_i\dot{\theta}^2) = F \sin \delta, \quad (6.9)$$

$$\bar{I}\ddot{\theta} + \sum_{i=1}^N m_i(s_i a_x - h_i \ddot{s}_i + 2s_i \dot{s}_i \dot{\theta}) + mba_z = M + Fp \sin \delta, \quad (6.10)$$

$$m_i(\ddot{s}_i + a_z - h_i \ddot{\theta} - s_i \dot{\theta}^2) + k_i s_i + c_i \dot{s}_i = 0, \quad \forall i, \quad (6.11)$$

where $(a_x, a_z) = (\dot{v}_x + \dot{\theta}v_z, \dot{v}_z - \dot{\theta}v_x)$ are the axial and transverse components of the acceleration of the center of tank, and

$$\bar{I} = I + I_0 + mb^2 + m_0h_0^2 + \sum_{i=1}^N m_i(h_i^2 + s_i^2).$$

Note that equations (6.11) represent N nonintegrable second-order relations and hence they can be viewed as second order nonholonomic constraints.

The control objective is to design feedback controllers so that the controlled spacecraft accomplishes a given planar maneuver, that is a change in the translational velocity vector and the attitude of the spacecraft, while suppressing the fuel slosh modes.

Multi-Pendulum Analogy

This section derives a multi-pendulum model of the sloshing fuel where the oscillation frequencies of the pendula represent the prominent sloshing modes (Sidi, 1997).

Consider a rigid spacecraft moving on a plane as indicated in Fig. 6.2, where v_x, v_z are the axial and transverse components, respectively, of the velocity of the center of the fuel tank, and θ denotes the attitude angle of the spacecraft with respect to a fixed reference. The fluid is modeled by moment of inertia I_0 assigned to a rigidly attached mass m_0 and masses $m_i, i = 1, \dots, N$, attached to pendula of lengths l_i . Moments of inertia of these masses are taken as zero. The locations h_0 and h_i are referenced to the center of the tank. A thrust F is produced by a gimballed thrust engine as shown in Fig. 6.2, where δ denotes the gimbal deflection angle, which is considered as one of the control inputs. A pitching moment M is also available for control purposes. The constants in the problem are the spacecraft mass m and moment of inertia I ; the fuel masses m_0, m_i ; the distance b between the body z -axis and the spacecraft center of mass location along the longitudinal axis, and the distance d from the gimbal pivot to the spacecraft center of mass. If the tank center is in front of the spacecraft center of mass then $b > 0$. The parameters m_i, h_i, l_i and b depend on the shape of the fuel tank, the characteristics of the fuel and the fill ratio of the fuel tank.

As in the multi-mass-spring model, the sum of all the fluid masses must be the same as the fuel mass m_f ; i.e., equation (6.4) is satisfied. In the multi-pendulum case, the rigidly attached mass location h_0 satisfies

$$m_0h_0 + \sum_{i=1}^N m_i(h_i - l_i) = 0. \quad (6.12)$$

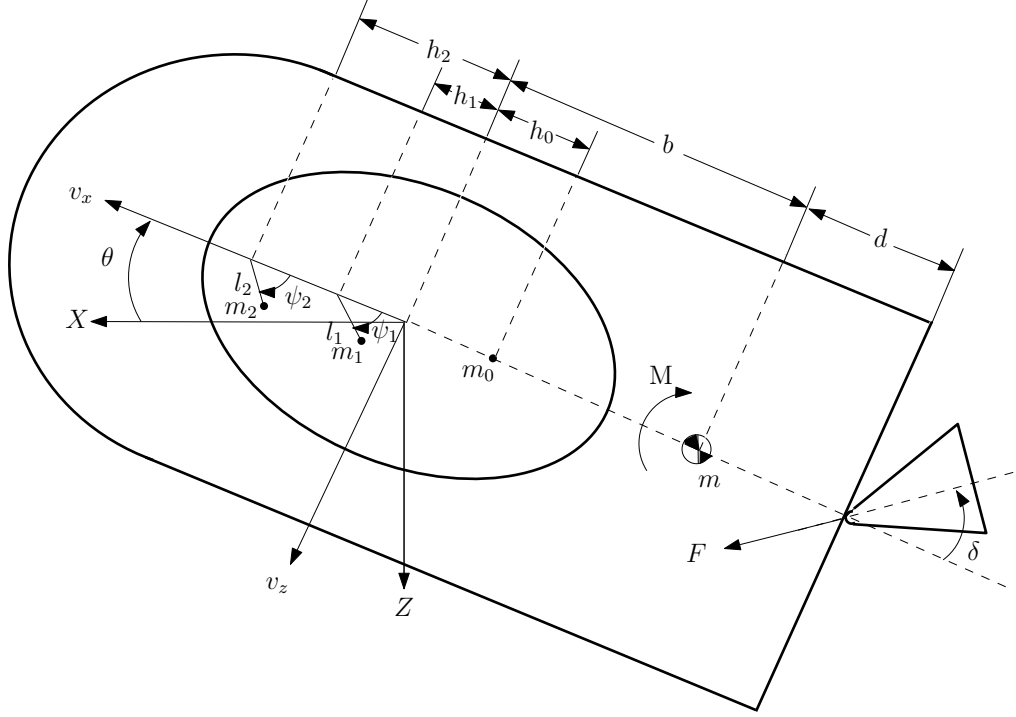


Figure 6.2: A multiple slosh pendula model for a spacecraft.

As in the previous case, the inertial position and velocity vectors in the spacecraft-fixed coordinate frame are given by equations (6.6) and (6.7), respectively.

The position vectors of the fuel masses m_0 , m_i , $\forall i$, in the spacecraft-fixed coordinate frame are given, respectively, by

$$\begin{aligned}\vec{r}_0 &= (x + h_0)\hat{i} + z\hat{k}, \\ \vec{r}_i &= (x + h_i - l_i \cos \psi_i)\hat{i} + (z + l_i \sin \psi_i)\hat{k}.\end{aligned}$$

Again assuming h_i are constants, the inertial velocities can be computed as

$$\begin{aligned}\dot{\vec{r}}_0 &= v_x\hat{i} + (v_z - h_0\dot{\theta})\hat{k}, \\ \dot{\vec{r}}_i &= [v_x + l_i(\dot{\theta} + \dot{\psi}_i) \sin \psi_i]\hat{i} + [v_z - h_i\dot{\theta} + l_i(\dot{\theta} + \dot{\psi}_i) \cos \psi_i]\hat{k}.\end{aligned}$$

The total kinetic energy can now be expressed as

$$T = \frac{1}{2}m\dot{\vec{r}}^2 + \frac{1}{2}m_0\dot{\vec{r}}_0^2 + \frac{1}{2}(I + I_0)\dot{\theta}^2 + \frac{1}{2}\sum_{i=1}^N m_i\dot{\vec{r}}_i^2.$$

Since gravitational effects are ignored, there is no potential energy. Thus, the

Lagrangian equals the kinetic energy, which can be expressed as

$$L = \frac{1}{2}m[v_x^2 + (v_z + b\dot{\theta})^2] + \frac{1}{2}m_0[v_x^2 + (v_z - h_0\dot{\theta})^2] + \frac{1}{2}(I + I_0)\dot{\theta}^2 \\ + \frac{1}{2}\sum_{i=1}^N m_i[(v_x + l_i(\dot{\theta} + \dot{\psi}_i)\sin\psi_i)^2 + (v_z - h_i\dot{\theta} + l_i(\dot{\theta} + \dot{\psi}_i)\cos\psi_i)^2].$$

Let ϵ_i denote the damping constants that represent the dissipative effects due to fuel slosh. Then, for this case, the Rayleigh dissipation function R can be expressed as

$$R = \frac{1}{2}\sum_{i=1}^N \epsilon_i \dot{\psi}_i^2.$$

Applying equations (6.1)-(6.3) with

$$\eta = \begin{bmatrix} \psi_1 \\ \vdots \\ \psi_N \end{bmatrix}, \quad v = \begin{bmatrix} v_x \\ 0 \\ v_z \end{bmatrix}, \quad \omega = \begin{bmatrix} 0 \\ \dot{\theta} \\ 0 \end{bmatrix}, \\ \tau_t = \begin{bmatrix} F \cos \delta \\ 0 \\ F \sin \delta \end{bmatrix}, \quad \tau_r = \begin{bmatrix} 0 \\ M + Fp \sin \delta \\ 0 \end{bmatrix},$$

the equations of motion can be obtained as

$$(m + m_f)a_x + \sum_{i=1}^N m_i l_i (\ddot{\theta} + \ddot{\psi}_i) \sin \psi_i + \bar{m} \bar{b} \ddot{\theta} + \sum_{i=1}^N m_i l_i (\dot{\theta} + \dot{\psi}_i)^2 \cos \psi_i = F \cos \delta, \quad (6.13)$$

$$(m + m_f)a_z + \sum_{i=1}^N m_i l_i (\ddot{\theta} + \ddot{\psi}_i) \cos \psi_i + \bar{m} \bar{b} \ddot{\theta} - \sum_{i=1}^N m_i l_i (\dot{\theta} + \dot{\psi}_i)^2 \sin \psi_i = F \sin \delta, \quad (6.14)$$

$$\bar{I} \ddot{\theta} - \sum_{i=1}^N m_i l_i h_i [(\ddot{\theta} + \ddot{\psi}_i) \cos \psi_i - (\dot{\theta} + \dot{\psi}_i)^2 \sin \psi_i] + \bar{m} \bar{b} a_z - \sum_{i=1}^N \epsilon_i \dot{\psi}_i = M + Fp \sin \delta, \quad (6.15)$$

$$m_i l_i [l_i (\ddot{\theta} + \ddot{\psi}_i) - h_i (\ddot{\theta} \cos \psi_i + \dot{\theta}^2 \sin \psi_i) + (a_x \sin \psi_i + a_z \cos \psi_i)] + \epsilon_i \dot{\psi}_i = 0, \quad \forall i, \quad (6.16)$$

where $(a_x, a_z) = (\dot{v}_x + \dot{\theta} v_z, \dot{v}_z - \dot{\theta} v_x)$ are the axial and transverse components of the acceleration of the center of tank, and

$$\bar{m} \bar{b} = mb - \sum_{i=1}^N m_i l_i,$$

$$\bar{I} = I + I_0 + mb^2 + m_0 h_0^2 + \sum_{i=1}^N m_i h_i^2.$$

Note that equations (6.16) represent N nonintegrable second-order relations and hence they can be viewed as second order nonholonomic constraints.

The control objective is again to design feedback controllers so that the controlled spacecraft accomplishes a given planar maneuver, that is a change in the translational velocity vector and the attitude of the spacecraft, while suppressing the fuel slosh modes.

6.1.1.2 Controllability and Stabilizability Analysis

This section presents a detailed development of feedback control laws through the model obtained via the multi-mass-spring analogy.

Consider the model of a spacecraft with a gimballed thrust engine shown in Fig. 6.1. If the thrust F during the fuel burn is a positive constant, and if the gimbal deflection angle and pitching moment are zero, $\delta = M = 0$, then the spacecraft and fuel slosh dynamics have a relative equilibrium defined by

$$v_z = \bar{v}_z, \theta = \bar{\theta}, \dot{\theta} = 0, s_i = 0, \dot{s}_i = 0, \forall i,$$

where \bar{v}_z and $\bar{\theta}$ are arbitrary constants. Without loss of generality, the subsequent analysis considers the relative equilibrium at the origin, i.e., $\bar{v}_z = \bar{\theta} = 0$. Note that the relative equilibrium corresponds to the vehicle axial velocity

$$v_x(t) = v_{x_0} + \bar{a}_x t, \quad t \leq t_b, \quad (6.17)$$

where v_{x_0} is the initial axial velocity of the spacecraft, t_b is the fuel burn time, and

$$\bar{a}_x = \frac{F}{m + m_f}.$$

Note that after the burnout v_x becomes a constant and thus it is bounded $\forall t$.

Since we have assumed that the axial acceleration term a_x is not significantly affected by small gimbal deflections, pitch changes and fuel motion (an assumption verified in simulations), equation (6.8) can be simplified to:

$$\dot{v}_x + \dot{\theta} v_z = \bar{a}_x. \quad (6.18)$$

Substituting this approximation leads to the following reduced equations of motion

for the transverse, pitch and slosh dynamics:

$$(m + m_f)(\dot{v}_z - \dot{\theta}v_x(t)) + mb\ddot{\theta} + \sum_{i=1}^N m_i(\ddot{s}_i - s_i\dot{\theta}^2) = F \sin \delta, \quad (6.19)$$

$$\bar{I}\ddot{\theta} + \sum_{i=1}^N m_i(\bar{a}_x s_i - h_i \ddot{s}_i + 2s_i \dot{s}_i \dot{\theta}) + mb(\dot{v}_z - \dot{\theta}v_x(t)) = M + Fp \sin \delta, \quad (6.20)$$

$$\ddot{s}_i + \dot{v}_z - \dot{\theta}v_x(t) - h_i \ddot{\theta} - s_i \dot{\theta}^2 + \frac{k_i}{m_i} s_i + \frac{c_i}{m_i} \dot{s}_i = 0, \quad \forall i, \quad (6.21)$$

where $v_x(t)$ is considered as an exogenous input. The subsequent analysis is based on the above equations of motion for the transverse, pitch and slosh dynamics of the vehicle.

Remark 6.1: *If one considers only small vehicle motions about the relative equilibrium at the origin, then the following linearized equations of motion can be obtained:*

$$(m + m_f)(\dot{v}_z - \dot{\theta}v_x(t)) + mb\ddot{\theta} + \sum_{i=1}^N m_i \ddot{s}_i = F\delta, \quad (6.22)$$

$$\bar{I}\ddot{\theta} + \sum_{i=1}^N m_i(\bar{a}_x s_i - h_i \ddot{s}_i) + mb(\dot{v}_z - \dot{\theta}v_x(t)) = M + Fp\delta, \quad (6.23)$$

$$\ddot{s}_i + \dot{v}_z - \dot{\theta}v_x(t) - h_i \ddot{\theta} + \frac{k_i}{m_i} s_i + \frac{c_i}{m_i} \dot{s}_i = 0, \quad \forall i. \quad (6.24)$$

The origin of the linearized time varying system (6.22)-(6.24) can be made uniformly asymptotically stable by linear state feedback. One of the difficulties in control design is the time variation representing the non-constant axial velocity of the vehicle that appears in the equations. This time variation formally prohibits the use of transfer function concepts, even for the linearized system (6.22)-(6.24). In the subsequent development, a Lyapunov-based control design approach is proposed for the nonlinear system (6.19)-(6.21) that overcomes this difficulty.

Eliminating \ddot{s}_i in (6.19) and (6.20) using (6.21) yields

$$(m + m_0)(\dot{v}_z - \dot{\theta}v_x(t)) + (mb - m_0 h_0)\ddot{\theta} - \sum_{i=1}^N (k_i s_i + c_i \dot{s}_i) = F \sin \delta, \quad (6.25)$$

$$(mb - m_0 h_0)(\dot{v}_z - \dot{\theta}v_x(t)) + (\bar{I} - \sum_{i=1}^N m_i h_i^2)\ddot{\theta} + N(s_i, \dot{s}_i, \dot{\theta}) = M + Fp \sin \delta, \quad (6.26)$$

where

$$N(s_i, \dot{s}_i, \dot{\theta}) = \sum_{i=1}^N \left[(m_i \bar{a}_x + k_i h_i) s_i + h_i c_i \dot{s}_i + 2m_i s_i \dot{s}_i \dot{\theta} - m_i h_i s_i \dot{\theta}^2 \right].$$

Note that the expressions (6.4) and (6.5) have been utilized to obtain equations (6.25) and (6.26) in the form above.

By defining control transformations from (δ, M) to new control inputs (u_1, u_2) :

$$\begin{bmatrix} u_1 \\ u_2 \end{bmatrix} = \begin{bmatrix} m + m_0 & mb - m_0 h_0 \\ mb - m_0 h_0 & \bar{I} - \sum_{i=1}^N m_i h_i^2 \end{bmatrix}^{-1} \begin{bmatrix} F \sin \delta + \sum_{i=1}^N (k_i s_i + c_i \dot{s}_i) \\ M + F p \sin \delta - N(s_i, \dot{s}_i, \dot{\theta}) \end{bmatrix},$$

the system (6.19)-(6.21) can be written as:

$$\dot{v}_z = u_1 + \dot{\theta} v_x(t), \quad (6.27)$$

$$\ddot{\theta} = u_2, \quad (6.28)$$

$$\ddot{s}_i = -\omega_i^2 s_i - 2\zeta_i \omega_i \dot{s}_i - u_1 + h_i u_2 + s_i \dot{\theta}^2, \quad \forall i, \quad (6.29)$$

where

$$\omega_i^2 = \frac{k_i}{m_i}, \quad 2\zeta_i \omega_i = \frac{c_i}{m_i}, \quad \forall i.$$

Here ω_i and ζ_i , $\forall i$, denote the undamped natural frequencies and damping ratios, respectively.

In order to apply the ideas of previous chapters, it is first noticed that equation (6.27) contains the time varying term $v_x(t)$. To deal with time dependence, the space state is expanded to also account for that term. Let

$$[\eta_1, \eta_2, \eta_3, \eta_4, \eta_{4+i}, \eta_{4+N+i}] = [v_x, v_z, \theta, \dot{\theta}, s_i, \dot{s}_i], \quad \forall i,$$

be the space state vector in \mathbb{R}^{4+2N} . Then, the system described by (6.27)-(6.29) together with (6.17) can be rewritten in a control form as

$$\dot{\eta}_1 = \bar{a}_x, \quad (6.30)$$

$$\dot{\eta}_2 = \eta_1 \eta_4 + u_1, \quad (6.31)$$

$$\dot{\eta}_3 = \eta_4, \quad (6.32)$$

$$\dot{\eta}_4 = u_2, \quad (6.33)$$

$$\dot{\eta}_{4+i} = \eta_{4+N+i}, \quad \forall i, \quad (6.34)$$

$$\dot{\eta}_{4+N+i} = -\omega_i^2 \eta_{4+i} - 2\zeta_i \omega_i \eta_{4+N+i} - u_1 + h_i u_2 + \eta_{4+i} \eta_4^2, \quad \forall i, \quad (6.35)$$

and the drift and control vector fields as

$$f = \bar{a}_x \frac{\partial}{\partial v_x} + \dot{\theta} v_x \frac{\partial}{\partial v_z} + \dot{\theta} \frac{\partial}{\partial \theta} + \dot{s}_i \frac{\partial}{\partial s_i} + (-\omega_i^2 s_i - 2\zeta_i \omega_i \dot{s}_i + s_i \dot{\theta}^2) \frac{\partial}{\partial \dot{s}_i}, \quad \forall i,$$

$$g_1 = \frac{\partial}{\partial v_z} - \frac{\partial}{\partial \dot{s}_i}, \quad i = 1, \dots, N, \quad g_2 = \frac{\partial}{\partial \dot{\theta}} + h_i \frac{\partial}{\partial \dot{s}_i}, \quad \forall i.$$

The space spanned by $[f, g_1, g_2, \text{ad}_f g_2, \text{ad}_{f^2} g_1], \forall i$, at the equilibrium determine an accessibility rank $4 + 2N$. Without loss of generality, assume the origin to be our equilibrium point. Then Theorem 4.3 is applied to the system projected to $[v_z, \theta, \dot{\theta}, s_i, \dot{s}_i], \forall i$, to prove small time local controllability of the system described by (6.27)-(6.29).

6.1.1.3 Feedback Control Laws

The main idea in the subsequent development is to first design feedback control laws for (u_1, u_2) and then use the following equations to obtain the feedback laws for the original controls (δ, M) for $t \leq t_b$:

$$\delta = \sin^{-1} \left([(m + m_0)u_1 + (mb - m_0 h_0)u_2 - \sum_{i=1}^N (k_i s_i + c_i \dot{s}_i)] / F \right), \quad (6.36)$$

$$M = (mb - m_0 h_0)u_1 + (\bar{I} - \sum_{i=1}^N m_i h_i^2)u_2 + N(s_i, \dot{s}_i, \dot{\theta}) - Fp \sin \delta. \quad (6.37)$$

Now, consider the following candidate Lyapunov function for the system (6.27)-(6.29):

$$V = \frac{r_1}{2} v_z^2 + \frac{r_2}{2} \theta^2 + \frac{r_3}{2} \dot{\theta}^2 + \frac{r_4}{2} \sum_{i=1}^N (\dot{s}_i^2 + \omega_i^2 s_i^2 - 2h_i \dot{s}_i \dot{\theta}),$$

where r_1, r_2, r_3 , and r_4 are positive constants. Assume that

$$\mu = r_3 - r_4 \sum_{i=1}^N h_i^2 > 0$$

so that the function V is positive definite.

Remark 6.2: Let $z = (\dot{\theta}, \dot{s}_1, \dots, \dot{s}_N)'$ and let $Q \in \mathbb{R}^{(N+1) \times (N+1)}$ denote the symmetric matrix corresponding to the quadratic form

$$z' Q z = r_3 \dot{\theta}^2 + r_4 \sum_{i=1}^N (\dot{s}_i^2 - 2h_i \dot{s}_i \dot{\theta}).$$

Clearly, this quadratic form is positive definite if and only if the leading principal minors of the matrix Q are all positive. It is easy to show that the condition holds if $\mu > 0$.

The time derivative of V along the trajectories of (6.27)-(6.29) is

$$\begin{aligned} \dot{V} = & -2r_4 \sum_{i=1}^N \zeta_i \omega_i \dot{s}_i^2 + [r_1 v_z - r_4 \sum_{i=1}^N (\dot{s}_i - h_i \dot{\theta})] u_1 + [r_1 v_x(t) v_z + r_2 \theta + \mu u_2 \\ & + r_4 \sum_{i=1}^N (h_i \omega_i^2 s_i + 2\zeta_i \omega_i h_i \dot{s}_i + s_i \dot{s}_i \dot{\theta} - h_i s_i \dot{\theta}^2)] \dot{\theta}. \end{aligned}$$

Clearly, the feedback laws

$$u_1 = -K_1[r_1 v_z - r_4 \sum_{i=1}^N (\dot{s}_i - h_i \dot{\theta})], \quad (6.38)$$

$$u_2 = -\frac{1}{\mu}[r_2 \dot{\theta} + K_2 \dot{\theta} + r_1 v_x(t) v_z + r_4 \sum_{i=1}^N (h_i \omega_i^2 s_i + 2\zeta_i \omega_i h_i \dot{s}_i + s_i \dot{s}_i \dot{\theta} - h_i s_i \dot{\theta}^2)], \quad (6.39)$$

where K_1 and K_2 are positive constants, yield

$$\dot{V} = -K_1[r_1 v_z - r_4 \sum_{i=1}^N (\dot{s}_i - h_i \dot{\theta})]^2 - K_2 \dot{\theta}^2 - 2r_4 \sum_{i=1}^N \zeta_i \omega_i \dot{s}_i^2,$$

which satisfies $\dot{V} \leq 0$.

Note that the closed-loop system becomes time-invariant after the burnout (since the time-varying term $v_x(t)$ becomes constant after the burnout). Using Krasovski-LaSalle invariance principle for time-varying systems (Khalil, 2002), it is easy to prove asymptotic stability of the origin of the closed loop defined by the equations (6.27)-(6.29) and the feedback control laws (6.38)-(6.39). Note also that the positive gains K_1 and K_2 can be chosen arbitrarily to achieve good closed loop responses.

Remark 6.3: *Following the above procedure, it is easy to show that the reduced equations for the multi-pendulum case are given by*

$$\dot{v}_z = u_1 + \dot{\theta} v_x(t), \quad (6.40)$$

$$\ddot{\theta} = u_2, \quad (6.41)$$

$$\ddot{\psi}_i = -c_i u_1 \cos \psi_i - d_i \sin \psi_i - (1 - c_i h_i \cos \psi_i) u_2 - e_i \dot{\psi}_i + c_i h_i \dot{\theta}^2 \sin \psi_i, \quad \forall i, \quad (6.42)$$

where

$$c_i = \frac{1}{l_i}, \quad d_i = \frac{F c_i}{m + m_f}, \quad e_i = \frac{\epsilon_i}{m_i l_i^2}, \quad \forall i,$$

and the controls (u_1, u_2) can be obtained as

$$u_1 = -K_1[r_1 v_z - r_4 \sum_{i=1}^N c_i(\dot{\psi}_i + \dot{\theta}(1 - c_i h_i \cos \psi_i)) \cos \psi_i], \quad (6.43)$$

$$\begin{aligned} u_2 = & -\frac{1}{\mu}[r_2 \dot{\theta} + K_2 \dot{\theta} + r_1 v_x(t) v_z + r_4 \sum_{i=1}^N e_i \dot{\psi}_i (c_i h_i \cos \psi_i - 1) \\ & + r_4 \sum_{i=1}^N c_i h_i ((\dot{\theta} + \dot{\psi}_i)^2 - 0.5 \dot{\theta} \dot{\psi}_i - d_i) \sin \psi_i \\ & + r_4 \sum_{i=1}^N c_i h_i (d_i - c_i h_i \dot{\theta}^2) \cos \psi_i \sin \psi_i]. \end{aligned} \quad (6.44)$$

Note also that as mentioned previously the control approaches developed for accelerating space vehicles have commonly employed methods of linear control design. The linear control laws for the suppression of the slosh dynamics inevitably lead to excitation of the transverse vehicle motion through nonlinear coupling effects. In this dissertation, this issue has been addressed by designing the nonlinear controller given by (6.36)-(6.39) based on the complete nonlinear dynamics formulation that allows simultaneous control of the transverse, pitch, and slosh dynamics.

6.1.1.4 Simulations

The feedback control laws developed in the previous section are implemented here for the AVUM upper stage spacecraft (Perez, 2006). The first two slosh modes are included to demonstrate the effectiveness of the control law. The physical parameters used in the simulations for the multi-mass-spring and multi-pendulum cases are given in Tables 6.1 and 6.2, respectively. The fluid parameters are obtained using the formulae in Dodge (2000).

The control objective in both cases is the stabilization of the spacecraft in orbital transfer, suppressing the transverse and pitching motion of the spacecraft and sloshing of fuel while the spacecraft is accelerating. In other words, the control objective is to stabilize the relative equilibrium corresponding to a constant axial spacecraft acceleration of 1.77 m/s^2 and $v_z = \theta = \dot{\theta} = 0$, $s_i = \dot{s}_i = 0$, $i = 1, 2$ (or $\psi_i = \dot{\psi}_i = 0$, $i = 1, 2$ in the multi-pendulum case). In the simulations, a fuel burn time of 660 s is assumed. Note that the following relation between the slosh variables can be used to compare the results for both cases:

$$s_i = l_i \sin \psi_i, \quad i = 1, 2.$$

6.1 Control of Space Vehicles with Fuel Slosh Dynamics

It must be noted that for the AVUM spacecraft the characteristic length of the propellant tank can be taken as ≈ 0.5 m and the propellant UMDH (Unsymmetrical Dimethyl Hydrazine) has a σ/ρ ratio of around $0.25 \times 10^{-4} \text{ m}^3/\text{s}^2$. Thus, accelerations that are larger than 0.1 m/s^2 correspond to a Bond number larger than 1000, which is clearly in the high-acceleration regime. The simulations indicate that during the main engine burn the vehicle acceleration exceeds 1 m/s^2 , and thus the mechanical-analogy models are valid.

Table 6.1: Physical parameters for a spacecraft (multi-mass-spring analogy).

Parameter	Value	Parameter	Value
m	975 kg	F	2450 N
I	$400 \text{ kg} \cdot \text{m}^2$	I_0	$14.85 \text{ kg} \cdot \text{m}^2$
m_0	358 kg	k_1	750 kg/s^2
m_1	89 kg	k_2	65 kg/s^2
m_2	2.7 kg	c_1	25.8 kg/s
h_0	-0.011 m	c_2	1.32 kg/s
h_1	0.035 m	b	-0.6 m
h_2	0.291 m	d	1.2 m

First the multi-mass-spring model is considered. The effectiveness of the Lyapunov-based controller (6.38)-(6.39) is demonstrated by applying the controller to the complete nonlinear system (6.8)-(6.11). Time responses shown in Figs. 6.3-6.5 correspond to the initial conditions $v_{x_0} = 3000 \text{ m/s}$, $v_{z_0} = 150 \text{ m/s}$, $\theta_0 = 5^\circ$, $\dot{\theta}_0 = 0$, $s_{1_0} = 0.15 \text{ m}$, $s_{2_0} = -0.15 \text{ m}$, and $\dot{s}_{1_0} = \dot{s}_{2_0} = 0$. As can be seen in the figures, the transverse velocity, attitude angle, and the slosh states converge to the relative equilibrium at zero while the axial velocity v_x increases and \dot{v}_x tends asymptotically to 1.77 m/s^2 . Note that there is a trade-off between good responses for the directly actuated degrees of freedom (the transverse and pitch dynamics) and good responses for the unactuated degree of freedom (the slosh dynamics); the controller given by (6.38)-(6.39) with parameters $r_1 = 8 \times 10^{-7}$, $r_2 = 2500$, $r_3 = 500$, $r_4 = 1 \times 10^{-5}$, $K_1 = 1 \times 10^4$, $K_2 = 1 \times 10^4$ represents one example of this balance.

Next the multi-pendulum model is considered. The effectiveness of the controller (6.43)-(6.44) is demonstrated by applying the controller to the complete nonlinear system (6.13)-(6.16). Time responses shown in Figs. 6.6-6.8 correspond to the same

initial conditions and the same controller parameters as in the previous case. Again, as can be seen in the figures, the transverse velocity, attitude angle, and the slosh states converge to the relative equilibrium at zero while the axial velocity v_x increases and \dot{v}_x tends asymptotically to 1.77 m/s^2 . Clearly, the simulation results show a close agreement in responses for both cases.

Table 6.2: Physical parameters for a spacecraft (multi-pendulum analogy).

Parameter	Value	Parameter	Value
m	975 kg	F	2450 N
I	$400 \text{ kg} \cdot \text{m}^2$	I_0	$14.85 \text{ kg} \cdot \text{m}^2$
m_0	358 kg	l_1	0.204 m
m_1	89 kg	l_2	0.070 m
m_2	2.7 kg	ϵ_1	$1.072 \text{ kg} \cdot \text{m}^2/\text{s}$
h_0	-0.011 m	ϵ_2	$0.007 \text{ kg} \cdot \text{m}^2/\text{s}$
h_1	0.239 m	b	-0.6 m
h_2	0.361 m	d	1.2 m

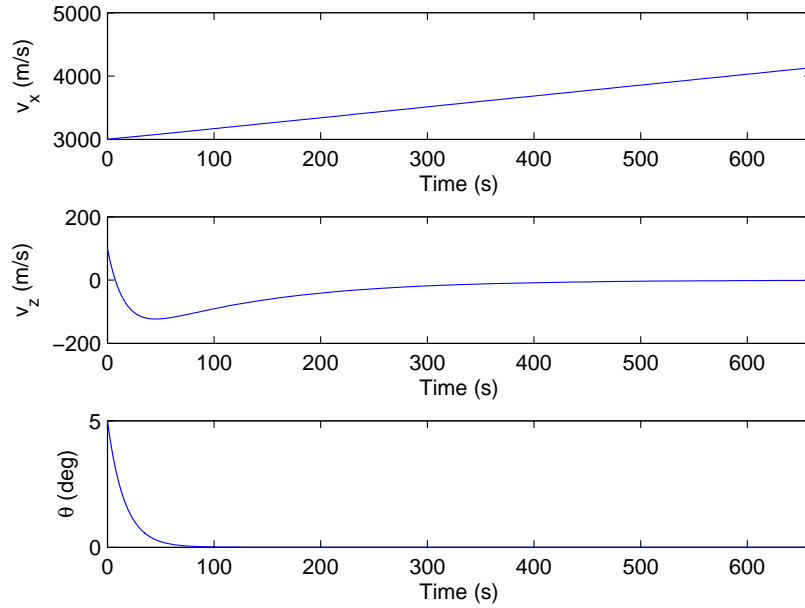


Figure 6.3: Time responses of v_x , v_z and θ (Multi-mass-spring case).

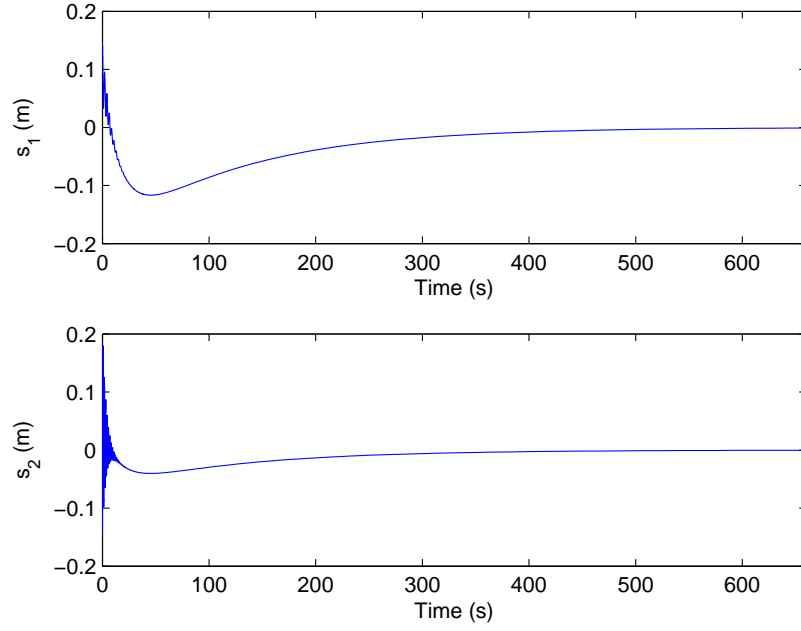


Figure 6.4: Time responses of s_1 and s_2 (Multi-mass-spring case).

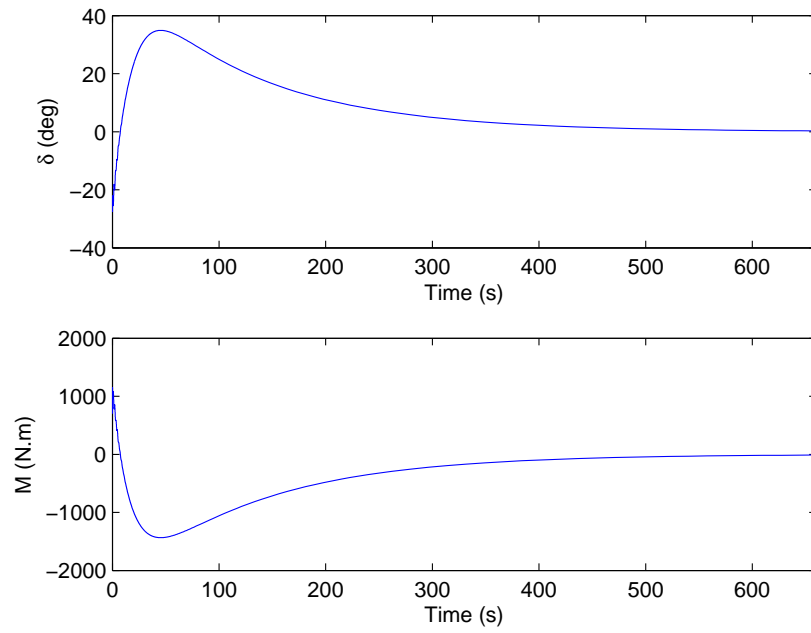


Figure 6.5: Gimbal deflection angle δ and pitching moment M (Multi-mass-spring case).

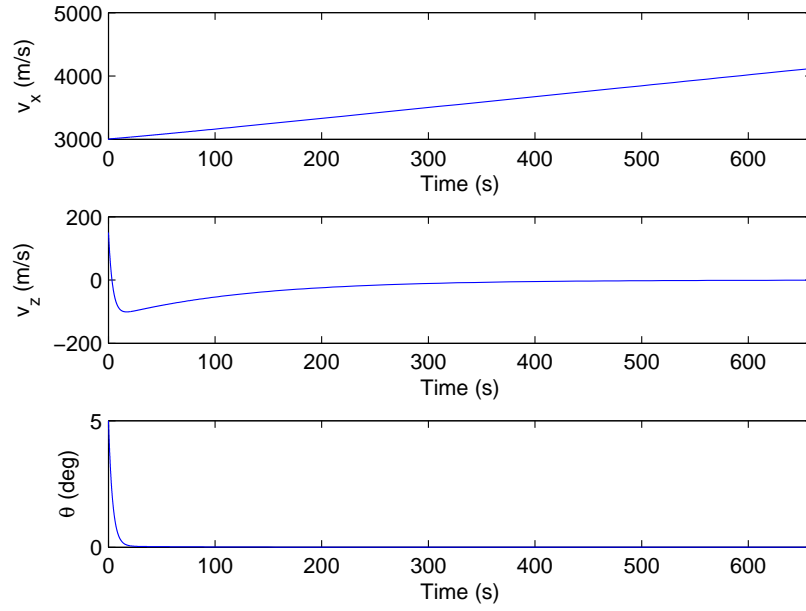


Figure 6.6: Time responses of v_x , v_z and θ (Multi-pendulum case).

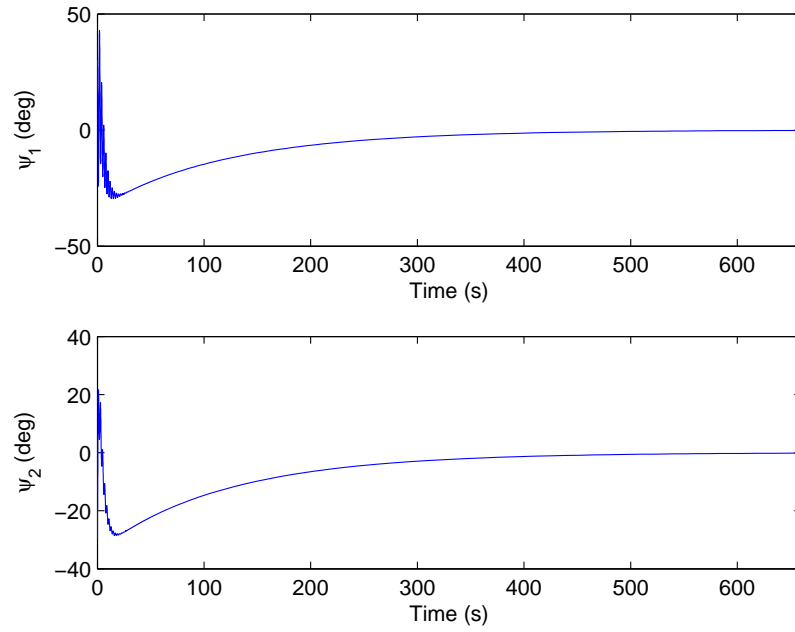


Figure 6.7: Time responses of ψ_1 and ψ_2 (Multi-pendulum case).

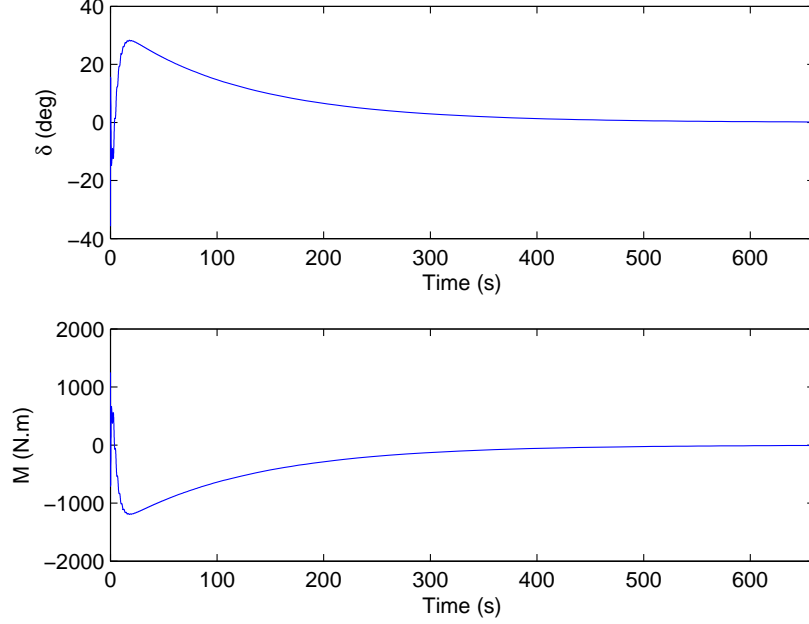


Figure 6.8: Gimbal deflection angle δ and pitching moment M (Multi-pendulum case).

6.1.2 Planar Thrust Vector Control of an Upper-Stage Rocket with Time-Varying Slosh Parameters

The previous sections considered a spacecraft with multiple fuel slosh modes assuming constant physical parameters. In this section, we take into account the time-varying nature of the slosh parameters, which renders stability analysis more difficult. The treatment is parallel to that in the previous section. The control inputs are defined by the gimbal deflection angle of a non-throttleable thrust engine and a pitching moment about the center of mass of the spacecraft. The control objective is to control the translational velocity vector and the attitude of the spacecraft, while attenuating the sloshing modes characterizing the internal dynamics. The results are applied to the AVUM upper stage—the fourth stage of the European launcher Vega (Perez, 2006). The main contributions here are (i) the development of a full nonlinear mathematical model with time-varying slosh parameters and (ii) the design of a nonlinear time-varying feedback controller. Simulation example is included to illustrate the effectiveness of the controller.

6.1.2.1 Model Formulation

Consider the multiple slosh mass-spring model for a spacecraft as described in Section 6.1.1 and let the slosh parameters be time-varying.

Assuming a constant fuel burn rate, we have

$$m_f = m_{ini} \left(1 - \frac{t}{t_f} \right), \quad (6.45)$$

where m_{ini} is the initial fuel mass in the tank and t_f is the time at which, at a constant rate, all the fuel is burned.

To compute the slosh parameters, a simple equivalent cylindrical tank is considered together with the model described in Dodge (2000), which can be summarized as follows. Assuming a constant propellant density, the height of still liquid inside the cylindrical tank is

$$h = \frac{4m_f}{\pi\varphi^2\rho}, \quad (6.46)$$

where φ and ρ denote the diameter of the tank and the propellant density, respectively. As shown in Dodge (2000), every slosh mode is defined by the parameters

$$m_i = m_f \left[\frac{\varphi \tanh(2\xi_i h/\varphi)}{\xi_i (\xi_i^2 - 1) h} \right], \quad (6.47)$$

$$h_i = \frac{h}{2} - \frac{\varphi}{2\xi_i} \left[\tanh(\xi_i h/\varphi) - \frac{1 - \cosh(2\xi_i h/\varphi)}{\sinh(2\xi_i h/\varphi)} \right], \quad (6.48)$$

$$k_i = \frac{m_i g}{\varphi} 2\xi_i \tanh(2\xi_i h/\varphi), \quad (6.49)$$

where ξ_i , $\forall i$, are constant parameters given by

$$\xi_1 = 1.841, \quad \xi_2 = 5.329, \quad \xi_i \simeq \xi_{i-1} + \pi,$$

and g is the axial acceleration of the spacecraft. For the rigidly attached mass, m_0 and h_0 are obtained from (6.4), (6.5), (6.45), and (6.46). Assuming that the liquid depth ratio for the cylindrical tank (i.e., h/φ) is less than two, the following relations apply

$$I_0 = \left(1 - 0.85 \frac{h}{\varphi} \right) m_f \left(\frac{3\varphi^2}{16} + \frac{h^2}{12} \right) - m_0 h_0^2 - \sum_{i=1}^N m_i h_i^2, \quad \text{if } \frac{h}{\varphi} < 1,$$

$$I_0 = \left(0.35 \frac{h}{\varphi} - 0.2 \right) m_f \left(\frac{3\varphi^2}{16} + \frac{h^2}{12} \right) - m_0 h_0^2 - \sum_{i=1}^N m_i h_i^2, \quad \text{if } 1 \leq \frac{h}{\varphi} < 2.$$

Let \hat{i} and \hat{k} be the unit vectors along the spacecraft-fixed longitudinal and transverse axes, respectively, and denote by (x, z) the inertial position of the center of

the fuel tank. The position vector of the center of mass of the vehicle can then be expressed in the spacecraft-fixed coordinate frame as

$$\vec{r} = (x - b)\hat{i} + z\hat{k}.$$

The inertial velocity and acceleration of the vehicle can be computed as

$$\begin{aligned}\dot{\vec{r}} &= v_x\hat{i} + (v_z + b\dot{\theta})\hat{k}, \\ \ddot{\vec{r}} &= (a_x + b\dot{\theta}^2)\hat{i} + (a_z + b\ddot{\theta})\hat{k},\end{aligned}$$

where we have used the fact that $(v_x, v_z) = (\dot{x} + z\dot{\theta}, \dot{z} - x\dot{\theta})$ and $(a_x, a_z) = (\dot{v}_x + v_z\dot{\theta}, \dot{v}_z - v_x\dot{\theta})$

Similarly, the position vectors of the fuel masses $m_0, m_i, \forall i$, in the spacecraft-fixed coordinate frame are given, respectively, by

$$\begin{aligned}\vec{r}_0 &= (x + h_0)\hat{i} + z\hat{k}, \\ \vec{r}_i &= (x + h_i)\hat{i} + (z + s_i)\hat{k}, \quad \forall i.\end{aligned}$$

The inertial accelerations of the fuel masses can be computed as

$$\begin{aligned}\ddot{\vec{r}}_0 &= (a_x - h_0\dot{\theta}^2 + \ddot{h}_0)\hat{i} + (a_z - 2\dot{h}_0\dot{\theta} - h_0\ddot{\theta})\hat{k}, \\ \ddot{\vec{r}}_i &= (a_x + s_i\ddot{\theta} - h_i\dot{\theta}^2 + \ddot{h}_i + 2\dot{s}_i\dot{\theta})\hat{i} + (a_z + \ddot{s}_i - h_i\ddot{\theta} - s_i\dot{\theta}^2 - 2\dot{h}_i\dot{\theta})\hat{k}, \quad \forall i.\end{aligned}$$

Now Newton's second law for the whole system can be written as

$$\vec{F} = m\ddot{\vec{r}} + \sum_{i=0}^N m_i\ddot{\vec{r}}_i, \quad (6.50)$$

where

$$\vec{F} = F(\hat{i} \cos \delta + \hat{k} \sin \delta).$$

The total torque with respect to the tank center can be expressed as

$$\vec{\tau} = (I + I_0)\ddot{\theta}\hat{j} + \vec{\rho} \times m\ddot{\vec{r}} + \sum_{i=0}^N \vec{\rho}_i \times m_i\ddot{\vec{r}}_i, \quad (6.51)$$

where

$$\vec{\tau} = \tau\hat{j} = [M + F(b + d)\sin \delta]\hat{j},$$

and $\vec{\rho}$, $\vec{\rho}_0$, and $\vec{\rho}_i$ are the positions of m , m_0 , and m_i relative to the tank center, respectively, i.e.,

$$\vec{\rho} = -b\hat{i}, \quad \vec{\rho}_0 = h_0\hat{i}, \quad \vec{\rho}_i = h_i\hat{i} + s_i\hat{k}, \quad \forall i.$$

The dissipative effects due to fuel slosh are included via damping constants c_i . When the damping is small, it can be represented accurately by equivalent linear viscous damping. Newton's second law for the fuel mass m_i can be written as

$$m_i a_{z_i} = -c_i \dot{s}_i - k_i s_i, \quad (6.52)$$

where

$$a_{z_i} = \ddot{s}_i + a_z - h_i \ddot{\theta} - s_i \dot{\theta}^2 - 2\dot{h}_i \dot{\theta}.$$

Using (6.50)-(6.52), the equations of motion can be obtained as

$$(m + m_f) a_x + mb\dot{\theta}^2 + \sum_{i=1}^N m_i (s_i \ddot{\theta} + 2\dot{s}_i \dot{\theta} + \ddot{h}_i) + m_0 \ddot{h}_0 = F \cos \delta, \quad (6.53)$$

$$(m + m_f) a_z + mb\ddot{\theta} + \sum_{i=1}^N m_i (\ddot{s}_i - s_i \dot{\theta}^2 - 2\dot{h}_i \dot{\theta}) - 2m_0 \dot{h}_0 \dot{\theta} = F \sin \delta, \quad (6.54)$$

$$\bar{I} \ddot{\theta} + \sum_{i=1}^N m_i \left(s_i a_x - h_i \ddot{s}_i + 2(s_i \dot{s}_i + h_i \dot{h}_i) \dot{\theta} + s_i \ddot{h}_i \right) + 2m_0 h_0 \dot{h}_0 \dot{\theta} + mba_z = \tau, \quad (6.55)$$

$$m_i (\ddot{s}_i + a_z - h_i \ddot{\theta} - s_i \dot{\theta}^2 - 2\dot{h}_i \dot{\theta}) + k_i s_i + c_i \dot{s}_i = 0, \quad \forall i, \quad (6.56)$$

where $p = b + d$ and

$$\bar{I} = I + I_0 + mb^2 + m_0 h_0^2 + \sum_{i=1}^N m_i (h_i^2 + s_i^2).$$

Note that equations (6.56) represent N nonintegrable second-order relations and hence they can be written as second order nonholonomic constraints.

The control objective is again to design feedback controllers so that the controlled spacecraft accomplishes a given planar maneuver, that is a change in the translational velocity vector and the attitude of the spacecraft, while suppressing the fuel slosh modes.

6.1.2.2 Feedback Control Laws

This section presents a detailed development of feedback control laws through the model obtained via the multi-mass-spring analogy.

Consider the model of a spacecraft with a gimballed thrust engine shown in Fig. 6.1. If the thrust F during the fuel burn is a positive constant, and if the gimbal deflection angle and pitching moment are zero, $\delta = M = 0$, then the spacecraft and fuel slosh dynamics have a relative equilibrium defined by

$$v_z = \bar{v}_z, \quad \theta = \bar{\theta}, \quad \dot{\theta} = 0, \quad s_i = 0, \quad \dot{s}_i = 0, \quad \forall i,$$

where \bar{v}_z and $\bar{\theta}$ are arbitrary constants. Without loss of generality, the subsequent analysis considers the relative equilibrium at the origin, i.e., $\bar{v}_z = \bar{\theta} = 0$. Note that the relative equilibrium corresponds to the vehicle axial velocity

$$v_x(t) = v_{x_0} + \bar{a}_x t, \quad t \leq t_b,$$

where v_{x_0} is the initial axial velocity of the spacecraft, t_b is the fuel burn time, and

$$\bar{a}_x = \frac{F}{m + m_f}.$$

Note that after the burnout v_x becomes a constant and thus it is bounded $\forall t$.

Now assume the axial acceleration term a_x is not significantly affected by small gimbal deflections, pitch changes and fuel motion (an assumption verified in simulations). Consequently, equation (6.53) becomes:

$$\dot{v}_x + \dot{\theta} v_z = \bar{a}_x. \quad (6.57)$$

Substituting this approximation leads to the following reduced equations of motion for the transverse, pitch and slosh dynamics:

$$(m + m_f)\bar{a}_z + mb\ddot{\theta} + \sum_{i=1}^N m_i(\ddot{s}_i - s_i\dot{\theta}^2 - 2\dot{h}_i\dot{\theta}) - 2m_0\dot{h}_0\dot{\theta} = F \sin \delta, \quad (6.58)$$

$$\bar{I}\ddot{\theta} + \sum_{i=1}^N m_i \left[\bar{a}_x s_i - h_i \ddot{s}_i + s_i \ddot{h}_i + 2(s_i \dot{s}_i + h_i \dot{h}_i) \dot{\theta} \right] + 2m_0 h_0 \dot{h}_0 \dot{\theta} + mb\bar{a}_z = \tau, \quad (6.59)$$

$$m_i(\ddot{s}_i + \bar{a}_z - h_i \ddot{\theta} - s_i \dot{\theta}^2 - 2\dot{h}_i \dot{\theta}) + k_i s_i + c_i \dot{s}_i = 0, \quad \forall i, \quad (6.60)$$

where $\bar{a}_z = \dot{v}_z - \dot{\theta} v_x(t)$. Here $v_x(t)$ is considered as an exogenous input. The subsequent analysis is based on the above equations of motion for the transverse, pitch and slosh dynamics of the vehicle.

Eliminating \ddot{s}_i in (6.58) and (6.59) using (6.60) yields

$$(m + m_0)\bar{a}_z + (mb - m_0 h_0)\ddot{\theta} - 2m_0 \dot{h}_0 \dot{\theta} - \sum_{i=1}^N (k_i s_i + c_i \dot{s}_i) = F \sin \delta, \quad (6.61)$$

$$(mb - m_0 h_0)\bar{a}_z + (\bar{I} - \sum_{i=1}^N m_i h_i^2)\ddot{\theta} + 2m_0 h_0 \dot{h}_0 \dot{\theta} + G = M + F p \sin \delta, \quad (6.62)$$

where

$$G = \sum_{i=1}^N \left[(m_i \bar{a}_x + m_i \ddot{h}_i + k_i h_i) s_i + h_i c_i \dot{s}_i + 2m_i s_i \dot{s}_i \dot{\theta} - m_i h_i s_i \dot{\theta}^2 \right].$$

Note that the expressions (6.4) and (6.5) have been utilized to obtain equations (6.61) and (6.62) in the form above.

By defining control transformations from (δ, M) to new control inputs (u_1, u_2) :

$$\begin{bmatrix} u_1 \\ u_2 \end{bmatrix} = \begin{bmatrix} m + m_0 & mb - m_0 h_0 \\ mb - m_0 h_0 & \bar{I} - \sum_{i=1}^N m_i h_i^2 \end{bmatrix}^{-1} \begin{bmatrix} F \sin \delta + 2m_0 \dot{h}_0 \dot{\theta} + \sum_{i=1}^N (k_i s_i + c_i \dot{s}_i) \\ M + Fp \sin \delta - 2m_0 h_0 \dot{h}_0 \dot{\theta} - G \end{bmatrix},$$

the system (6.58)-(6.60) can be written as:

$$\dot{v}_z = u_1 + \dot{\theta} v_x(t), \quad (6.63)$$

$$\ddot{\theta} = u_2, \quad (6.64)$$

$$\ddot{s}_i = -\omega_i^2 s_i - 2\zeta_i \omega_i \dot{s}_i - u_1 + h_i u_2 + s_i \dot{\theta}^2 + 2\dot{h}_i \dot{\theta}, \quad \forall i, \quad (6.65)$$

where

$$\omega_i^2 = \frac{k_i}{m_i}, \quad 2\zeta_i \omega_i = \frac{c_i}{m_i}, \quad \forall i.$$

Here ω_i and ζ_i , $\forall i$, denote the undamped natural frequencies and damping ratios, respectively.

The main idea in the subsequent development is to first design feedback control laws for (u_1, u_2) and then use the following equations to obtain the feedback laws for the original controls (δ, M) for $t \leq t_b$:

$$\delta = \sin^{-1} \left([(m + m_0)u_1 + (mb - m_0 h_0)u_2 - 2m_0 \dot{h}_0 \dot{\theta} - \sum_{i=1}^N (k_i s_i + c_i \dot{s}_i)] / F \right), \quad (6.66)$$

$$M = (mb - m_0 h_0)u_1 + (\bar{I} - \sum_{i=1}^N m_i h_i^2)u_2 + 2m_0 h_0 \dot{h}_0 \dot{\theta} + G - Fp \sin \delta. \quad (6.67)$$

Consider the following candidate Lyapunov function to stabilize the subsystem defined by the equations (6.63) and (6.64):

$$V = \frac{r_1}{2} v_z^2 + \frac{r_2}{2} \theta^2 + \frac{r_3}{2} \dot{\theta}^2,$$

where r_1 , r_2 , and r_3 are positive constants so that the function V is positive definite.

The time derivative of V along the trajectories of (6.63) and (6.64) can be computed as

$$\dot{V} = r_1 v_z \dot{v}_z + r_2 \theta \dot{\theta} + r_3 \dot{\theta} \ddot{\theta},$$

or rewritten in terms of the new control inputs

$$\dot{V} = (r_1 v_z) u_1 + (r_1 v_x v_z + r_2 \theta + r_3 u_2) \dot{\theta}.$$

Clearly, the feedback laws

$$u_1 = -l_1 v_z, \quad (6.68)$$

$$u_2 = -\frac{1}{r_3} \left(r_2 \theta + l_2 \dot{\theta} \right), \quad (6.69)$$

where l_1, l_2 are positive constants and taking into account that

$$r_1 v_x v_z \dot{\theta} \leq \left(\frac{\dot{\theta}^2}{2} + \frac{(r_1 v_x v_z)^2}{2} \right),$$

yield

$$\dot{V} = -l_1 r_1 v_z^2 - l_2 \dot{\theta}^2 + r_1 v_x v_z \dot{\theta} \leq -r_1 \left(l_1 - \frac{r_1 v_x^2}{2} \right) v_z^2 - \left(l_2 - \frac{1}{2} \right) \dot{\theta}^2.$$

which satisfies $\dot{V} \leq 0$ if $l_1 > 0.5 r_1 v_x^2$ and $l_2 > 0.5$, where v_x is bounded at any time t .

The closed-loop system for (v_z, θ) -dynamics can be written as

$$\dot{v}_z = -l_1 v_z + \dot{\theta} v_x(t), \quad (6.70)$$

$$\ddot{\theta} = -K_1 \theta - K_2 \dot{\theta}, \quad (6.71)$$

where $K_1 = r_2/r_3$ and $K_2 = l_2/r_3$.

Equation (6.71) can be easily solved in the case of $K_2^2 > 4K_1$ as

$$\theta(t) = A e^{-\lambda_1 t} + B e^{-\lambda_2 t},$$

where A, B are integration constants and $-\lambda_1, -\lambda_2$ are the eigenvalues of the linear system (6.71). Therefore, $\theta(t)$ and $\dot{\theta}(t)$ can be upper bounded as

$$|\theta(t)| \leq C e^{-\lambda t}, \quad |\dot{\theta}(t)| \leq D e^{-\lambda t},$$

respectively, where C, D are positive constants and $\lambda = \min(\lambda_1, \lambda_2)$. Now, assuming that $\lambda \neq l_1$, equation (6.70) can be integrated to obtain an upper bound for $v_z(t)$ as:

$$|v_z(t)| \leq \alpha e^{-\beta t},$$

where α, β are positive constants. Therefore, it can be concluded that the (v_z, θ) -dynamics are exponentially stable under the control laws (6.68) and (6.69).

To analyze the stability of the N equations defined by (6.65), it will be first shown that the system described by the equation

$$\ddot{s}_i + 2\zeta_i \omega_i(t) \dot{s}_i + \omega_i^2(t) s_i = 0, \quad (6.72)$$

is exponentially stable.

From equations (6.47) and (6.49)

$$\omega_i(t) = \sqrt{\frac{2g\xi_i}{\varphi} \tanh\left(\frac{2\xi_i h(t)}{\varphi}\right)} \in C^1.$$

The following properties can be shown to hold:

$$\begin{aligned} \omega_i^2(t) &\geq \varepsilon_1^2, \quad p(t) = \frac{1}{2} \frac{\dot{\omega}_i(t)}{\omega_i(t)} + 2\zeta_i \omega_i(t) \geq \varepsilon_2^2, \\ |2\zeta_i \omega_i(t)| &\leq 2\zeta_i \sqrt{\frac{2g\xi_i}{\varphi}} = M_1, \quad |\omega_i^2(t)| \leq \frac{2g\xi_i}{\varphi} = M_2, \\ |2\dot{\omega}_i(t) \omega_i(t)| &\leq g \left(\frac{2\xi_i}{\varphi}\right)^2 = M_3, \end{aligned}$$

where ε_1 and ε_2 are small positive parameters given the fact that the tank will never be totally empty, but a small amount of fuel will always remain inside. For this same reason $h(t) > 0$, $\forall t$. Therefore, by Corollary A.1 (see Appendix), the system (6.72) is exponentially stable.

Now write equation (6.65) as

$$\dot{x} = (A_1(t) + A_2(t))x + H(t), \tag{6.73}$$

where $x = [s_i, \dot{s}_i]'$ and

$$\begin{aligned} A_1(t) &= \begin{bmatrix} 0 & 1 \\ -\omega_i^2(t) & -2\zeta_i \omega_i(t) \end{bmatrix}, \quad A_2(t) = \begin{bmatrix} 0 & 0 \\ \dot{\theta}^2(t) & 0 \end{bmatrix}, \\ H(t) &= \begin{bmatrix} 0 \\ -\bar{a}_z(t) + h_i(t)\ddot{\theta}(t) + 2\dot{h}_i(t)\dot{\theta}(t) \end{bmatrix}. \end{aligned}$$

Under the stated assumptions, $A_1(t)$ is exponentially stable and there exist positive constants λ_0 , λ_1 and λ_2 such that

$$\int_0^\infty \|A_2(t)\| dt \leq \lambda_0, \quad \|H(t)\| \leq \lambda_1 e^{-\lambda_2 t}, \quad \forall t \geq 0.$$

Hence, for any initial condition the state of the system (6.58)-(6.60) converges exponentially to zero since the conditions in Lemma A.1 are satisfied.

6.1.2.3 Simulations

The feedback control law developed in the previous section is implemented here for the fourth stage of the European launcher Vega. The first two slosh modes are

6.1 Control of Space Vehicles with Fuel Slosh Dynamics

Table 6.3: Physical parameters for a spacecraft (time-varying slosh parameters).

Parameter	Value	Parameter	Value
F	2450 N	b	-0.6 m
m	975 kg	d	1.2 m
m_{ini}	580 kg	φ	1 m
I	$400 \text{ kg} \cdot \text{m}^2$	t_b	650 s
ρ	1180 kg/m^3	t_f	667 s

included to demonstrate the effectiveness of the controller (6.66)-(6.69) by applying to the complete nonlinear system (6.53)-(6.56). The physical parameters used in the simulations are given in Table 6.3.

We consider stabilization of the spacecraft in orbital transfer, suppressing the transverse and pitching motion of the spacecraft and sloshing of fuel while the spacecraft is accelerating. In other words, the control objective is to attract the relative equilibrium corresponding to a specific spacecraft axial acceleration and $v_z = \theta = \dot{\theta} = s_i = \dot{s}_i = 0$, $i = 1, 2$.

Time responses shown in Figs. 6.9-6.11. correspond to the initial conditions $v_{x_0} = 3000 \text{ m/s}$, $v_{z_0} = 100 \text{ m/s}$, $\theta_0 = 5^\circ$, $\dot{\theta}_0 = 0$, $s_{1_0} = 0.1 \text{ m}$, $s_{2_0} = -0.1 \text{ m}$, and $\dot{s}_{1_0} = \dot{s}_{2_0} = 0$. We assume a fuel burn time of 650 s. As can be seen, the transverse velocity, attitude angle, and the slosh states converge to the relative equilibrium at zero while the axial velocity v_x increases and \dot{v}_x tends asymptotically to $F/(m + m_f)$. Note that there is a trade-off between good responses for the directly actuated degrees of freedom (the transverse and pitch dynamics) and good responses for the internal degrees of freedom (the slosh dynamics); the controller given by (6.66)-(6.69) with parameters $r_1 = 8 \times 10^{-7}$, $r_2 = 1000$, $r_3 = 500$, $l_1 = 10^4$, $l_2 = 4 \times 10^4$ represents one example of this balance.

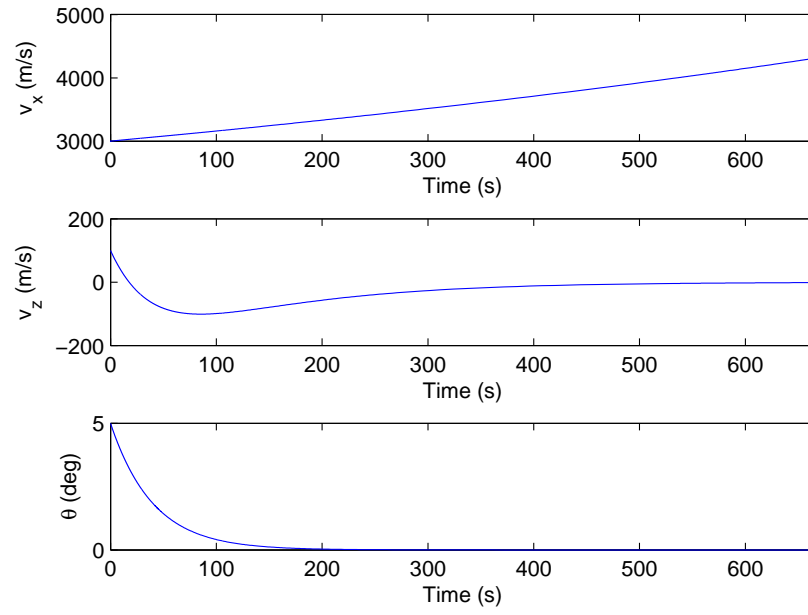


Figure 6.9: Time responses of v_x , v_z and θ .

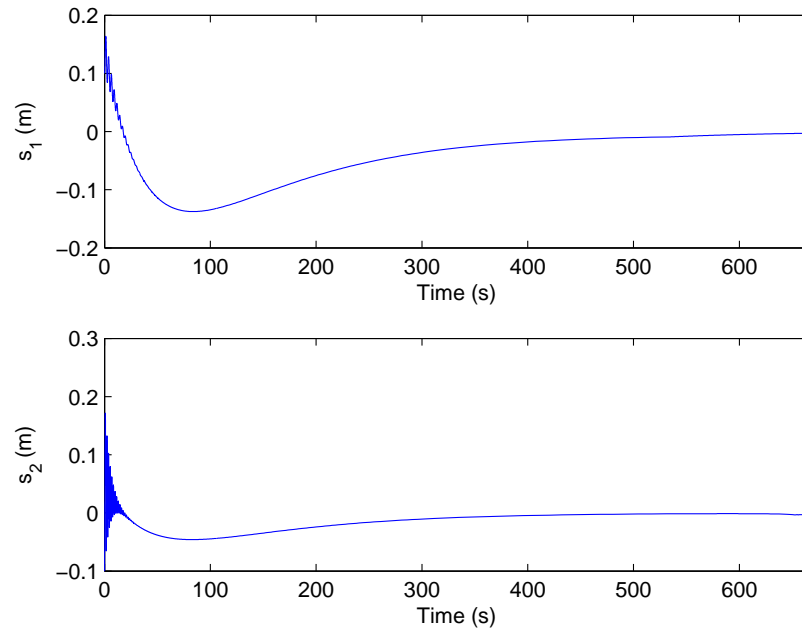


Figure 6.10: Time responses of s_1 and s_2 .

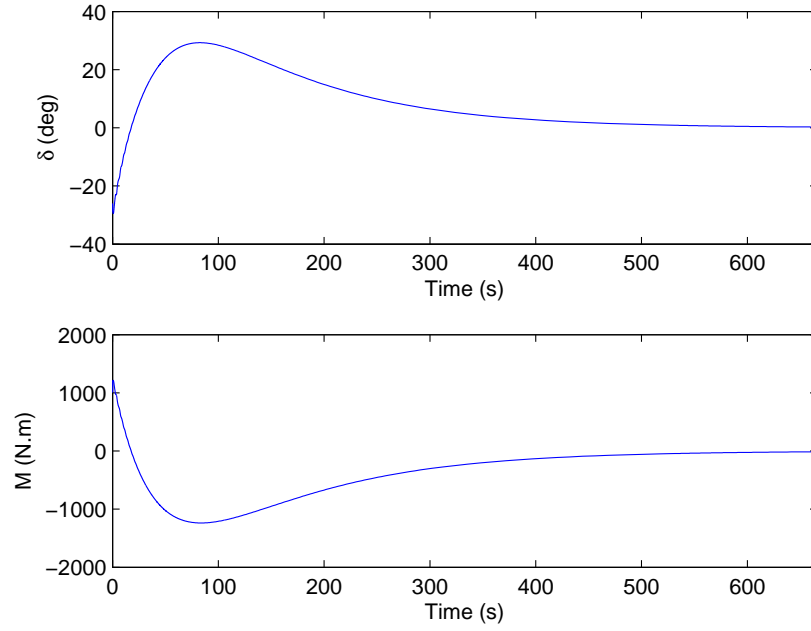


Figure 6.11: Gimbal deflection angle δ and pitching moment M .

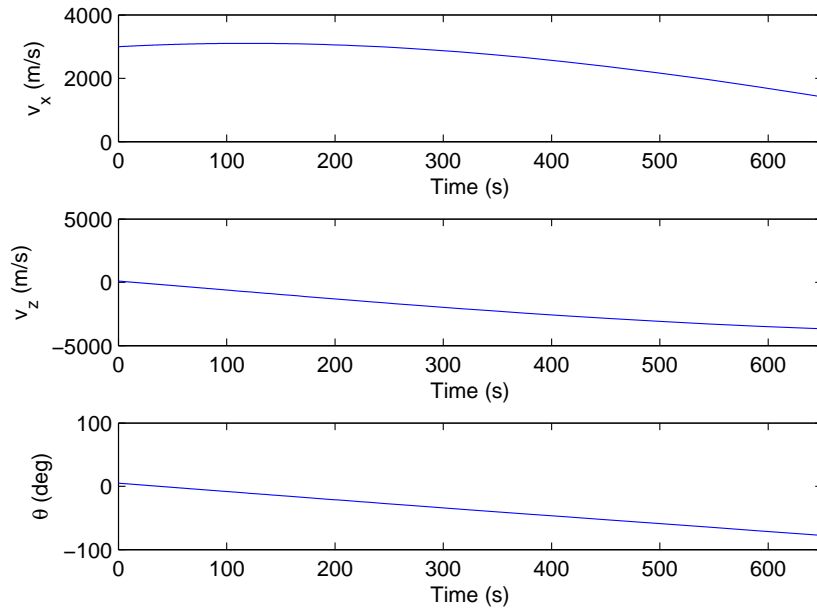


Figure 6.12: Time responses of v_x , v_z and θ (zero control case).

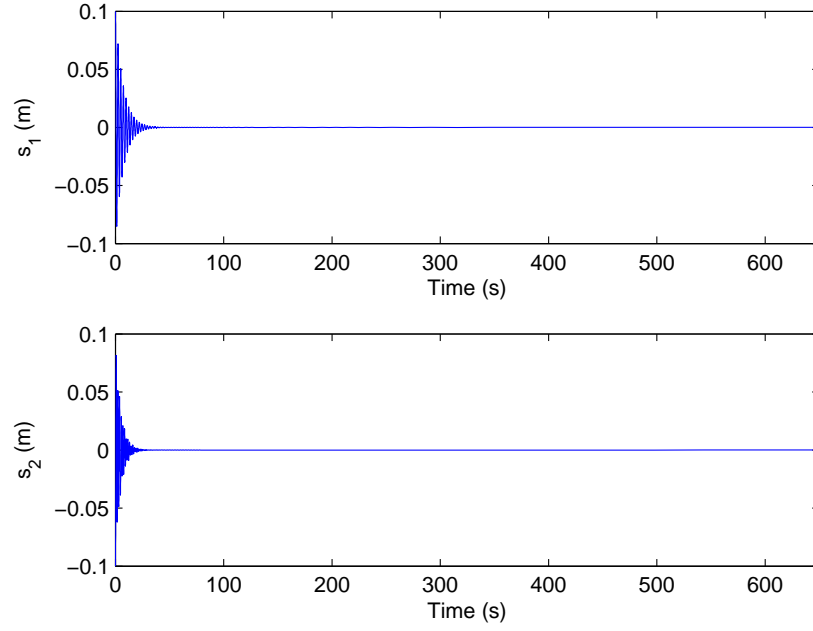


Figure 6.13: Time responses of s_1 and s_2 (zero control case).

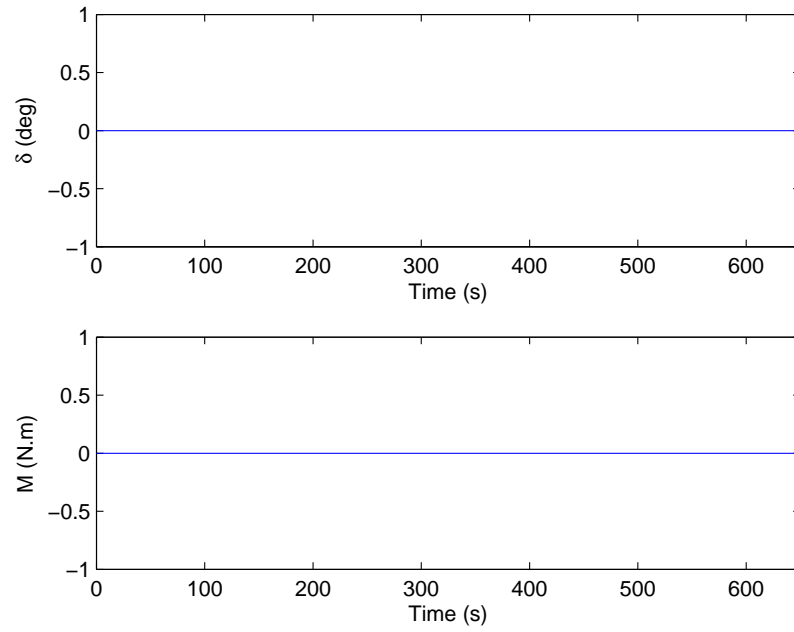


Figure 6.14: Gimbal deflection angle δ and pitching moment M (zero control case).

6.1.3 Thrust-Vector Control of a Three-Axis Stabilized Spacecraft with Fuel Slosh Dynamics

This section formulates the dynamics of a three-axis stabilized spacecraft with a single fuel tank and model the sloshing propellant as a multi-mass-spring system. The equations of motion are expressed in terms of the three dimensional spacecraft translational velocity vector, the attitude, the angular velocity, and the internal (shape) coordinates representing the slosh modes. A Lyapunov-based nonlinear feedback control law is proposed to control the translational velocity vector and the attitude of the spacecraft, while attenuating the sloshing modes characterizing the internal dynamics. A simulation example is included to illustrate the effectiveness of the control law.

6.1.3.1 Model Formulation

This section formulates the dynamics of a three-axis stabilized spacecraft with a single propellant tank including the prominent fuel slosh modes. The spacecraft is represented as a rigid body (base body) and the sloshing fuel masses as internal bodies.

We now derive a multi-mass-spring model of the sloshing fuel where the oscillation frequencies of the mass-spring elements represent the prominent sloshing modes (see e.g., Reyhanoglu and Rubio Hervas (2011b, 2012b); Rubio Hervas and Reyhanoglu (2012a,b)). Consider a rigid spacecraft moving in a three-dimensional space as shown in Fig. 6.15, where F denotes the constant thrust produced by a gimballed thrust engine. The gimbal deflection angles δ_1 and δ_2 about the spacecraft fixed y -axis and z -axis, respectively, are considered as control inputs. The input torque $M = [M_x, M_y, M_z]'$, generated by gas jet pairs or control moment gyroscopes, is also available for control purposes. For simplicity, xyz axes are assumed to be principal axes. The fluid is modeled by moment of inertia I_0 assigned to a rigidly attached isoinertial mass m_0 and point masses m_i , $i = 1, \dots, N$, whose relative positions along the spacecraft fixed y and z -axis are denoted by ξ_i and η_i , respectively. Moments of inertia of these masses are taken as zero. The locations h_0 and h_i are referenced to the center of mass of undisturbed propellant. Restoring forces $-k_{y_i}\xi_i$ and $-k_{z_i}\eta_i$ act on the mass m_i whenever the mass is displaced from its neutral position $\xi_i = 0$ and $\eta_i = 0$, respectively. Damping constants c_{y_i} and c_{z_i} characterize the dissipative effects of the fuel slosh. In this dissertation, for simplicity it is assumed that $k_{y_i} = k_{z_i} = k_i$

and $c_{y_i} = c_{z_i} = c_i$. The spacecraft mass m , moments of inertia (J_x, J_y, J_z) , the fuel masses (m_0, m_i) , the distance b between the origin of body xyz axes and the spacecraft center of mass location along the longitudinal axis, and the distance d from the gimbal pivot to the spacecraft center of mass are assumed to be constant. If the tank center is in front of the spacecraft center of mass then $b > 0$. The parameters m_i, h_i, k_i, c_i and b depend on the shape of the fuel tank, the characteristics of the fuel and the fill ratio of the fuel tank. To preserve the static properties of the liquid, the sum of all the masses must be the same as the fuel mass m_f , and the center of mass of the model must be at the same elevation as that of the fuel; i.e., equations (6.4) and (6.5) are satisfied.

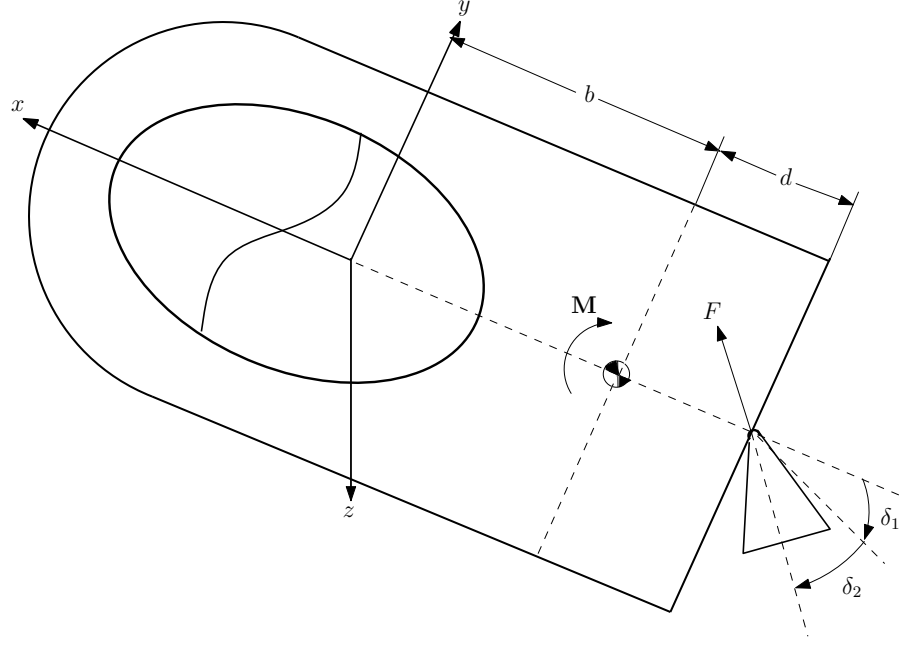


Figure 6.15: A spacecraft with a liquid propellant tank.

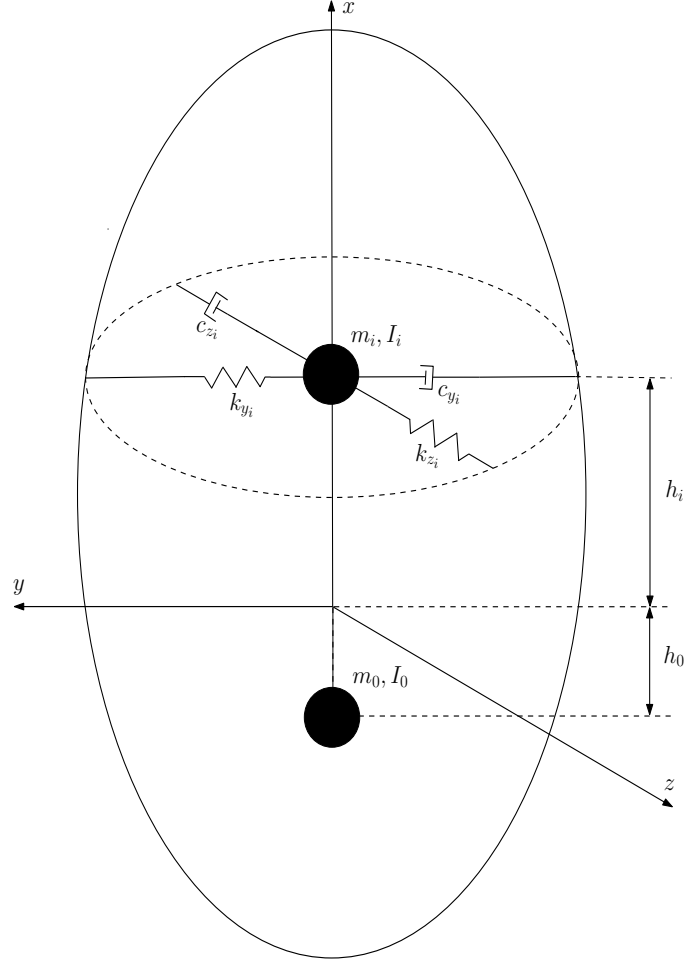


Figure 6.16: A multi mass-spring model of sloshing.

Denote by

$$r = [x, y, z]'$$

the inertial position of the center of mass of the undisturbed fuel in the spacecraft-fixed coordinate frame. The position vectors of the center of mass of the vehicle and the fuel masses $m_0, m_i, \forall i$, in the spacecraft-fixed coordinate frame are then given, respectively, by

$$\begin{aligned} r_c &= [(x - b), y, z]', \\ r_0 &= [x + h_0, y, z]', \\ r_i &= [x + h_i, y + \xi_i, z + \eta_i]', \forall i. \end{aligned}$$

Clearly, the inertial velocity of the center of mass of the undisturbed fuel can be expressed as

$$v = \dot{r} + \omega \times r,$$

where $\omega = [\omega_x, \omega_y, \omega_z]'$ is the angular velocity vector. The inertial velocities v_c , v_0 , and v_i , $\forall i$, can be computed similarly.

The total kinetic energy neglecting the moment of inertia of the sloshing masses, can now be expressed as

$$T = \frac{1}{2}m\|v_c\|^2 + \frac{1}{2}\sum_{j=0}^N m_j\|v_j\|^2 + \frac{1}{2}\omega'(J + J_0)\omega,$$

where $J = \text{diag}\{J_x, J_y, J_z\}$ and $J_0 = \text{diag}\{I_0, I_0, I_0\}$.

Since gravitational effects are ignored, there is no gravitational potential energy. The acceleration of the rocket gives rise to the elastic potential energy given by

$$U = \frac{1}{2}\sum_{i=1}^N k_i(\xi_i^2 + \eta_i^2).$$

Typically, k_i would be a function of the axial acceleration. However, in this section it is assumed that the axial acceleration is not significantly affected by small gimbal deflections, attitude changes and fuel motion so that k_i remains constant.

Dissipative effects due to fuel slosh are included via damping constants c_i so that the Rayleigh dissipation function R can be expressed as

$$R = \frac{1}{2}\sum_{i=1}^N c_i(\dot{\xi}_i^2 + \dot{\eta}_i^2).$$

Applying equations (6.1)-(6.3) with $L = T - U$ and

$$s = \begin{bmatrix} \xi \\ \eta \end{bmatrix}, \quad v = \begin{bmatrix} v_x \\ v_y \\ v_z \end{bmatrix}, \quad \tau_t = \begin{bmatrix} F \cos \delta_1 \cos \delta_2 \\ F \sin \delta_2 \\ -F \sin \delta_1 \cos \delta_2 \end{bmatrix},$$

$$\omega = \begin{bmatrix} \omega_x \\ \omega_y \\ \omega_z \end{bmatrix}, \quad \tau_r = \begin{bmatrix} M_x \\ M_y - Fp \sin \delta_1 \cos \delta_2 \\ M_z - Fp \sin \delta_2 \end{bmatrix},$$

where $p = b + d$, the equations of motion can be obtained as

$$(m+m_f)a_x + mb(\omega_y^2 + \omega_z^2) + \sum_{i=1}^N m_i [2\omega_y \dot{\eta}_i - 2\omega_z \dot{\xi}_i + \eta_i(\dot{\omega}_y + \omega_x \omega_z) - \xi_i(\dot{\omega}_z - \omega_x \omega_y)] = F \cos \delta_1 \cos \delta_2, \quad (6.74)$$

$$(m+m_f)a_y - mb(\dot{\omega}_z + \omega_x \omega_y) + \sum_{i=1}^N m_i [\ddot{\xi}_i - 2\omega_x \dot{\eta}_i - \eta_i(\dot{\omega}_x - \omega_y \omega_z) - \xi_i(\omega_x^2 + \omega_z^2)] = F \sin \delta_2, \quad (6.75)$$

$$(m+m_f)a_z + mb(\dot{\omega}_y - \omega_x \omega_z) + \sum_{i=1}^N m_i [\ddot{\eta}_i + 2\omega_x \dot{\xi}_i - \eta_i(\omega_x^2 + \omega_y^2) - \xi_i(\dot{\omega}_x + \omega_y \omega_z)] = -F \sin \delta_1 \cos \delta_2, \quad (6.76)$$

$$(I_0 + J_x)\dot{\omega}_x + (J_z - J_y)\omega_y \omega_z + \sum_{i=1}^N m_i [\xi_i \ddot{\eta}_i - \eta_i \ddot{\xi}_i - \eta_i(a_y - \eta_i(\dot{\omega}_x + \omega_y \omega_z) - h_i(\dot{\omega}_z + \omega_x \omega_y)) + 2(\eta_i \dot{\eta}_i + \xi_i \dot{\xi}_i)\omega_x + \xi_i(a_z + \xi_i(\dot{\omega}_x + \omega_y \omega_z) - h_i(\dot{\omega}_y + \omega_x \omega_z))] = M_x, \quad (6.77)$$

$$(I_0 + J_y + \bar{I})\dot{\omega}_y + (J_x - J_z - \bar{I})\omega_x \omega_z + mba_z + \sum_{i=1}^N m_i [-h_i \ddot{\eta}_i + 2\eta_i \dot{\eta}_i \omega_y - 2\dot{\xi}_i(\omega_z \eta_i + h_i \omega_x) + \eta_i(a_x + \eta_i(\dot{\omega}_y + \omega_x \omega_z) + h_i(\omega_x^2 - \omega_z^2)) - h_i \xi_i(\dot{\omega}_x + \omega_y \omega_z) - \eta_i \xi_i(\dot{\omega}_z - \omega_x \omega_y)] = M_y - Fp \sin \delta_1 \cos \delta_2, \quad (6.78)$$

$$(I_0 + J_z + \bar{I})\dot{\omega}_z + (J_y - J_x + \bar{I})\omega_x \omega_y - mba_y + \sum_{i=1}^N m_i [h_i \ddot{\xi}_i + 2\xi_i \dot{\xi}_i \omega_z - 2\dot{\eta}_i(\omega_y \xi_i + h_i \omega_x) - \xi_i(a_x - \xi_i(\dot{\omega}_z - \omega_x \omega_y) - h_i(\omega_y^2 - \omega_x^2)) - h_i \eta_i(\dot{\omega}_x - \omega_y \omega_z) - \eta_i \xi_i(\dot{\omega}_y + \omega_x \omega_z)] = M_z - Fp \sin \delta_2, \quad (6.79)$$

$$m_i[\ddot{\xi}_i + a_y - 2\dot{\eta}_i \omega_x - \eta_i(\dot{\omega}_x - \omega_y \omega_z) - \xi_i(\omega_x^2 + \omega_z^2) - h_i(\dot{\omega}_z - \omega_x \omega_y)] + k_i \xi_i + c_i \dot{\xi}_i = 0, \quad \forall i, \quad (6.80)$$

$$m_i[\ddot{\eta}_i + a_z + 2\dot{\xi}_i \omega_x + \xi_i(\dot{\omega}_x + \omega_y \omega_z) - \eta_i(\omega_x^2 + \omega_y^2) - h_i(\dot{\omega}_y - \omega_x \omega_z)] + k_i \eta_i + c_i \dot{\eta}_i = 0, \quad \forall i, \quad (6.81)$$

where $a = [a_x, a_y, a_z]'$ is the acceleration of the center of mass of the fuel in the spacecraft-fixed frame and

$$\bar{I} = mb^2 + m_0 h_0^2 + \sum_{i=1}^N m_i h_i^2.$$

Note that equations (6.80)-(6.81) represent $2N$ nonintegrable second-order relations and hence they can be viewed as second order nonholonomic constraints.

Let $\theta = [\theta_1, \theta_2, \theta_3]'$ denote the vector of Euler angles. Assuming 321 Euler angle sequence, the angular velocity can be expressed as

$$\omega = Q(\theta)\dot{\theta}, \quad (6.82)$$

where

$$Q(\theta) = \begin{bmatrix} 1 & 0 & -\sin \theta_2 \\ 0 & \cos \theta_1 & \sin \theta_1 \cos \theta_2 \\ 0 & -\sin \theta_1 & \cos \theta_1 \cos \theta_2 \end{bmatrix}.$$

The control objective is to design feedback controllers so that the controlled spacecraft accomplishes a given three-dimensional maneuver while suppressing the fuel slosh modes.

6.1.3.2 Feedback Control Laws

Consider the model of a spacecraft with a gimballed thrust engine shown in Fig. 6.15-6.16. If the thrust F during the fuel burn is a positive constant, and if the gimbal deflection angles and moments are zero, $\delta_1 = \delta_2 = M_x = M_y = M_z = 0$, then the spacecraft and fuel slosh dynamics have a relative equilibrium defined by

$$v_y = \bar{v}_y, \quad v_z = \bar{v}_z, \quad \theta = \bar{\theta}, \quad \dot{\theta} = 0, \quad s = \dot{s} = 0,$$

where \bar{v}_y , \bar{v}_z and $\bar{\theta}$, are arbitrary constants. Without loss of generality, the subsequent analysis considers the relative equilibrium at the origin, i.e., $\bar{v}_y = \bar{v}_z = \bar{\theta} = 0$. Note that the relative equilibrium corresponds to the vehicle axial velocity

$$v_x(t) = v_{x_0} + \bar{a}_x t, \quad t \leq t_b,$$

where v_{x_0} is the initial axial velocity of the spacecraft, t_b is the fuel burn time, and $\bar{a}_x = F/(m + m_f)$. Note that after the burnout v_x becomes a constant and thus it is bounded $\forall t$.

Now assume the axial acceleration term a_x is not significantly affected by small gimbal deflections, attitude changes and fuel motion (an assumption verified in simulations). Consequently, equation (6.74) becomes:

$$\dot{v}_x + \omega_2 v_z - \omega_3 v_y = \bar{a}_x. \tag{6.83}$$

Substituting this approximation into (6.75)-(6.81) leads to the following reduced equations of motion for the transverse, attitude and slosh dynamics, where $v_x(t)$ is considered as an exogenous input. The subsequent analysis is based on these equations of motion for the transverse, attitude and slosh dynamics of the vehicle.

We now design a nonlinear controller to stabilize the relative equilibrium at the origin of the equations (6.75)-(6.81). Our control design is based on a Lyapunov function approach. By defining control transformations from $(\delta_1, \delta_2, M_x, M_y, M_z)$ to

new control inputs $(u_1, u_2, u_3, u_4, u_5)$, the equations (6.75)-(6.81) can be written as:

$$\dot{v}_y = u_1 - v_x \omega_z + v_z \omega_x, \quad (6.84)$$

$$\dot{v}_z = u_2 + v_x \omega_y - v_y \omega_x, \quad (6.85)$$

$$\ddot{\theta}_1 = u_3, \quad (6.86)$$

$$\ddot{\theta}_2 = u_4, \quad (6.87)$$

$$\ddot{\theta}_3 = u_5, \quad (6.88)$$

$$\ddot{\xi}_i = -\Omega_i^2 \xi_i - 2\zeta_i \Omega_i \dot{\xi}_i - u_1 + 2\dot{\eta}_i \omega_x + \eta_i (\dot{\omega}_x - \omega_y \omega_z) + \xi_i (\omega_x^2 + \omega_z^2) + h_i (\dot{\omega}_z - \omega_x \omega_y), \quad (6.89)$$

$$\ddot{\eta}_i = -\Omega_i^2 \eta_i - 2\zeta_i \Omega_i \dot{\eta}_i - u_2 - 2\dot{\xi}_i \omega_x - \xi_i (\dot{\omega}_x + \omega_y \omega_z) + \eta_i (\omega_x^2 + \omega_y^2) + h_i (\dot{\omega}_y - \omega_x \omega_z), \quad (6.90)$$

where

$$\Omega_i^2 = \frac{k_i}{m_i}, \quad 2\zeta_i \Omega_i = \frac{c_i}{m_i}, \quad \forall i.$$

Here Ω_i and ζ_i , $\forall i$, denote the undamped natural frequencies and damping ratios, respectively.

Now, consider the following candidate Lyapunov function for the system (6.84)-(6.90):

$$\begin{aligned} V = & \frac{r_1}{2} v_y^2 + \frac{r_2}{2} v_z^2 + \frac{r_3}{2} \theta_1^2 + \frac{r_4}{2} \dot{\theta}_1^2 + \frac{r_5}{2} \theta_2^2 + \frac{r_6}{2} \dot{\theta}_2^2 + \frac{r_7}{2} \theta_3^2 \\ & + \frac{r_8}{2} \dot{\theta}_3^2 + \frac{r_9}{2} \sum_{i=1}^N (\dot{\xi}_i^2 + \Omega_i^2 \xi_i^2 - 2h_i \dot{\xi}_i \omega_z - 2\eta_i \dot{\xi}_i \omega_x) \\ & + \frac{r_{10}}{2} \sum_{i=1}^N (\dot{\eta}_i^2 + \Omega_i^2 \eta_i^2 - 2h_i \dot{\eta}_i \omega_y + 2\xi_i \dot{\eta}_i \omega_x), \end{aligned} \quad (6.91)$$

where r_i , $i = 1, \dots, 10$, are positive constants. Assume that $r_4 = r_6 = r_8 \gg 1 \gg r_9 = r_{10}$. Then it is easy to show that the function V is positive definite.

The time derivative of V along the trajectories of (6.84)-(6.90) is

$$\begin{aligned} \dot{V} = & -2r_9 \sum_{i=1}^N \zeta_i \Omega_i \dot{\xi}_i^2 - 2r_{10} \sum_{i=1}^N \zeta_i \Omega_i \dot{\eta}_i^2 + [r_1 v_y - r_9 \sum_{i=1}^N (\dot{\xi}_i - h_i \omega_z - \eta_i \omega_x)] u_1 \\ & + [r_2 v_z - r_{10} \sum_{i=1}^N (\dot{\eta}_i - h_i \omega_y + \xi_i \omega_x)] u_2 + \sum_{i=1}^3 (f_{i1} u_3 + f_{i2} u_4 + f_{i3} u_5 + g_i) \dot{\theta}_i, \end{aligned} \quad (6.92)$$

where f_{ij} , g_i , $i, j = 1, 2, 3$, are functions of v_y , v_z , θ , $\dot{\theta}$, s , and \dot{s} .

Assume $F = [f_{ij}]$ is a 3×3 invertible matrix $\forall t$. Then, the feedback laws

$$u_1 = -l_1[r_1 v_y - r_9 \sum_{i=1}^N (\dot{\xi}_i - h_i \omega_z - \eta_i \omega_x)], \quad (6.93)$$

$$u_2 = -l_2[r_2 v_z - r_{10} \sum_{i=1}^N (\dot{\eta}_i - h_i \omega_y + \xi_i \omega_x)], \quad (6.94)$$

$$\begin{bmatrix} u_3 \\ u_4 \\ u_5 \end{bmatrix} = -F^{-1} \begin{bmatrix} g_1 + l_3 \dot{\theta}_1 \\ g_2 + l_4 \dot{\theta}_2 \\ g_3 + l_5 \dot{\theta}_3 \end{bmatrix}, \quad (6.95)$$

where l_i , $i = 1, \dots, 5$, are positive constants, yield

$$\begin{aligned} \dot{V} = & -2r_9 \sum_{i=1}^N \zeta_i \Omega_i \dot{\xi}_i^2 - 2r_{10} \sum_{i=1}^N \zeta_i \Omega_i \dot{\eta}_i^2 - l_1 [r_1 v_y - r_9 \sum_{i=1}^N (\dot{\xi}_i - h_i \omega_z - \eta_i \omega_x)]^2 \\ & - l_2 [r_2 v_z - r_{10} \sum_{i=1}^N (\dot{\eta}_i - h_i \omega_y + \xi_i \omega_x)]^2 - l_3 \dot{\theta}_1^2 - l_4 \dot{\theta}_2^2 - l_5 \dot{\theta}_3^2, \end{aligned}$$

which satisfies $\dot{V} \leq 0$. Using Krasovski-LaSalle invariance principle, it is easy to prove the asymptotic stability of the origin of the closed loop defined by equations (6.84)-(6.90) and the feedback control laws (6.93)-(6.95). Note that the positive gains l_j , $j = 1, \dots, 5$, can be chosen arbitrarily to achieve good close loop responses.

Remark 6.4: *If we assume small Euler angles, the formulation above can be made more tractable. This assumption simplifies the form of the control laws (6.95) while still reflecting main features of the three-dimensional sloshing problem. In this case, $\omega = \dot{\theta}$, and f_{ij} , g_i , $i = 1, 2, 3$, take the following form:*

$$\begin{aligned} f_{11} &= r_4 - \sum_{i=1}^N (r_9 \eta_i^2 + r_{10} \xi_i^2), \quad f_{12} = f_{21} = r_{10} \sum_{i=1}^N h_i \xi_i, \\ f_{22} &= r_6 - r_{10} \sum_{i=1}^N h_i^2, \quad f_{13} = f_{31} = -r_9 \sum_{i=1}^N h_i \eta_i, \\ f_{33} &= r_8 - r_9 \sum_{i=1}^N h_i^2, \quad f_{23} = f_{32} = 0 \end{aligned}$$

$$\begin{aligned}
g_1 &= (r_1 - r_2)v_y v_z + r_3 \theta_1 + r_9 \sum_{i=1}^N [2\dot{\xi}_i \dot{\eta}_i + \dot{\theta}_1 \xi_i \dot{\xi}_i - \dot{\theta}_2 h_i \dot{\xi}_i - 2(h_i \dot{\theta}_3 + \dot{\theta}_1 \eta_i) \dot{\eta}_i \\
&\quad + \Omega_i^2 \xi_i \eta_i + 2\zeta_i \Omega_i \eta_i \dot{\xi}_i] - r_{10} \sum_{i=1}^N [2\dot{\xi}_i \dot{\eta}_i - \dot{\theta}_1 \eta_i \dot{\eta}_i + \dot{\theta}_3 h_i \dot{\eta}_i - 2(h_i \dot{\theta}_2 - \dot{\theta}_1 \xi_i) \dot{\xi}_i \\
&\quad + \Omega_i^2 \xi_i \eta_i + 2\zeta_i \Omega_i \xi_i \dot{\eta}_i], \\
g_2 &= r_2 v_x v_z + r_5 \theta_2 - r_{10} \sum_{i=1}^N (\dot{\theta}_3 \xi_i \dot{\eta}_i - \dot{\theta}_2 \eta_i \dot{\eta}_i - h_i \Omega_i^2 \eta_i - 2h_i \zeta_i \Omega_i \dot{\eta}_i) - r_9 \sum_{i=1}^N \dot{\theta}_3 \eta_i \dot{\xi}_i, \\
g_3 &= -r_1 v_x v_y + r_7 \theta_3 + r_9 \sum_{i=1}^N (\dot{\theta}_3 \xi_i \dot{\xi}_i + h_i \Omega_i^2 \xi_i + 2h_i \zeta_i \Omega_i \dot{\xi}_i).
\end{aligned}$$

6.1.3.3 Simulations

The feedback control laws developed in the previous section are implemented here for the AVUM upper stage spacecraft (Perez, 2006). The first two slosh modes are included to demonstrate the effectiveness of the control law. The physical parameters used in the simulation is given in Table 6.4. The fluid parameters are obtained using the formulae in Dodge (2000). The control objective is to stabilize the relative equilibrium corresponding to a constant axial spacecraft acceleration of 1.720 m/s^2 and $v_y = v_z = 0$, $\theta = \dot{\theta} = 0$, $s = \dot{s} = 0$.

It must be noted that for the AVUM spacecraft the characteristic length of the propellant tank can be taken as $\approx 0.375 \text{ m}$ and the propellant UMDH (Unsymmetrical Dimethyl Hydrazine) has a σ/ρ ratio of around $0.25 \times 10^{-4} \text{ m}^3/\text{s}^2$. Thus, accelerations that are larger than 0.1 m/s^2 correspond to a Bond number larger than 1000, which is clearly in the high-acceleration regime. The simulation indicates that during the main engine burn the vehicle acceleration exceeds 1 m/s^2 , and thus the mechanical-analogy model is valid.

The effectiveness of the Lyapunov-based control laws is demonstrated by applying the controller defined by (6.93)-(6.95) to the complete nonlinear system (6.74)-(6.82). Time responses shown in Figs. 6.17-6.22 correspond to the initial conditions

$$\begin{aligned}
v_0 &= [3000, 75, 25]' \text{ m/s}, \quad \theta_0 = [5^\circ, 2^\circ, -5^\circ]', \\
s_0 &= [0.15, 0.05, -0.1, 0.15]' \text{ m}, \quad \dot{\theta}_0 = 0, \quad \dot{s}_0 = 0.
\end{aligned}$$

As can be seen in the figures, the transverse velocities, attitude angles, and the slosh states converge to the relative equilibrium at zero while the axial velocity v_x

6.1 Control of Space Vehicles with Fuel Slosh Dynamics

Table 6.4: Physical parameters for a spacecraft (three-dimensional case).

Parameter	Value	Parameter	Value
m	975 kg	F	2450 N
J_x	600 kg · m ²	t_b	600 s
J_y	800 kg · m ²	b	−0.6 m
J_z	400 kg · m ²	d	1.2 m
m_0	358 kg	h_0	−0.011 m
m_1	89 kg	h_1	0.035 m
m_2	2.7 kg	h_2	0.291 m
I_0	14.85 kg · m ²	\bar{a}_x	1.720 m/s ²
k_1	750 kg/s ²	c_1	25.8 kg/s
k_2	65 kg/s ²	c_2	1.32 kg/s

increases and \dot{v}_x tends asymptotically to 1.720 m/s². Note that there is a trade-off between good responses for the directly actuated degrees of freedom (the transverse and attitude dynamics) and good responses for the unactuated degree of freedom (the slosh dynamics); the controller given by (6.93)-(6.95) with parameters $r_1 = r_2 = 8 \times 10^{-7}$, $r_3 = r_5 = r_7 = 1000$, $r_4 = r_6 = r_8 = 500$, $r_9 = r_{10} = 1 \times 10^{-5}$, $l_1 = l_2 = 1 \times 10^4$, $l_3 = l_4 = l_5 = 4 \times 10^4$ represents one example of this balance.

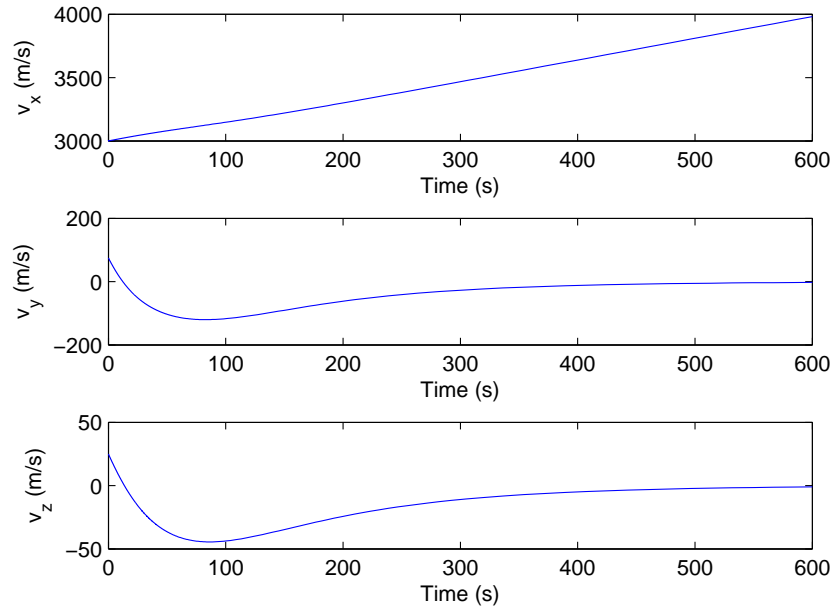


Figure 6.17: Time responses of v_x , v_y and v_z .

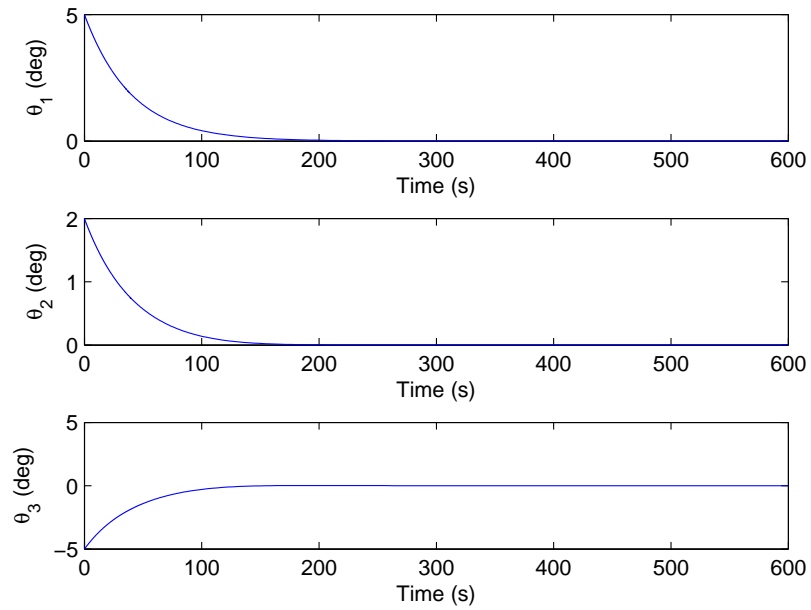


Figure 6.18: Time responses of θ_1 , θ_2 and θ_3 .

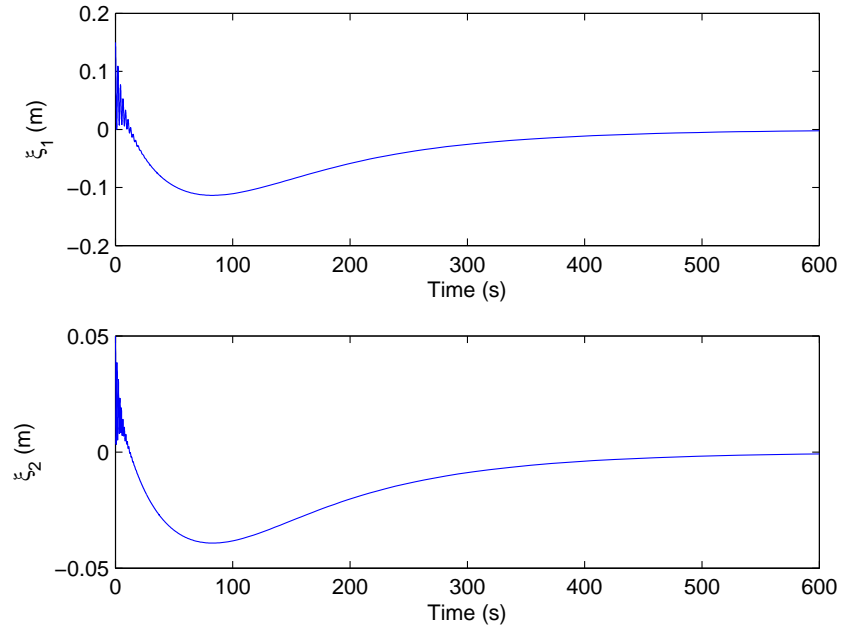


Figure 6.19: Time responses of ξ_1 and ξ_2 .

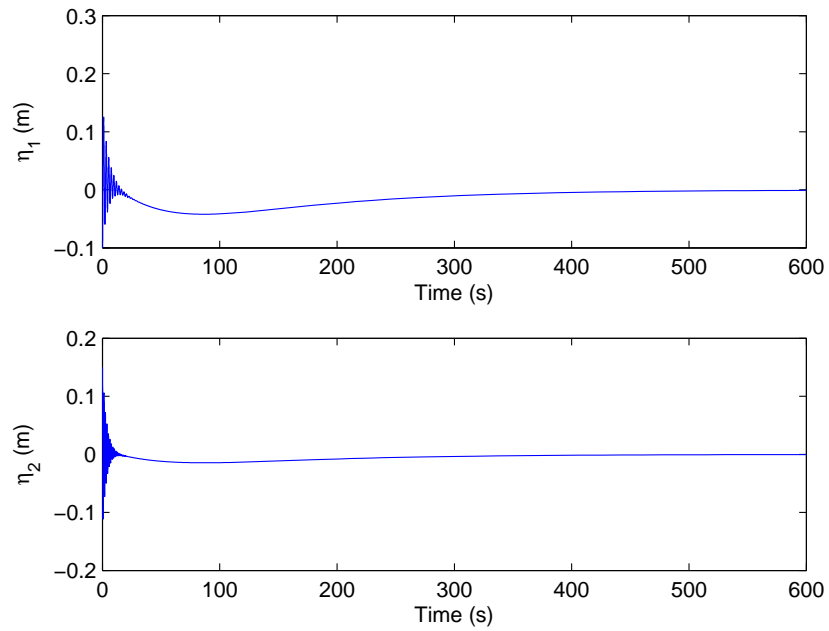


Figure 6.20: Time responses of η_1 and η_2 .

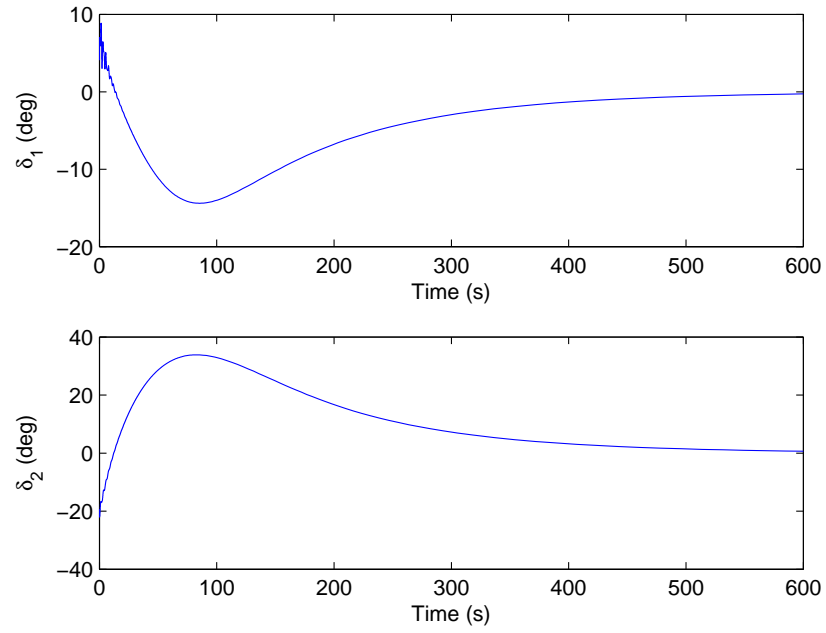


Figure 6.21: Gimbal deflection angles δ_1 and δ_2 .

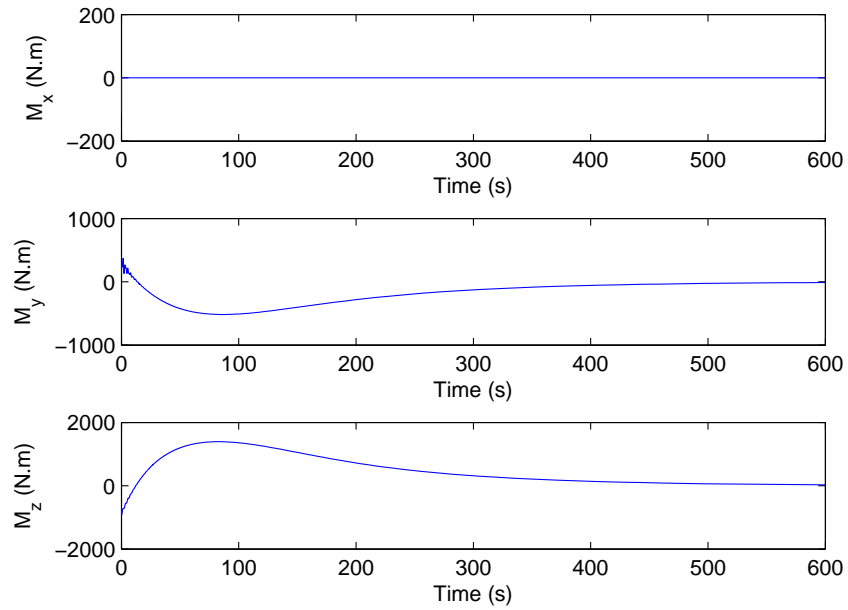


Figure 6.22: Control moments M_x , M_y and M_z .

6.2 Liquid Container Transfer via a PPR Robot

This section studies the point-to-point liquid container transfer control problem for a PPR robot, i.e., a robot with two prismatic and one revolute joint. The robot manipulator is represented as three rigid links, and the liquid slosh dynamics are included using a multi-mass-spring model. It is assumed that two forces and a torque applied to the prismatic joints and the revolute joint, respectively, are available as control inputs. The objective is to control the robot end-effector movement while suppressing the sloshing modes. A nonlinear mathematical model that reflects all of these assumptions is first introduced. Then, Lyapunov-based feedback controllers are designed to achieve the control objective. Two cases are considered: partial-state feedback that does not use slosh state information and full-state feedback that uses both robot state and slosh state measurements or estimations. Computer simulations are included to illustrate the effectiveness of the proposed control laws.

The active slosh control approaches developed for robotic systems moving liquid filled containers (Feddema et al., 1997; Gandhi and Duggal, 2009; Grundelius and Bernhardsson, 1999; Grundelius, 2000; Pridgen et al., 2010; Terashima and Schmidt, 1994; Yano et al., 2001a,b; Yano and Terashima, 2001) are mostly based on linear control design methods (Aboel-Hassan et al., 2009; Bryson, 1994; Sidi, 1997; Wie, 1998) and adaptive control methods (Adler et al., 1991). Most of the existing literature on the liquid slosh problem considers only the first sloshing mode represented by a single pendulum model or a single mass-spring model. The literature that incorporates more than one sloshing mode in modeling the slosh dynamics includes (Dodge, 2000; Reyhanoglu and Rubio Hervas, 2012a, 2013).

This section presents novel methods for the fast robotic delivery of an open container of liquid without residual end point sloshing. In particular, a planar Prismatic-Prismatic-Revolute (PPR) robot moving a liquid filled container is considered. The control inputs for the PPR robot are two forces and a torque applied to the prismatic joints and the revolute joint, respectively. The control objective is to control the robot movement while suppressing the sloshing modes. The main contributions in this section are (i) the development of a full nonlinear mathematical model of the coupled robot motion and slosh dynamics and (ii) the design of Lyapunov-based feedback controllers that achieve the control objective. Two cases are considered: partial-state feedback that does not use slosh state information and full-state feedback that uses both robot state and slosh state measurements or estimations. Simulation examples are included to illustrate the effectiveness of the controllers.

6.2.1 Model Formulation

This section formulates the dynamics of a PPR robot moving a liquid filled container including the prominent liquid slosh modes. In particular, the sloshing liquid is modeled as a multi-mass-spring system where the oscillation frequencies of the mass-spring elements represent the prominent sloshing modes.

Consider a planar PPR robot moving in a vertical plane as shown in Fig. 6.23, where (x, y) denotes the position of the revolute joint and θ the orientation of the third link. Let the forces F_x and F_y be the control inputs to the two prismatic joints and the torque τ_θ be the input to the revolute joint. The constants for the robot are the link masses M_1, M_2, M_3 ; the moment of inertia I_3 of the third link about its center of mass; the distance l between the revolute joint and the center of mass of the third link, and the distance b from the center of mass of the third link to the end-effector. As shown in Fig. 6.24, the liquid filled container is a cylinder of radius r and height h_c . The mass and moment of inertia of the container (with respect to its own center of mass) are denoted by m_c and I_c , respectively. The fluid is modeled by moment of inertia I_0 assigned to a rigidly attached mass m_0 and point masses m_i , $i = 1, \dots, N$, whose relative positions along the container-fixed lateral axis are denoted by s_i . The locations h_0 and h_i are referenced to the center of mass of undisturbed liquid. For simplicity, it is assumed that the center of mass of the container is at the same location as the center of mass of the undisturbed liquid. A restoring force $-k_i s_i$ acts on the mass m_i whenever the mass is displaced from its neutral position $s_i = 0$. The parameters $m_0, h_0, I_0, m_i, h_i, k_i$ depend on the shape of the container, the characteristics of the liquid, and the fill ratio of the container.

As in the previous cases, to preserve the static properties of the liquid, the sum of all the masses must be the same as the liquid mass m_f , and the center of mass of the model must be at the same elevation as that of the liquid, i.e.,

$$m_0 + \sum_{i=1}^N m_i = m_f, \quad m_0 h_0 + \sum_{i=1}^N m_i h_i = 0.$$

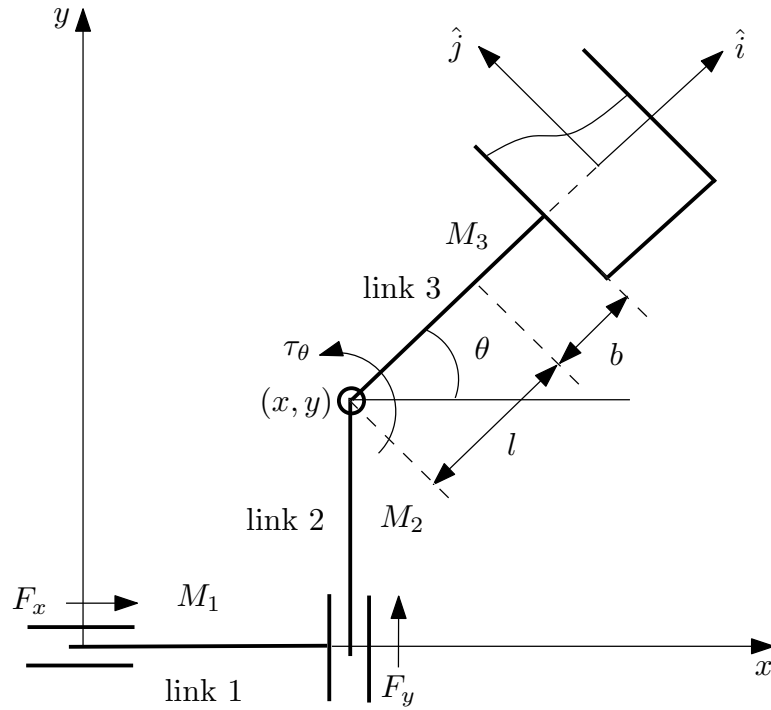


Figure 6.23: A PPR robot moving a liquid filled container.

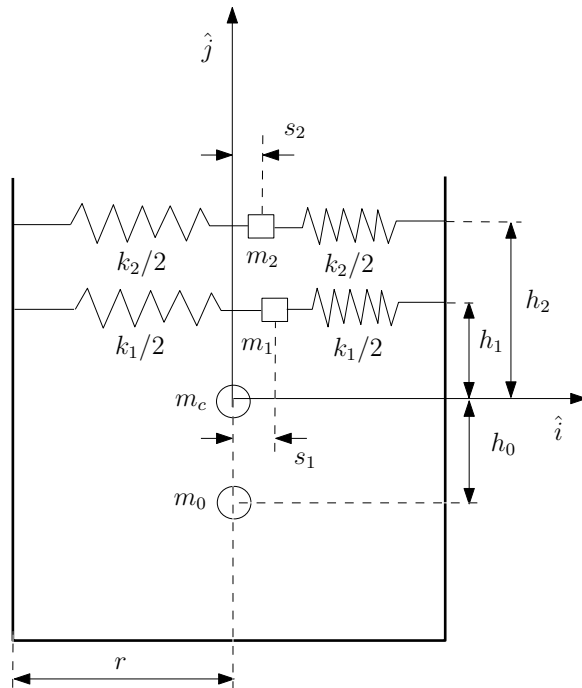


Figure 6.24: A multi-mass-spring model of liquid slosh.

Let \hat{i} and \hat{j} be the unit vectors along the container-fixed transverse (along the third link) and cylindrical axes, respectively. Then the inertial position of revolute joint

and the container center can be expressed in the container-fixed coordinate frame as

$$\begin{aligned}\vec{r}_r &= (x \cos \theta + y \sin \theta)\hat{i} + (-x \sin \theta + y \cos \theta)\hat{j}, \\ \vec{r}_c &= \vec{r}_r + (l + b + r)\hat{i}.\end{aligned}$$

Similarly, the position vectors of the liquid masses $m_0, m_i, \forall i$, in the container-fixed coordinate frame are given, respectively, by

$$\begin{aligned}\vec{r}_0 &= \vec{r}_c + h_0\hat{j}, \\ \vec{r}_i &= \vec{r}_c + s_i\hat{i} + h_i\hat{j}.\end{aligned}$$

The kinetic energies of the robot, the container, and the liquid can be computed as

$$\begin{aligned}T_r &= \frac{1}{2}(M_1 + M_2)\dot{x}^2 + \frac{1}{2}M_2\dot{y}^2 + \frac{1}{2}I_3\dot{\theta}^2 + \frac{1}{2}M_3[(\dot{x} - l\dot{\theta} \sin \theta)^2 + (\dot{y} + l\dot{\theta} \cos \theta)^2], \\ T_c &= \frac{1}{2}m_c\dot{\vec{r}}_c^2 + \frac{1}{2}I_c\dot{\theta}^2, \\ T_l &= \frac{1}{2}m_0\dot{\vec{r}}_0^2 + \frac{1}{2}I_0\dot{\theta}^2 + \frac{1}{2}\sum_{i=1}^N m_i\dot{\vec{r}}_i^2.\end{aligned}$$

The potential energies of the robot, the container, and the liquid can be expressed as

$$\begin{aligned}U_r &= M_2gy + M_3g(y + l \sin \theta), \\ U_c &= m_cg[y + (l + b + r) \sin \theta], \\ U_l &= m_0g[y + (l + b + r) \sin \theta + h_0 \cos \theta] + \frac{1}{2}\sum_{i=1}^N k_i s_i^2 \\ &\quad + \sum_{i=1}^N m_i g[y + (l + b + r) \sin \theta + h_i \cos \theta].\end{aligned}$$

The Lagrangian can now be given as

$$L = T_r + T_c + T_l - U_r - U_c - U_l.$$

The dissipative effects due to fuel slosh are described by damping coefficients c_i . A fraction of kinetic energy of sloshing fuel is dissipated during each cycle of the motion. The damping is included via a Rayleigh dissipation function R given by

$$R = \frac{1}{2}\sum_{i=1}^N c_i \dot{s}_i^2.$$

Applying Lagrange's formulation with dissipation, the equations of motion can be obtained as

$$(\bar{M} + \bar{m}_f)\ddot{x} - \bar{m}\bar{l}(\dot{\theta}^2 \cos \theta + \ddot{\theta} \sin \theta) + \sum_{i=1}^N m_i(\ddot{s}_i \cos \theta - 2\dot{s}_i\dot{\theta} \sin \theta) = F_x, \quad (6.96)$$

$$(M_2 + M_3)\ddot{y} - \bar{m}\bar{l}(\dot{\theta}^2 \sin \theta - \ddot{\theta} \cos \theta) + \sum_{i=1}^N m_i(\ddot{s}_i \sin \theta + 2\dot{s}_i\dot{\theta} \cos \theta) + (M_2 + M_3 + \bar{m}_f)g = F_y, \quad (6.97)$$

$$\bar{I}\ddot{\theta} - \bar{m}\bar{l}(\ddot{x} \sin \theta - \ddot{y} \cos \theta) - \sum_{i=1}^N m_i[h_i\ddot{s}_i - 2\dot{\theta}(a + s_i)\dot{s}_i] + (M_3l + \bar{m}_fa)g \cos \theta = \tau_\theta, \quad (6.98)$$

$$m_i[\ddot{s}_i + \ddot{x} \cos \theta + \ddot{y} \sin \theta - h_i\ddot{\theta} - (a + s_i)\dot{\theta}^2] + k_i s_i + c_i \dot{s}_i = 0, \quad \forall i, \quad (6.99)$$

where

$$\bar{M} = M_1 + M_2 + M_3,$$

$$\bar{m}_f = m_c + m_f,$$

$$a = l + b + r,$$

$$\bar{m}\bar{l} = M_3l + \bar{m}_fa + \sum_{i=1}^N m_i s_i,$$

$$\bar{I} = I_3 + I_c + I_0 + M_3l^2 + \bar{m}_fa^2 + m_0h_0^2 + \sum_{i=1}^N m_i(h_i^2 + s_i^2 + 2s_ia).$$

Note that equations (6.99) represent N nonintegrable second-order relations and hence they can be viewed as second order nonholonomic constraints.

Let $r = [x, y, \theta]'$ and $s = [s_1, \dots, s_N]'$ be the configuration vectors of the robot and slosh masses, respectively; and let $q = [r', s']'$ denote the $(N+3)$ -vector of generalized coordinates. Denote by $\tau_r = [F_x, F_y, \tau_\theta]'$ the control input vector for the PPR robot.

Then the system (6.96)-(6.99) can be written as

$$M(q)\ddot{q} + C(q, \dot{q})\dot{q} + G(q) = \tau, \quad (6.100)$$

where \dot{q} and \ddot{q} are $(N+3)$ -vectors of generalized velocities and generalized accelerations, respectively, and

$$M = \left[\begin{array}{c|c} M_{rr} & M_{rs} \\ \hline M_{sr} & M_{ss} \end{array} \right] = \left[\begin{array}{ccc|c} \bar{M} + \bar{m}_f & 0 & -\bar{m}\bar{l} \sin \theta & m' \cos \theta \\ 0 & M_2 + M_3 & \bar{m}\bar{l} \cos \theta & m' \sin \theta \\ -\bar{m}\bar{l} \sin \theta & \bar{m}\bar{l} \cos \theta & \bar{I} & -h' \mathcal{D}(m) \\ \hline m \cos \theta & m \sin \theta & -\mathcal{D}(m)h & \mathcal{D}(m) \end{array} \right],$$

$$C = \left[\begin{array}{c|c} C_{rr} & C_{rs} \\ \hline C_{sr} & C_{ss} \end{array} \right] = \left[\begin{array}{ccc|c} 0 & 0 & -\bar{m}\bar{l}\dot{\theta} \cos \theta - \dot{s}'m \sin \theta & -m'\dot{\theta} \sin \theta \\ 0 & 0 & -\bar{m}\bar{l}\dot{\theta} \sin \theta + \dot{s}'m \cos \theta & m'\dot{\theta} \cos \theta \\ 0 & 0 & \dot{s}'\mathcal{D}(m)(s+1a) & [am' + s'\mathcal{D}(m)]\dot{\theta} \\ 0 & 0 & -[am + \mathcal{D}(m)s]\dot{\theta} & 0 \end{array} \right],$$

$$G = \left[\frac{G_r}{\mathcal{D}(k)s} \right], \quad \tau = \left[\frac{\tau_r}{-\mathcal{D}(c)\dot{s}} \right],$$

where $1 = [1, \dots, 1]' \in \mathbb{R}^N$ and

$$G_r = \begin{bmatrix} 0 \\ (M_2 + M_3 + \bar{m}_f)g \\ (M_3l + \bar{m}_fa)g \cos \theta \end{bmatrix}.$$

Here m , h , k , and c denote the N -vectors of sloshing masses, distances, spring constants, and damping coefficients, respectively; and for any n -vector v , $\mathcal{D}(v)$ denotes the diagonal matrix $\text{diag}\{v_1, \dots, v_n\}$.

It is assumed that the manipulator parameters are chosen such that the symmetric $(N+3) \times (N+3)$ generalized inertia matrix is positive definite for all $\theta \in \mathbb{S}$, $s_i \in (-r, r)$, $i = 1, \dots, N$. It can be shown that the dynamic model (6.100) satisfy the following property:

Property: $\dot{M} - 2C$ is a skew-symmetric matrix.

The control objective is to design feedback controllers so that the controlled PPR accomplishes a point-to-point transfer of the liquid container, while suppressing the slosh modes. It must be pointed out that in the above formulation it is assumed that no control forces or torques exist that directly control the slosh dynamics. The objective is to simultaneously control the robot dynamics and the slosh dynamics using only control effectors that act on the PPR robot; the control of the slosh dynamics must be achieved through the system coupling. In this regard, equations (6.96)-(6.99) model interesting examples of underactuated mechanical systems. The published literature on the dynamics and control of such systems includes the development of theoretical controllability and stabilizability results for a large class of systems using tools from nonlinear control theory (Reyhanoglu et al., 1999) and the development of effective nonlinear control design methodologies (Reyhanoglu et al., 2000) that are applied to several practical examples, including underactuated space vehicles (Krishnan et al., 1992; Reyhanoglu, 2003) and underactuated manipulators (Mahindrakar et al., 2005).

6.2.2 Controllability and Stabilizability Analysis

In this section, tools from differential geometric control theory are applied to derive the controllability and stabilizability properties. In this context, equation (6.99) can be considered as a second order nonholonomic constraint. To analyze this system define

$$\ddot{x} = v_1, \quad (6.101)$$

$$\ddot{y} = v_2, \quad (6.102)$$

$$\ddot{\theta} = v_3, \quad (6.103)$$

$$\ddot{s}_i = -v_1 \cos \theta - v_2 \sin \theta + h_i v_3 + (a + s_i)\dot{\theta}^2 - \omega_i^2 s_i - 2\zeta_i \omega_i \dot{s}_i, \quad \forall i. \quad (6.104)$$

For simplicity, we will consider only the first two modes (i.e., $i = 1, 2$), however, we will show that this is easily generalizable for any number of modes.

Let $q = [x, y, \theta, s_1, s_2]'$ denote the configuration vector and define the following state variables

$$(\eta_1, \dots, \eta_{10}) = (x, y, \theta, s_1, s_2, \dot{x}, \dot{y}, \dot{\theta}, \dot{s}_1, \dot{s}_2).$$

Then, we can rewrite (6.101)-(6.104) as

$$\dot{\eta}_1 = \eta_6,$$

$$\dot{\eta}_2 = \eta_7,$$

$$\dot{\eta}_3 = \eta_8,$$

$$\dot{\eta}_4 = \eta_9,$$

$$\dot{\eta}_5 = \eta_{10},$$

$$\dot{\eta}_6 = v_1,$$

$$\dot{\eta}_7 = v_2,$$

$$\dot{\eta}_8 = v_3,$$

$$\dot{\eta}_9 = -v_1 \cos \eta_3 - v_2 \sin \eta_3 + h_1 v_3 + (a + \eta_4)\eta_8^2 - \omega_1^2 \eta_4 - 2\zeta_1 \omega_1 \eta_9,$$

$$\dot{\eta}_{10} = -v_1 \cos \eta_3 - v_2 \sin \eta_3 + h_2 v_3 + (a + \eta_5)\eta_8^2 - \omega_2^2 \eta_5 - 2\zeta_2 \omega_2 \eta_{10}.$$

It can be shown that the linearization around the equilibrium configuration is completely controllable if $\omega_i \neq 0, \forall i$. There exist solutions to the problem of controlling the PPR robot moving a liquid filled container.

A nonlinear approach can be used to illustrate Theorem 4.3 and the relationship between linear and nonlinear controllability for this kind of systems.

It is clear that the drift and control vector fields are

$$\begin{aligned}
 f &= \dot{x} \frac{\partial}{\partial x} + \dot{y} \frac{\partial}{\partial y} + \dot{\theta} \frac{\partial}{\partial \theta} + \dot{s}_1 \frac{\partial}{\partial s_1} + \dot{s}_2 \frac{\partial}{\partial s_2} + [(a + s_1)\dot{\theta}^2 - \omega_1^2 s_1 - 2\zeta_1 \omega_1 \dot{s}_1] \frac{\partial}{\partial \dot{s}_1} \\
 &\quad + [(a + s_2)\dot{\theta}^2 - \omega_2^2 s_2 - 2\zeta_2 \omega_2 \dot{s}_2] \frac{\partial}{\partial \dot{s}_2}, \\
 g_1 &= \frac{\partial}{\partial \dot{x}} - \cos \theta \frac{\partial}{\partial \dot{s}_1} - \cos \theta \frac{\partial}{\partial \dot{s}_2}, \\
 g_2 &= \frac{\partial}{\partial \dot{y}} - \sin \theta \frac{\partial}{\partial \dot{s}_1} - \sin \theta \frac{\partial}{\partial \dot{s}_2}, \\
 g_3 &= \frac{\partial}{\partial \dot{\theta}} + h_1 \frac{\partial}{\partial \dot{s}_1} + h_2 \frac{\partial}{\partial \dot{s}_2}.
 \end{aligned}$$

Define $q = (q_1, q_2)$ as $q_1 = (x, y, \theta) \in \mathbb{R}^3$ and $q_2 = (s_1, s_2) \in \mathbb{R}^2$ such that the movement of the liquid filled container moved by the PPR robot can be expressed as a second-order nonholonomic system where $p = 2$, $m = 3$, and $n = 5$. As shown in Theorems 4.3, 4.4 and Corollary 4.1, the small time local controllability of this system can be studied by the properties of the matrices J and R . If we rewrite the $(n - m)$ nonholonomic constraints as

$$\begin{aligned}
 \begin{bmatrix} \dot{\eta}_9 \\ \dot{\eta}_{10} \end{bmatrix} &= \begin{bmatrix} -\cos \eta_3 & -\sin \eta_3 & h_1 \\ -\cos \eta_3 & -\sin \eta_3 & h_2 \end{bmatrix} \begin{bmatrix} v_1 \\ v_2 \\ v_3 \end{bmatrix} + \\
 &\quad \begin{bmatrix} (a + \eta_4)\eta_8^2 - \omega_1^2 \eta_4 - 2\zeta_1 \omega_1 \eta_9 \\ (a + \eta_5)\eta_8^2 - \omega_2^2 \eta_5 - 2\zeta_2 \omega_2 \eta_{10} \end{bmatrix},
 \end{aligned}$$

it is easy to identify

$$\begin{aligned}
 J_1 &= \begin{bmatrix} -\cos \eta_3 \\ -\cos \eta_3 \end{bmatrix}, \quad J_2 = \begin{bmatrix} -\sin \eta_3 \\ -\sin \eta_3 \end{bmatrix}, \quad J_3 = \begin{bmatrix} h_1 \\ h_2 \end{bmatrix}, \\
 R &= \begin{bmatrix} (a + \eta_4)\eta_8^2 - \omega_1^2 \eta_4 - 2\zeta_1 \omega_1 \eta_9 \\ (a + \eta_5)\eta_8^2 - \omega_2^2 \eta_5 - 2\zeta_2 \omega_2 \eta_{10} \end{bmatrix}.
 \end{aligned}$$

Note that since J_i , $i = 1, \dots, 3$, does not depend on $(\eta_6, \dots, \eta_{10})$, Theorem 4.4 is not applicable to prove small time local controllability.

We now apply Corollary 4.1 by defining the following matrices evaluated at the

equilibrium $(\eta_1^e, \dots, \eta_5^e, 0, \dots, 0)$:

$$\begin{aligned} \beta_0 &= \begin{bmatrix} 1 & 0 \\ 0 & 1 \end{bmatrix}, \quad \beta_1 = \frac{\partial R}{\partial \dot{q}_2} \beta_0 = \begin{bmatrix} -2\zeta_1 \omega_1 & 0 \\ 0 & -2\zeta_2 \omega_2 \end{bmatrix}, \\ \beta_2 &= \frac{\partial R}{\partial q_2} \beta_0 + \frac{\partial R}{\partial \dot{q}_2} \beta_1 = \begin{bmatrix} \omega_1^2(4\zeta_1^2 - 1) & 0 \\ 0 & \omega_2^2(4\zeta_2^2 - 1) \end{bmatrix}, \\ b_1 &= \begin{bmatrix} 1 \\ 0 \\ 0 \\ -\cos \eta_3^e \\ -\cos \eta_3^e \end{bmatrix}, \quad b_2 = \begin{bmatrix} 0 \\ 1 \\ 0 \\ -\sin \eta_3^e \\ -\sin \eta_3^e \end{bmatrix}, \quad b_3 = \begin{bmatrix} 0 \\ 0 \\ 1 \\ h_1 \\ h_2 \end{bmatrix}. \end{aligned}$$

Then the matrix A_1 is given by

$$\begin{aligned} (a_1)_1 &= \beta_0 \frac{\partial R}{\partial \dot{q}} b_1 = \begin{bmatrix} 2\zeta_1 \omega_1 \cos \eta_3^e \\ 2\zeta_2 \omega_2 \cos \eta_3^e \end{bmatrix}, \\ (a_2)_1 &= \beta_0 \frac{\partial R}{\partial q} b_1 + \beta_1 \frac{\partial R}{\partial \dot{q}} b_1 = \begin{bmatrix} \omega_1^2(1 - 4\zeta_1^2) \cos \eta_3^e \\ \omega_2^2(1 - 4\zeta_2^2) \cos \eta_3^e \end{bmatrix}, \\ (a_3)_1 &= \beta_1 \frac{\partial R}{\partial q} b_1 + \beta_2 \frac{\partial R}{\partial \dot{q}} b_1 = \begin{bmatrix} -4\omega_1^3 \zeta_1(1 - 2\zeta_1^2) \cos \eta_3^e \\ -4\omega_2^3 \zeta_2(1 - 2\zeta_2^2) \cos \eta_3^e \end{bmatrix} \end{aligned}$$

as

$$A_1 = \begin{bmatrix} 2\zeta_1 \omega_1 \cos \eta_3^e & \omega_1^2(1 - 4\zeta_1^2) \cos \eta_3^e \\ 2\zeta_2 \omega_2 \cos \eta_3^e & \omega_2^2(1 - 4\zeta_2^2) \cos \eta_3^e \\ \omega_1^2(1 - 4\zeta_1^2) \cos \eta_3^e & -4\omega_1^3 \zeta_1(1 - 2\zeta_1^2) \cos \eta_3^e \\ \omega_2^2(1 - 4\zeta_2^2) \cos \eta_3^e & -4\omega_2^3 \zeta_2(1 - 2\zeta_2^2) \cos \eta_3^e \end{bmatrix}.$$

Similar expressions can be obtained for $(a_j)_i$, $i = 2, 3$, $j = 1, \dots, 3$, to construct

$$A_2 = \begin{bmatrix} 2\zeta_1 \omega_1 \sin \eta_3^e & \omega_1^2(1 - 4\zeta_1^2) \sin \eta_3^e \\ 2\zeta_2 \omega_2 \sin \eta_3^e & \omega_2^2(1 - 4\zeta_2^2) \sin \eta_3^e \\ \omega_1^2(1 - 4\zeta_1^2) \sin \eta_3^e & -4\omega_1^3 \zeta_1(1 - 2\zeta_1^2) \sin \eta_3^e \\ \omega_2^2(1 - 4\zeta_2^2) \sin \eta_3^e & -4\omega_2^3 \zeta_2(1 - 2\zeta_2^2) \sin \eta_3^e \end{bmatrix}$$

and

$$A_3 = \begin{bmatrix} -2\zeta_1 \omega_1 h_1 & -\omega_1^2(1 - 4\zeta_1^2) h_1 \\ -2\zeta_2 \omega_2 h_2 & -\omega_2^2(1 - 4\zeta_2^2) h_2 \\ -\omega_1^2(1 - 4\zeta_1^2) h_1 & 4\omega_1^3 \zeta_1(1 - 2\zeta_1^2) h_1 \\ -\omega_2^2(1 - 4\zeta_2^2) h_2 & 4\omega_2^3 \zeta_2(1 - 2\zeta_2^2) h_2 \end{bmatrix}.$$

Thus we can construct the matrix $[A_1 \ A_2 \ A_3]$ of rank 4 and it follows from Corollary 4.1 that the system is small time locally controllable. Note that $\omega_i \neq 0$, $\forall i$, and $h_1 \neq h_2$ are assumed.

The result above is easily applicable to any number of modes N constructing a matrix $[A_1 \ A_2 \ A_3]$ of rank $2N$.

6.2.3 Feedback Control Laws

In this section, Lyapunov-based feedback controllers are designed to achieve the control objective. Two cases are considered; partial-state feedback that does not use slosh state information and full-state feedback that uses both robot state and slosh state measurements or estimations.

6.2.3.1 Partial-State Feedback

Consider the model of a PPR robot moving a liquid filler container shown in Figs. 6.23 and 6.24. The equilibrium solution corresponding to

$$\bar{F}_x = 0, \bar{F}_y = (M_2 + M_3 + \bar{m}_f)g, \bar{\tau}_\theta = (M_3l + \bar{m}_fa)g \cos \bar{\theta}$$

is given by $x = \bar{x}$, $y = \bar{y}$, $\theta = \bar{\theta}$, $s_i = \dot{s}_i = 0$, $\forall i$. Without loss of generality in our subsequent analysis, we consider the equilibrium at the origin, i.e., $\bar{x} = \bar{y} = \bar{\theta} = 0$.

To design a partial-state feedback controller that stabilizes the system (6.100) at the origin, consider the following candidate Lyapunov function:

$$V = \frac{1}{2}[r'\mathcal{D}(\alpha)r + s'\mathcal{D}(k)s + \dot{q}'M\dot{q}],$$

where $\alpha = [\alpha_1, \alpha_2, \alpha_3]'$, $\alpha_i > 0$, $i = 1, 2, 3$.

Using the fact that $\dot{M} - 2C$ is a skew-symmetric matrix, the time derivative of V along the trajectories of (6.100) can be computed as

$$\dot{V} = \dot{r}'[\tau_r - G_r + \mathcal{D}(\alpha)r] - \dot{s}'\mathcal{D}(c)\dot{s}.$$

Clearly, the control law

$$\tau_r = G_r - \mathcal{D}(\alpha)r - \mathcal{D}(\lambda)\dot{r}, \quad (6.105)$$

where $\lambda = [\lambda_1, \lambda_2, \lambda_3]'$, $\lambda_i > 0$, $i = 1, 2, 3$, yields

$$\dot{V} = -\dot{r}'\mathcal{D}(\lambda)\dot{r} - \dot{s}'\mathcal{D}(c)\dot{s},$$

which satisfies $\dot{V} \leq 0$. Using LaSalle's principle (Khalil, 2002), it is easy to prove the asymptotic stability of the origin of the closed-loop system defined by (6.100) and the feedback control law (6.105). Note that the control parameters α and λ can be chosen arbitrarily to achieve good closed-loop responses.

We now present the following result.

Proposition 6.1: *Consider the system (6.100) with the feedback control law (6.105), where the constant control parameters satisfy $\alpha_i > 0$, $\lambda_i > 0$, $i = 1, 2, 3$. Then the closed-loop system is uniformly asymptotically stable at the origin.*

6.2.3.2 Full-State Feedback

In order to apply the theory developed for underactuated mechanical systems (Reyhanoglu et al., 1999), rewrite the system (6.100) as

$$M_{rr}(q)\ddot{r} + M_{rs}(q)\ddot{s} + F_r(q, \dot{q}) = \tau_r, \quad (6.106)$$

$$M_{sr}(q)\ddot{r} + M_{ss}(q)\ddot{s} + F_s(q, \dot{q}) = 0, \quad (6.107)$$

where

$$F_r(q, \dot{q}) = C_{rr}\dot{r} + C_{rs}\dot{s} + G_r,$$

$$F_s(q, \dot{q}) = C_{sr}\dot{r} + \mathcal{D}(c)\dot{s} + \mathcal{D}(k)s.$$

Following Reyhanoglu et al. (1999), \ddot{s} can be expressed as

$$\ddot{s} = -M_{ss}^{-1}(q)[M_{sr}(q)\ddot{r} + F_s(q, \dot{q})],$$

and substituted into (6.106) to obtain

$$\bar{M}(q)\ddot{r} + \bar{F}(q, \dot{q}) = \tau_r,$$

where

$$\bar{M}(q) = M_{rr}(q) - M_{rs}(q)M_{ss}^{-1}(q)M_{sr}(q),$$

$$\bar{F}(q, \dot{q}) = F_r(q, \dot{q}) - M_{rs}(q)M_{ss}^{-1}(q)F_s(q, \dot{q}).$$

Consequently, using the partial feedback linearizing controller

$$\tau_r = \bar{M}(q)u + \bar{F}(q, \dot{q}), \quad (6.108)$$

the system (6.106)-(6.107) can be rewritten as

$$\ddot{r} = u, \quad (6.109)$$

$$\ddot{s} = J(q)u + R(q, \dot{q}), \quad (6.110)$$

where

$$J(q) = -[1 \cos \theta \quad 1 \sin \theta \quad -h],$$

$$R(q, \dot{q}) = -\mathcal{D}^2(\omega)s - 2\mathcal{D}(\zeta)\mathcal{D}(\omega)\dot{s} + (s + 1a)\dot{\theta}^2.$$

Here $\omega = [\omega_1, \dots, \omega_N]' \in \mathbb{R}^N$, $\zeta = [\zeta_1, \dots, \zeta_N]' \in \mathbb{R}^N$, and $\omega_i = \sqrt{\frac{k_i}{m_i}}$ and $\zeta_i = \frac{c_i}{2\omega_i m_i}$, $i = 1, \dots, N$, denote the undamped natural frequencies and damping ratios,

respectively. Equations (6.109)-(6.110) have a special triangular or cascade form that appropriately captures the important attributes of underactuated mechanical systems. Equation (6.109) defines the linearized dynamics for the 3 completely actuated degrees of freedom of the robot. Equation (6.110) defines the dynamics of the N unactuated degrees of freedom of the slosh masses.

To design a full-state feedback controller to stabilize the system (6.109)-(6.110) at the origin, consider the following candidate Lyapunov function:

$$V = \frac{1}{2} [r' \mathcal{D}(\alpha) r + \dot{r}' \mathcal{D}(\lambda) \dot{r} + \beta [\dot{s}' \dot{s} + s' \mathcal{D}^2(\omega) s - 2 \dot{s}' J \dot{r}]] .$$

It is assumed that

$$\dot{r}' \mathcal{D}(\lambda) \dot{r} + \beta [\dot{s}' \dot{s} + s' \mathcal{D}^2(\omega) s - 2 \dot{s}' J \dot{r}] > 0 \quad (6.111)$$

so that the function V is positive definite.

Remark 6.4: Let $Q \in \mathbb{R}^{(N+3) \times (N+3)}$ denote the symmetric matrix corresponding to the quadratic form

$$\dot{q}' Q \dot{q} = \dot{r}' \mathcal{D}(\lambda) \dot{r} + \beta [\dot{s}' \dot{s} + s' \mathcal{D}^2(\omega) s - 2 \dot{s}' J \dot{r}] .$$

Clearly, this quadratic form is positive definite if and only if the leading principal minors of the matrix Q are all positive.

Let $\lambda_1 = \lambda_2 = \lambda_3 = \lambda$. Then, for $N = 2$ the following conditions guarantee that the quadratic form is positive definite:

$$\begin{aligned} \alpha_1(\lambda - \beta h_1^2) - \beta(\alpha_1 + \lambda) &> 0, \\ \lambda[\lambda - \beta(h_1^2 + h_2^2)] - \beta[2\lambda - (h_1 - h_2)^2] &> 0. \end{aligned}$$

The time derivative of V along the trajectories of (6.109)-(6.110) is

$$\begin{aligned} \dot{V} &= \dot{r}' \left[\mathcal{D}(\alpha) \dot{r} + \mathcal{D}(\lambda) u - \beta [J' \dot{s} + J'(Ju + R)] \right] + \beta \dot{s}' (s + 1a) \dot{\theta}^2 \\ &\quad - 2\beta \dot{s}' \mathcal{D}(\omega) \mathcal{D}(\zeta) \dot{s} \\ &= \dot{r}' [Bu + H] - 2\beta \dot{s}' \mathcal{D}(\omega) \mathcal{D}(\zeta) \dot{s}, \end{aligned}$$

where

$$\begin{aligned} B &= \mathcal{D}(\lambda) - \beta J' J, \\ H &= \beta \left[-J' \dot{s} + 2J' \mathcal{D}(\omega) \mathcal{D}(\zeta) \dot{s} + J' \mathcal{D}^2(\omega) s - J'(s + 1a) \dot{\theta}^2 + \dot{s}' (s + 1a) \dot{\theta} e_3 \right] \\ &\quad + \mathcal{D}(\alpha) r. \end{aligned}$$

Here $e_3 = [0, 0, 1]'$ is the third standard basis vector in \mathbb{R}^3 .

Remark 6.5: Note that B and H are given in open form as

$$B = \begin{bmatrix} \lambda_1 - N\beta \cos^2 \theta & -0.5N\beta \sin 2\theta & \beta \cos \theta \sum_{i=1}^N h_i \\ -0.5N\beta \sin 2\theta & \lambda_2 - N\beta \sin^2 \theta & \beta \sin \theta \sum_{i=1}^N h_i \\ \beta \cos \theta \sum_{i=1}^N h_i & \beta \sin \theta \sum_{i=1}^N h_i & \lambda_3 - \beta \sum_{i=1}^N h_i^2 \end{bmatrix},$$

$$H = \begin{bmatrix} -\beta \sum_{i=1}^N [(\omega_i^2 s_i + 2\zeta_i \omega_i \dot{s}_i - (a + s_i)\dot{\theta}^2) \cos \theta + \dot{s}_i \dot{\theta} \sin \theta] + \alpha_1 x \\ -\beta \sum_{i=1}^N [(\omega_i^2 s_i + 2\zeta_i \omega_i \dot{s}_i - (a + s_i)\dot{\theta}^2) \sin \theta - \dot{s}_i \dot{\theta} \cos \theta] + \alpha_2 y \\ -\beta \sum_{i=1}^N [(a + s_i)\dot{\theta}^2 - \omega_i^2 s_i - 2\zeta_i \omega_i \dot{s}_i] h_i - (a + s_i) \dot{s}_i \dot{\theta} + \alpha_3 \theta \end{bmatrix}.$$

The feedback control law

$$u = -B^{-1}(q)[H(q, \dot{q}) + \mathcal{D}(\gamma)\dot{r}], \quad (6.112)$$

where $\gamma = [\gamma_1, \gamma_2, \gamma_3]'$, $\gamma_i > 0$, $i = 1, 2, 3$, yields

$$\dot{V} = -\dot{r}'\mathcal{D}(\gamma)\dot{r} - 2\beta\dot{s}'\mathcal{D}(\omega)\mathcal{D}(\zeta)\dot{s},$$

which satisfies $\dot{V} \leq 0$. Using LaSalle's principle (Khalil, 2002), it is easy to prove asymptotic stability of the origin of the closed loop defined by the equations (6.109)-(6.110) and the feedback control law (6.112). Note that the control parameters β , α , λ and γ can be chosen arbitrarily to achieve good closed loop responses. The full-state feedback law can be written in terms of the original control inputs using the relation (6.108) as:

$$\tau_r = -\bar{M}(q)B^{-1}(q)[H(q, \dot{q}) + \mathcal{D}(\gamma)\dot{r}] + \bar{F}(q, \dot{q}). \quad (6.113)$$

We now present the following result.

Proposition 6.2: Consider the system (6.100) with the feedback control law (6.113), where the control parameters are chosen such that the constant parameters $\beta > 0$, $\alpha_i > 0$, $\lambda_i > 0$, $i = 1, 2, 3$, satisfy the condition given by (6.111) and $\gamma_j > 0$, $j = 1, 2, 3$. Then the closed-loop system is uniformly asymptotically stable at the origin.

6.2.4 Simulations

The feedback control laws developed in the previous sections are implemented here. The first two slosh modes are included to demonstrate the effectiveness of the control laws. The physical parameters used in the simulations are given in Table 6.5. The fluid parameters are obtained using the formulae in Dodge (2000).

Table 6.5: Physical parameters for a PPR robot and liquid container.

Parameter	Value	Parameter	Value
M_1	5 kg	m_0	7.95 kg
M_2	10 kg	m_1	1.43 kg
M_3	15 kg	m_2	0.04 kg
h_0	−0.008 m	m_c	1.5 kg
h_1	0.042 m	I_c	0.011 kg · m ²
h_2	0.113 m	I_0	0.042 kg · m ²
k_1	258 N/m	c_1	0.038 N · s/m
k_2	22.5 N/m	c_2	0.002 N · s/m
l	0.25 m	b	0.25 m
r	0.1 m	I_3	0.3125 kg · m ²

We consider a fast point-to-point transfer of the container while suppressing the slosh modes. Simulations correspond to the initial conditions

$$(x_0, y_0, s_{1_0}, s_{2_0}) = (1, 1, 0.03, -0.01) \text{ (m)},$$

$$\theta_0 = \pi/4, \dot{x}_0 = \dot{y}_0 = \dot{\theta}_0 = \dot{s}_{1_0} = \dot{s}_{2_0} = 0.$$

First the partial-state feedback case is considered. The effectiveness of the Lyapunov-based controller (6.105) is demonstrated by applying the controller to the complete nonlinear system (6.96)-(6.99). The control parameters were chosen as

$$\alpha = [25, 25, 25]', \lambda = [50, 50, 50]'$$

Time responses shown in Figs. 6.25-6.27 demonstrate that although the robot states converge to the origin in about 7 seconds, the slosh modes do not converge to zero fast enough due to insufficient damping.

6.2 Liquid Container Transfer via a PPR Robot

Next the full-state feedback case is considered. The effectiveness of the Lyapunov-based controller (6.113) is demonstrated by applying the controller to the complete nonlinear system (6.96)-(6.99). Time responses shown in Figs. 6.28-6.30 correspond to the same initial conditions. The control parameters in this case were chosen as

$$\alpha = [15, 15, 15]', \lambda = [6, 6, 6]', \beta = 1, \gamma = [30, 50, 30]'$$

As can be seen in the figures, the robot and the slosh states converge to the equilibrium at zero very fast. In both cases, the force on the second prismatic joint and the torque on the revolute joint converge to $\bar{F}_y = 352.4 \text{ N}$ and $\bar{\tau}_\theta = 101.1 \text{ N} \cdot \text{m}$, respectively.

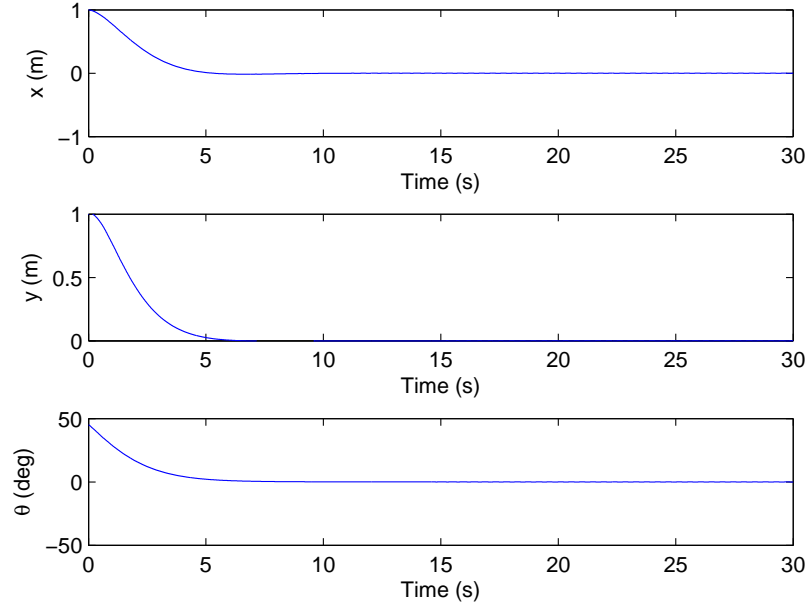


Figure 6.25: Time responses of x , y and θ (Partial-state feedback).

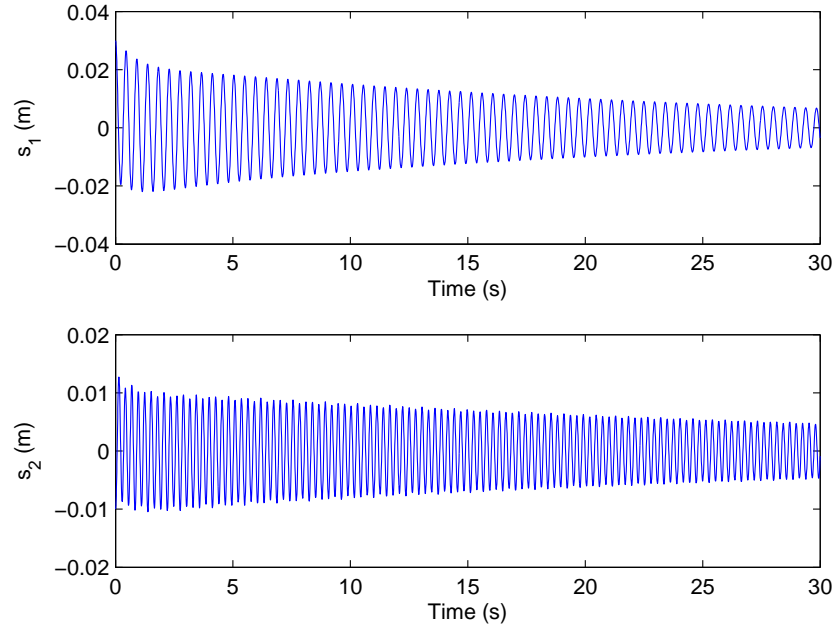


Figure 6.26: Time responses of s_1 and s_2 (Partial-state feedback).

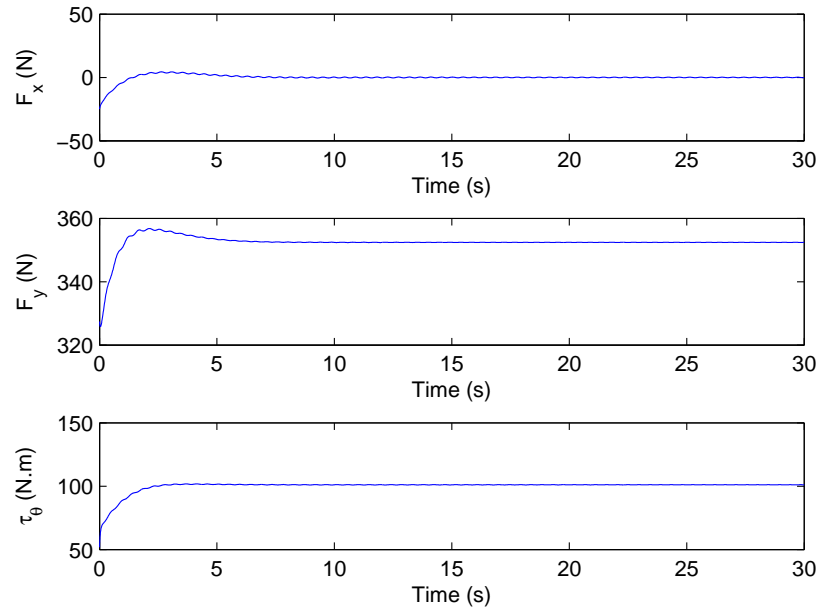


Figure 6.27: Time responses of F_x , F_y and τ_θ (Partial-state feedback).

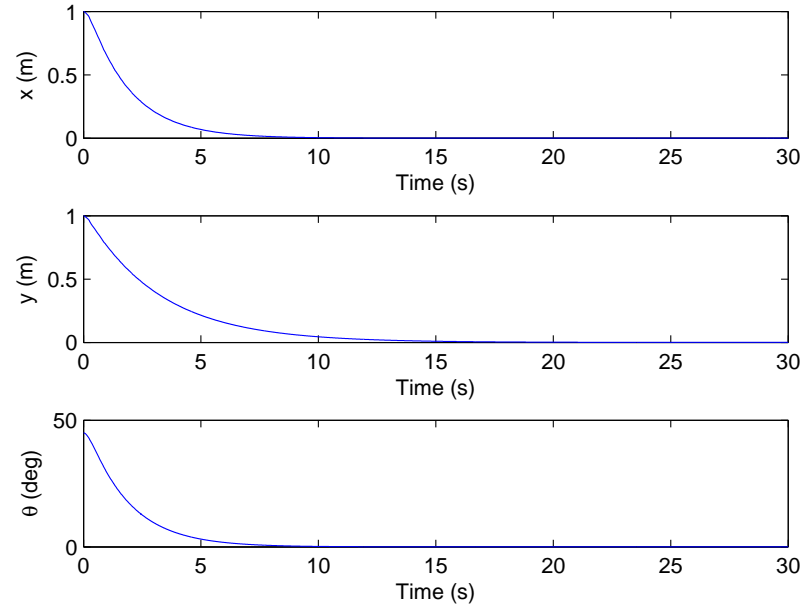


Figure 6.28: Time responses of x , y and θ (Full-state feedback).

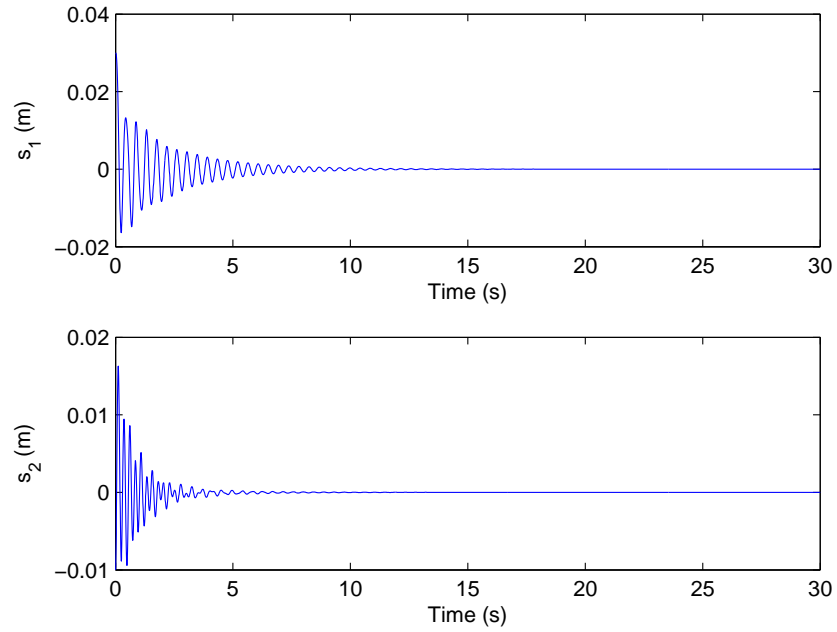


Figure 6.29: Time responses of s_1 and s_2 (Full-state feedback).

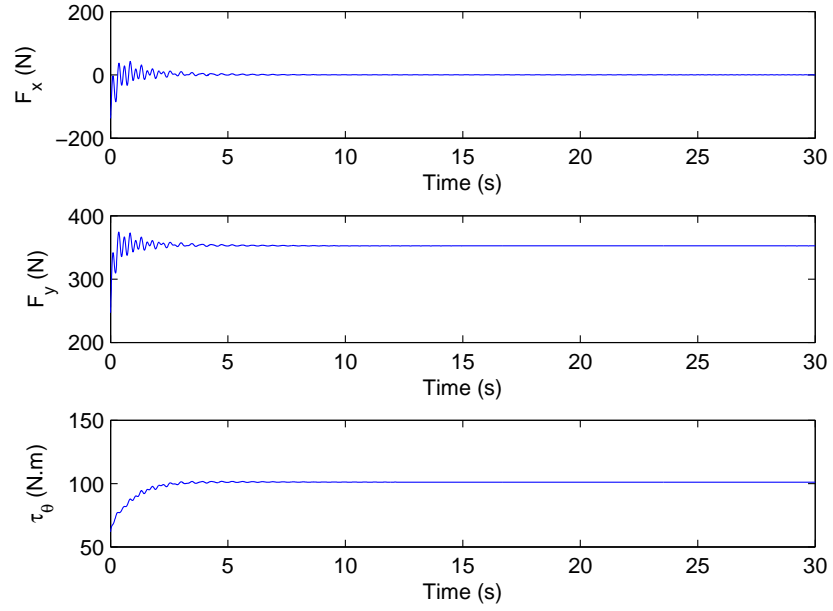


Figure 6.30: Time responses of F_x , F_y and τ_θ (Full-state feedback).

7

EXAMPLES: THIRD-ORDER NONHOLONOMIC SYSTEMS

This chapter is based on papers by Rubio Hervas and Reyhanoglu (2013a,b,c,d,e). We study two examples of systems that do not admit asymptotically stabilizing continuous static or dynamic state feedback: a planar PPR robot manipulator subject to a jerk constraint and a point mass moving on a constant torsion curve in a three dimensional space.

7.1 Control of a Manipulator with a Jerk Constraint

Jerk is defined as the time derivative of the acceleration, and thus is an interesting example of third-order constraints. In the context of robot manipulators, it is associated with rapidly changing actuator forces. Excessive jerk leads to premature wear on the actuators, resonant vibrations in the robot's structure, and is difficult for a controller to track accurately; even some experiments indicate that our brain realizes a version of minimum-jerk in planning grasping motions for our arms (Freeman, 2012).

7.1.1 Model Formulation

Following the ideas in Reyhanoglu et al. (1999), consider a planar PPR robot, i.e., a robot with two prismatic and one revolute joint, moving on a horizontal plane so that gravity can be ignored. Also assume that the joints are actuated by control inputs (F_x, F_y, T) . An idealized model of this manipulator is shown in Fig. 7.1. The model consists of a base body, which can translate and rotate freely in the plane, and a massless arm at the tip of which the end-effector is attached. The base body is connected to the massless arm. The Cartesian position (x_B, y_B) of the base body as well as the angle θ through which the base body is rotated can be controlled. Assume that the end effector is required to track a trajectory such that the transverse jerk component is zero.

Let (x, y) denote the end-effector position of the manipulator. Also, let the base body have mass M and rotational inertia I , the end-effector and payload combination have mass m , and let l be the length of the massless arm.

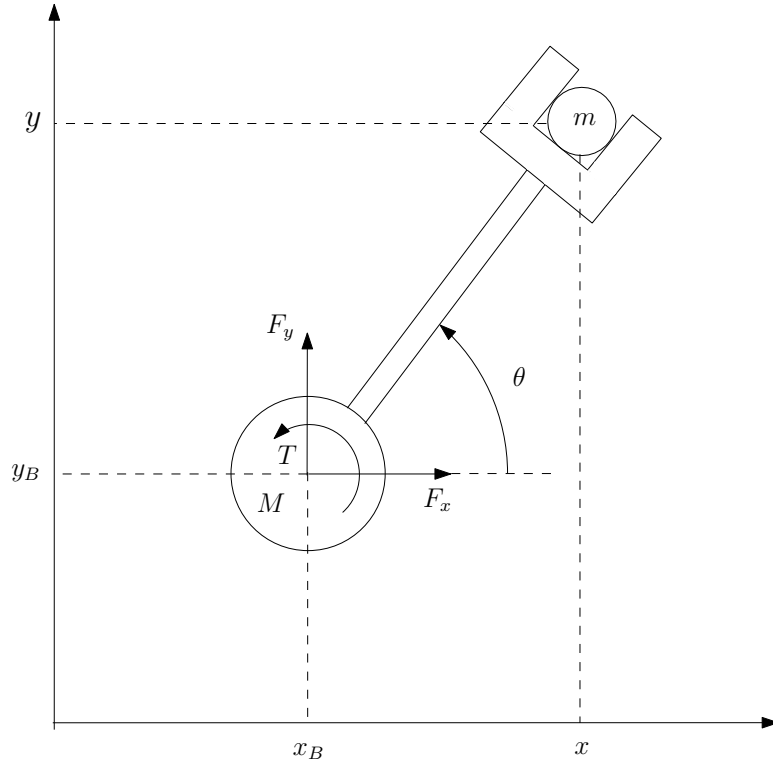


Figure 7.1: Simplified model of a PPR manipulator.

The control problem is to move the manipulator between any given initial configuration (x^0, y^0, θ^0) and final configuration (x^f, y^f, θ^f) such that the resultant transverse

7.1 Control of a Manipulator with a Jerk Constraint

jerk at the end-effector is zero, i.e.,

$$\ddot{y} = \ddot{x} \tan \theta, \forall t \geq 0.$$

For simplicity, assume $(x^f, y^f, \theta^f) = (0, 0, 0)$ and $\theta \in (-\pi/2, \pi/2)$.

We use the ideas introduced previously to formulate the above problem as a non-linear control problem. Let $(F_x, F_y, T) \in \mathbb{R}^3$ denote the vector of control inputs applied to the base body, where (F_x, F_y) are the force inputs in the x and y direction, respectively, and T is the torque input. The Lagrangian of the system is given by

$$L = \frac{1}{2}(M + m)(\dot{x}^2 + \dot{y}^2) + \frac{1}{2}(I + Ml^2)\dot{\theta}^2 + Ml\dot{\theta}(\dot{x} \sin \theta - \dot{y} \cos \theta).$$

The virtual work can be computed as

$$\delta W = F_x \delta(x - l \cos \theta) + F_y \delta(y - l \sin \theta) + T \delta \theta.$$

Following the development in the previous chapters, the constrained equations of motion can be written as

$$(M + m)(\ddot{x} \cos \theta + \ddot{y} \sin \theta) + Ml\ddot{\theta}^2 = F_x \cos \theta + F_y \sin \theta, \quad (7.1)$$

$$Ml(\ddot{x} \sin \theta - \ddot{y} \cos \theta) + (I + Ml^2)\ddot{\theta} = T + l(F_x \sin \theta - F_y \cos \theta), \quad (7.2)$$

together with the constraint

$$\ddot{y} = \ddot{x} \tan \theta. \quad (7.3)$$

It is easy to check that (7.3) satisfies Definition 2.1 and hence represents a non-integrable jerk relation, which implies that the transverse jerk component of the end-effector is zero. This condition can be viewed as a design constraint.

7.1.2 Controllability and Stabilizability Analysis

In this section, we consider the third-order nonholonomic constraint system (7.1)-(7.2) and study its control-theoretic properties.

Assuming $\theta \in (-\pi/2, \pi/2)$, equation (7.3) can be expressed as

$$\ddot{x} = u_1, \quad (7.4)$$

$$\ddot{\theta} = u_2, \quad (7.5)$$

$$\ddot{y} = u_1 \tan \theta, \quad (7.6)$$

Note that we have used

$$F_y = (M + m)\ddot{y}. \quad (7.7)$$

7.1 Control of a Manipulator with a Jerk Constraint

so that the original control inputs can be recovered from the relations

$$\dot{F}_x = (M + m)u_1 + Ml \frac{\dot{\theta}}{\cos \theta} (2\ddot{\theta} + \dot{\theta}^2 \tan \theta), \quad (7.8)$$

$$\dot{T} = (I + Ml^2)u_2 - ml\dot{\theta}(\ddot{x} \cos \theta + \ddot{y} \sin \theta) - Ml^2\dot{\theta}(2\ddot{\theta} \tan \theta + \frac{\dot{\theta}^2}{\cos^2 \theta}). \quad (7.9)$$

Now the control problem is reduced to designing controls u_1 and u_2 for the system (7.4)-(7.6). Once these controls are designed, one can use relations (7.7), (7.8) and (7.9) to determine the controls F_y , F_x and T , respectively.

Let $q = [x, \theta, y]'$ denote the configuration vector and define by

$$(q, \dot{q}, \ddot{q}) \in \mathbf{M} = \mathbb{R} \times (-\pi/2, \pi/2) \times \mathbb{R} \times \mathbb{R}^3 \times \mathbb{R}^3$$

the state. Clearly, the set of equilibrium solutions corresponding to $u = 0$ is given by

$$\mathbf{M}_e = \{(q, \dot{q}, \ddot{q}) \in \mathbf{M} \mid \dot{q} = \ddot{q} = 0\}.$$

The control system can be expressed in the usual form (4.10) such that the drift and control vector fields are given by

$$\begin{aligned} f &= \dot{x} \frac{\partial}{\partial x} + \dot{\theta} \frac{\partial}{\partial \theta} + \dot{y} \frac{\partial}{\partial y} + \ddot{x} \frac{\partial}{\partial \dot{x}} + \ddot{\theta} \frac{\partial}{\partial \dot{\theta}} + \ddot{y} \frac{\partial}{\partial \dot{y}}, \\ g_1 &= \frac{\partial}{\partial \ddot{x}} + \tan \theta \frac{\partial}{\partial \ddot{y}}, \quad g_2 = \frac{\partial}{\partial \ddot{\theta}}. \end{aligned}$$

Note that for this system $p = n = 3$ and $m = 2$.

Since $R \equiv 0$, there is no time-invariant continuous feedback law which asymptotically stabilizes the system to a given equilibrium solution $(q^e, 0, 0)$. On the other hand, the space spanned by the vectors

$$\begin{aligned} &g_1, g_2, [f, g_1], [f, g_2], [f, [f, g_1]], [f, [f, g_2]], [g_2, [f, [f, g_1]]], \\ &[f, [g_2, [f, [f, g_1]]]], [f, [f, [g_2, [f, [f, g_1]]]]] \end{aligned}$$

has dimension 9 at any $(q, \dot{q}, \ddot{q}) \in \mathbf{M}$ and hence the system is strongly accessible. Moreover, since the bad brackets of order 1, 3, and 5 are zero at any equilibrium solution $(q^e, 0, 0) \in \mathbf{M}_e$, Sussmann's sufficient conditions for small time local controllability (Sussmann, 1987a) are satisfied. Clearly, the system is a real analytic system, and therefore there exist both time-invariant piecewise analytic feedback laws (Sussmann, 1979) and time-periodic continuous feedback laws (Coron, 1990) which asymptotically stabilize $(q^e, 0, 0)$.

We now state the following results which characterize the controllability and stabilizability properties of the constrained manipulator dynamics.

Proposition 7.1: *Let $(q^e, 0, 0) \in \mathbf{M}_e$ denote an equilibrium solution. The following hold for the constrained manipulator dynamics described by equations (7.4)-(7.6).*

1. *The system is strongly accessible since the constraint (7.3) is third-order non-holonomic.*
2. *The system is small time locally controllable at $(q^e, 0, 0)$ since the sufficient conditions for small time local controllability are satisfied.*
3. *There exist both time-invariant piecewise analytic feedback laws and time-periodic continuous feedback laws which asymptotically stabilize $(q^e, 0, 0)$.*
4. *There is no time-invariant continuous feedback law which asymptotically stabilizes the closed loop to $(q^e, 0, 0)$.*

The controllability properties given in Proposition 7.1 guarantee the existence of the solution to the problem of controlling the manipulator with zero jerk at its end.

7.1.3 Feedback Control Laws

A control strategy for the system (7.4)-(7.6) is proposed in four steps as follows:

Step 1) Drive the system to a nonzero equilibrium such that $\tan \theta^e \neq 0$ in finite time using

$$\begin{aligned} u_1 &= 0, \\ u_2 &= -l_1 |\theta - \theta^e|^{\beta_1} \text{sign}(\theta - \theta^e) - l_2 |\dot{\theta}|^{\beta_2} \text{sign} \dot{\theta} - l_3 |\ddot{\theta}|^{\beta_3} \text{sign} \ddot{\theta}, \end{aligned}$$

Step 2) Drive the y variable to zero while keeping the $\theta = \theta^e$ using

$$\begin{aligned} u_1 &= -\frac{1}{\tan \theta^e} (k_1 |y|^{\alpha_1} \text{sign } y + k_2 |\dot{y}|^{\alpha_2} \text{sign } \dot{y} + k_3 |\ddot{y}|^{\alpha_3} \text{sign } \ddot{y}), \\ u_2 &= -l_1 |\theta - \theta^e|^{\beta_1} \text{sign}(\theta - \theta^e) - l_2 |\dot{\theta}|^{\beta_2} \text{sign} \dot{\theta} - l_3 |\ddot{\theta}|^{\beta_3} \text{sign} \ddot{\theta}, \end{aligned}$$

Step 3) Drive the θ variable to zero while keeping the $y \equiv 0$ using

$$\begin{aligned} u_1 &= -k_1 |y|^{\alpha_1} \text{sign } y - k_2 |\dot{y}|^{\alpha_2} \text{sign } \dot{y} - k_3 |\ddot{y}|^{\alpha_3} \text{sign } \ddot{y}), \\ u_2 &= -l_1 |\theta|^{\beta_1} \text{sign } \theta - l_2 |\dot{\theta}|^{\beta_2} \text{sign } \dot{\theta} - l_3 |\ddot{\theta}|^{\beta_3} \text{sign } \ddot{\theta}, \end{aligned}$$

Step 4) Drive the x variable to zero while keeping the $\theta \equiv 0$ using

$$\begin{aligned} u_1 &= -k_1 |x|^{\alpha_1} \text{sign } x - k_2 |\dot{x}|^{\alpha_2} \text{sign } \dot{x} - k_3 |\ddot{x}|^{\alpha_3} \text{sign } \ddot{x}, \\ u_2 &= -l_1 |\theta|^{\beta_1} \text{sign } \theta - l_2 |\dot{\theta}|^{\beta_2} \text{sign } \dot{\theta} - l_3 |\ddot{\theta}|^{\beta_3} \text{sign } \ddot{\theta}. \end{aligned}$$

Here k_i , l_i , α_i , β_i satisfy the sufficient conditions of Bhat and Bernstein (2005) for the finite-time stability of triple integrators. Note that Step 1 prevents from dividing by zero in the next steps. On the other hand, if the initial condition is one such that $\theta \neq 0$, then Step 1 is not needed.

7.1.4 Simulations

We now illustrate the previous ideas through a numerical simulation. The physical parameters used in the simulations are given in Table 7.1.

Table 7.1: Physical parameters for a PPR robot manipulator.

Parameter	Value
M	10 kg
m	2 kg
l	1 m
I	0.16 kg · m ²

Assume an initial condition

$$(x_0, y_0) = (1, -1) \text{ (m)}, \quad \theta_0 = \pi/4 \text{ (rads)},$$

$$\dot{x}_0 = \ddot{x}_0 = \dot{y}_0 = \ddot{y}_0 = \dot{\theta}_0 = \ddot{\theta}_0 = 0.$$

The control architecture is implemented here with

$$(k_1, k_2, k_3) = (l_1, l_2, l_3) = (1.0, 1.5, 1.5),$$

$$(\alpha_1, \alpha_2, \alpha_3) = (\beta_1, \beta_2, \beta_3) = (0.5, 0.6, 0.75).$$

Time responses are shown in Figs. 7.2-7.4. As can be seen in the figures, the robot converges to the equilibrium at zero in 30 s. Resultant forces and torques do not exceed 10 N and 5 N · m, respectively. Note also that the jerk constraint is satisfied at any point including the discontinuities.

7.1 Control of a Manipulator with a Jerk Constraint

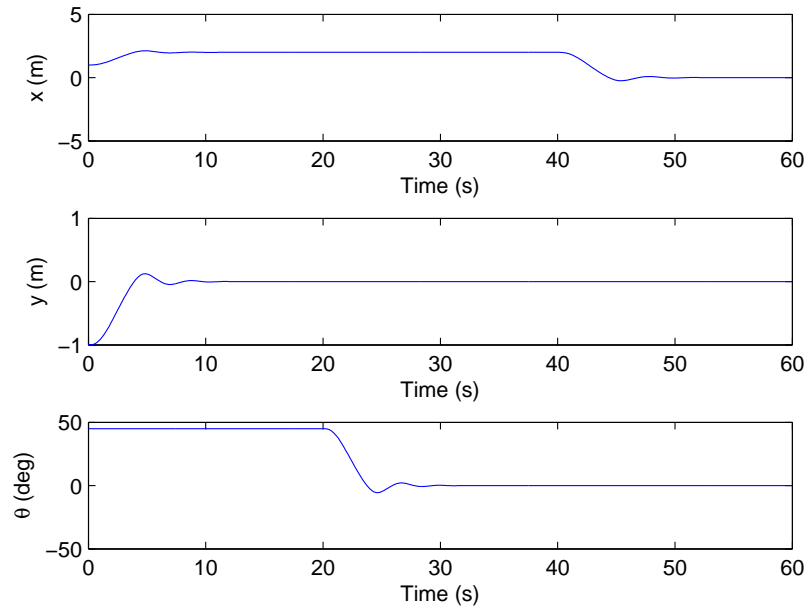


Figure 7.2: Time responses of x , y and θ .

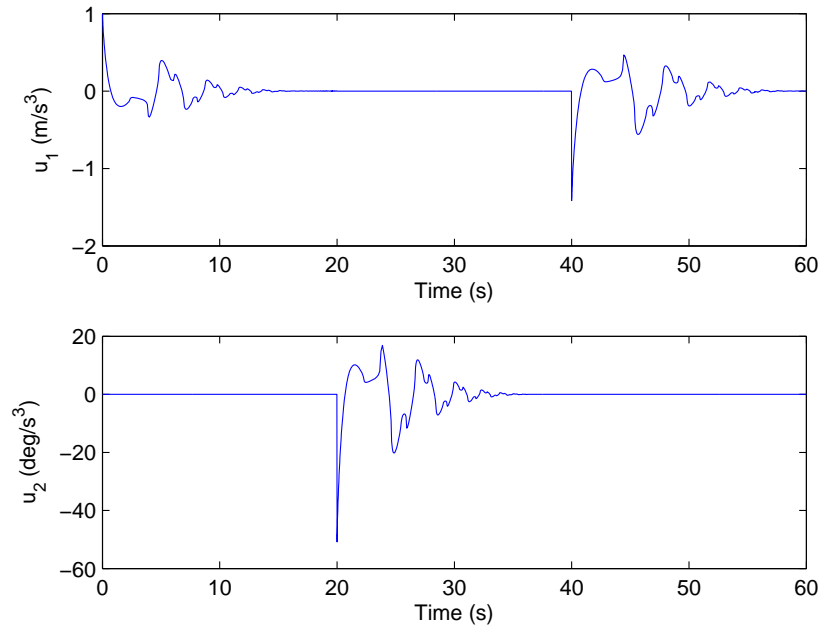
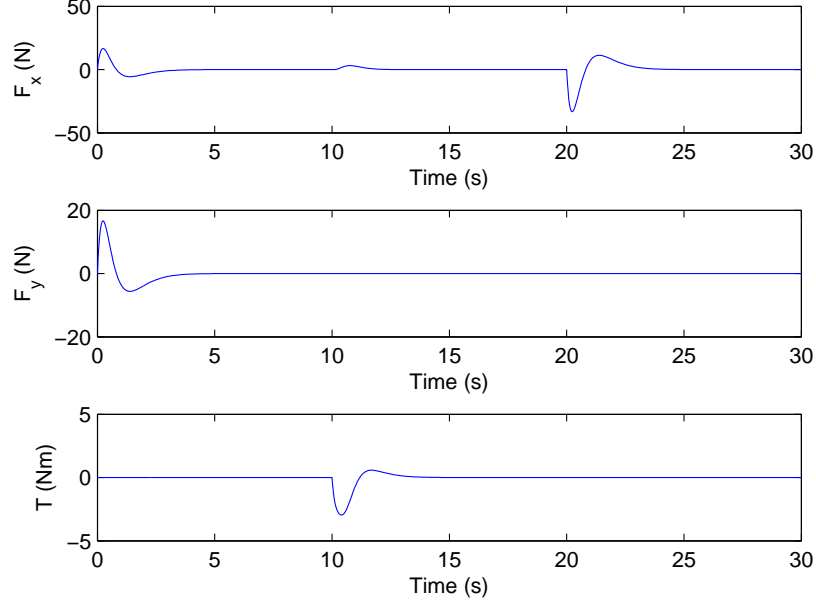


Figure 7.3: Time responses of u_1 and u_2 .


 Figure 7.4: Time responses of F_x , F_y and T .

7.2 A Point Mass Moving on a Constant-Torsion Curve

Consider a point mass M moving on a curve of constant torsion in a three dimensional space. The parametric equation of a curve in \mathbb{R}^3 can be expressed as $\vec{r} = \vec{r}(t)$, where t refers to any parameter, typically time. Assuming that the parametrization is regular and that the curvature does not vanish, the torsion can be computed by the formula

$$\tau = \frac{(\dot{\vec{r}} \times \ddot{\vec{r}}) \cdot \dddot{\vec{r}}}{\|\dot{\vec{r}} \times \ddot{\vec{r}}\|^2}, \quad (7.10)$$

which can be expressed in a Cartesian reference frame with $\vec{r}(t) = x(t)\vec{i} + y(t)\vec{j} + z(t)\vec{k}$ as

$$\tau = \frac{\ddot{x}(\dot{y}\ddot{z} - \ddot{y}\dot{z}) + \ddot{y}(\dot{x}\ddot{z} - \ddot{x}\dot{z}) + \ddot{z}(\dot{x}\ddot{y} - \ddot{x}\dot{y})}{(\dot{y}\ddot{z} - \ddot{y}\dot{z})^2 + (\dot{x}\ddot{z} - \ddot{x}\dot{z})^2 + (\dot{x}\ddot{y} - \ddot{x}\dot{y})^2}. \quad (7.11)$$

Thus, a curve with constant torsion ($\tau = c$) is a constraint of the form

$$\ddot{x}(\dot{y}\ddot{z} - \ddot{y}\dot{z}) + \ddot{y}(\dot{x}\ddot{z} - \ddot{x}\dot{z}) + \ddot{z}(\dot{x}\ddot{y} - \ddot{x}\dot{y}) = c[(\dot{y}\ddot{z} - \ddot{y}\dot{z})^2 + (\dot{x}\ddot{z} - \ddot{x}\dot{z})^2 + (\dot{x}\ddot{y} - \ddot{x}\dot{y})^2]. \quad (7.12)$$

7.2 A Point Mass Moving on a Constant-Torsion Curve

The control problem is to move the point mass between any given initial configuration (x^0, y^0, z^0) and final configuration (x^f, y^f, z^f) such that the constant torsion condition (7.12) is satisfied. We assume that the mass is actuated by a force $F = [F_x, F_y, F_z]'$.

Assuming $\dot{x}\ddot{y} - \ddot{x}\dot{y} \neq 0$, equation (7.12) can be expressed as

$$\ddot{z} = J_1 \ddot{x} + J_2 \ddot{y} + R, \quad (7.13)$$

where

$$J_1 = -\frac{\dot{y}\ddot{z} - \ddot{y}\dot{z}}{\dot{x}\ddot{y} - \ddot{x}\dot{y}}, \quad J_2 = -\frac{\ddot{x}\dot{z} - \dot{x}\ddot{z}}{\dot{x}\ddot{y} - \ddot{x}\dot{y}}, \quad R = c \frac{(\dot{y}\ddot{z} - \ddot{y}\dot{z})^2 + (\ddot{x}\dot{z} - \dot{x}\ddot{z})^2 + (\dot{x}\ddot{y} - \ddot{x}\dot{y})^2}{\dot{x}\ddot{y} - \ddot{x}\dot{y}}.$$

The Lagrangian of the system is given by

$$L = \frac{1}{2}M(\dot{x}^2 + \dot{y}^2 + \dot{z}^2) - Mgz.$$

Denote by $q = [x, y, z]'$ the configuration vector and partition it as $q_1 = [x, y]'$ and $q_2 = z$. Then equation (3.21) results in

$$M\ddot{q}_1 + J'M(\ddot{q}_2 + g) = u_1 + J'u_2, \quad (7.14)$$

where $J = [J_1, J_2]$, $u_1 = [F_x, F_y]'$, and $u_2 = F_z$.

Using a right inverse with

$$C(q, \dot{q}, \ddot{q}) = \begin{bmatrix} 1 \\ J(q, \dot{q}, \ddot{q}) \end{bmatrix},$$

we can solve (7.14) for u as

$$\begin{bmatrix} u_1 \\ u_2 \end{bmatrix} = M \begin{bmatrix} (1 + J'J)^{-1} & \frac{J'}{1+JJ'} \\ \frac{J}{1+JJ'} & \frac{JJ'}{1+JJ'} \end{bmatrix} \begin{bmatrix} \ddot{q}_1 \\ \ddot{q}_2 + g \end{bmatrix}. \quad (7.15)$$

By defining $v = \ddot{q}_1$ together with the state variables

$$(\eta_1, \dots, \eta_9) = (x, y, z, \dot{x}, \dot{y}, \dot{z}, \ddot{x}, \ddot{y}, \ddot{z}),$$

the system can be expressed in a control-affine form as

$$\dot{\eta} = f(\eta) + g(\eta)v, \quad (7.16)$$

where $f(\eta) = [\eta_4, \eta_5, \eta_6, \eta_7, \eta_8, \eta_9, 0, 0, R]'$, $v = [v_1, v_2]'$ and

$$g(\eta) = \begin{bmatrix} 1 & 0 \\ 0 & 1 \\ J_1 & J_2 \end{bmatrix}.$$

7.2 A Point Mass Moving on a Constant-Torsion Curve

Note that the drift and control vector fields are given by

$$f = \dot{x} \frac{\partial}{\partial x} + \dot{y} \frac{\partial}{\partial y} + \dot{z} \frac{\partial}{\partial z} + \ddot{x} \frac{\partial}{\partial \dot{x}} + \ddot{y} \frac{\partial}{\partial \dot{y}} + \ddot{z} \frac{\partial}{\partial \dot{z}} + R, \quad (7.17)$$

$$g_1 = \frac{\partial}{\partial \ddot{x}} + J_1 \frac{\partial}{\partial \ddot{z}}, \quad g_2 = \frac{\partial}{\partial \ddot{y}} + J_2 \frac{\partial}{\partial \ddot{z}}. \quad (7.18)$$

The control design strategy would consist of first constructing the control input v using (7.16) and then deriving the control inputs u_1 and u_2 (or F_x , F_y and F_z) using (7.15).

It can be shown that if the constant torsion is not zero the system (7.16) satisfies a number of controllability and stabilizability properties which guarantee the existence of solutions for the above motion planning problem. If the torsion of a regular curve with non-vanishing curvature is identically zero, then this curve belongs to a fixed plane defined by the initial condition and, therefore, the constraint (7.12) has a first integral. That is, the trajectory cannot leave the fixed plane and thus points that do not lie on the plane cannot be reached. Also note that a curve with constant curvature and constant torsion is a helix.

CONCLUSIONS AND FUTURE RESEARCH

The nonlinear modeling problem for systems with higher-order nonholonomic constraints has been studied using tools from theoretical mechanics. A number of control-theoretic properties such as nonintegrability, accessibility, controllability, and stabilizability have been derived using tools from differential geometry. We have studied a special class of systems with higher-order nonholonomic constraints. Specific assumptions have been introduced that define this class, which includes important models of robotic system examples. One of the main results of the dissertation is the construction of a discontinuous nonlinear feedback controller for which the closed loop equilibrium at the origin is made globally attractive. The control construction approach has been described in detail, and a proof of attractiveness has been presented. The applicability of the theoretical development has been illustrated through several examples including second and third order nonholonomic constraints: space vehicles with multiple slosh modes, planar PPR robot manipulators moving liquid containers, a planar PPR robot manipulator subject to a jerk constraint, and a point mass moving on a constant torsion curve in a three dimensional space.

The many avenues considered for future research include the development of more general control algorithms applicable to such systems as well as the design of control laws that achieve robustness, insensitivity to system and control parameters, and improved disturbance rejection. New examples present promising avenues of research. Future research directions for the examples studied in this dissertation include:

-
1. Space vehicle with multiple slosh modes: The design of nonlinear control observers to estimate the slosh states. Problems involving multiple propellant tanks. The control system design in this dissertation is based on the assumption that the axial acceleration term of the spacecraft is not significantly affected by small gimbal deflections, pitch changes, and fuel motion so that it remains constant. Relaxing this assumption presents another promising avenue of research.
 2. Point-to-point liquid container transfer: The design of nonlinear control observers to estimate the slosh states. Problems involving link and joint flexibilities, multiple liquid containers, and three dimensional transfers offer challenges that need to be overcome.
 3. Planar PPR robot manipulator subject to a jerk constraint: Problems involving link and joint flexibilities, multiple end-effectors, and three dimensional maneuvers represent new research directions.
 4. Point mass moving on a constant torsion curve in a three dimensional space: The study of its theoretic-control properties dealing with the singularities issues they present as well as the development of feedback control laws.

APPENDIX

Consider the system

$$\ddot{s} + f(t) \dot{s} + g(t) s = 0, \quad (8.1)$$

where $g(t) \in C^1$, $|f(t)| < M_1$, $|g(t)| < M_2$, $|\dot{g}(t)| < M_3$.

Theorem A.1: If $g(t) > \varepsilon_1^2$ and $p(t) = \frac{1}{2} \frac{\dot{g}(t)}{g(t)} + f(t) > \varepsilon_2^2$, then the origin is globally uniformly asymptotically stable.

Proof: Given the conditions above, the following bounds can be set

$$\begin{aligned} -M_1 &< f(t) < M_1, \quad \alpha_1^2 < g(t) < M_2, \\ -M_3 &< \dot{g}(t) < M_3, \quad \varepsilon_2^2 < p(t) < \frac{M_3}{2\varepsilon_1^2} + M_1. \end{aligned}$$

Consider the following candidate Lyapunov function

$$V(z, t) = \frac{1}{2} \left(s^2 + 2\beta \frac{s\dot{s}}{\sqrt{g(t)}} + \frac{\dot{s}^2}{g(t)} \right),$$

where $z = [s \ \dot{s}]^T$ is the state vector and β is a positive constant. This function can be rewritten in a matrix form as

$$V(z, t) = \frac{1}{2} \begin{bmatrix} s & \dot{s} \end{bmatrix} \begin{bmatrix} 1 & \frac{\beta}{\sqrt{g}} \\ \frac{\beta}{\sqrt{g}} & \frac{1}{g} \end{bmatrix} \begin{bmatrix} s \\ \dot{s} \end{bmatrix},$$

which is positive definite if $\beta < 1$.

Recalling that a positive definite quadratic function $z^T P z$ satisfies

$$\lambda_{\min}(P) z^T z \leq z^T P z \leq \lambda_{\max}(P) z^T z,$$

where

$$\lambda_{\min}(P) = \frac{1+g}{2g} \left[1 - \sqrt{1 - 4g \frac{1-\beta^2}{(1+g)^2}} \right],$$

$$\lambda_{\max}(P) = \frac{1+g}{2g} \left[1 + \sqrt{1 - 4g \frac{1-\beta^2}{(1+g)^2}} \right],$$

and thus the following hold:

$$\gamma_1 \|z\|^2 \leq V \leq \gamma_2 \|z\|^2,$$

where γ_1 and γ_2 are positive constants.

Taking the time derivative of $V(z, t)$ yields

$$\dot{V} = -\frac{\beta}{\sqrt{g(t)}} \left[g(t) s^2 + p(t) s \dot{s} + \left(\frac{p(t)}{\beta \sqrt{g(t)}} - 1 \right) \dot{s}^2 \right],$$

which can be rewritten as

$$\dot{V} = -\frac{\beta}{\sqrt{g}} \begin{bmatrix} s & \dot{s} \end{bmatrix} \begin{bmatrix} g & \frac{p}{2} \\ \frac{p}{2} & \frac{p^2}{\beta \sqrt{g}} - 1 \end{bmatrix} \begin{bmatrix} s \\ \dot{s} \end{bmatrix} < 0.$$

Clearly, $\dot{V} < 0$ if

$$\beta < \frac{16\varepsilon_1^5 \varepsilon_2^2}{16M_2 \varepsilon_1^4 + (M_3 + 2\varepsilon_1^2 M_1)^2}.$$

Note that \dot{V} satisfies

$$\dot{V} \leq -\frac{\beta}{\sqrt{g}} \lambda_{\min}(Q) \|z\|^2.$$

It can be shown that if

$$\beta < \min \left\{ 1, \frac{16\varepsilon_1^5 \varepsilon_2^2}{16M_2 \varepsilon_1^4 + (M_3 + 2\varepsilon_1^2 M_1)^2} \right\},$$

then, using Theorem 4.10 of Khalil (2002), it can be concluded that the origin is exponentially stable. Hence, the following result can be stated.

Corollary A.1: There exist $\alpha, \beta > 0$ such that

$$|s| < \beta e^{-\alpha(t-t_0)}, \quad |\dot{s}| < \beta e^{-\alpha(t-t_0)}, \quad \forall t \geq t_0.$$

The following result is a modified version of that presented in Reyhanoglu et al. (2000).

Lemma A.1: Consider a system which is described by the linear time-varying differential equation

$$\dot{x} = (A_1(t) + A_2(t))x + H(t), \quad x \in \mathbb{R}^n. \quad (8.2)$$

If the matrix $A_1(t)$ is exponentially stable and there exist positive constants λ_0, λ_1 and λ_2 such that

$$(i) \int_0^\infty \|A_2(t)\| dt \leq \lambda_0, (ii) \|H(t)\| \leq \lambda_1 e^{-\lambda_2 t}, \forall t \geq 0,$$

then all the solutions of (8.2) approach zero exponentially as t goes to ∞ .

Bibliography

- Aboel-Hassan, A., Arafa, M., and Nassef, A. (2009). Design and optimization of input shapers for liquid slosh suppression. *Journal of Sound and Vibration*, 320, 1–15.
- Adler, J. M., Lee, M. S., and Saugen, J. D. (1991). Adaptive control of propellant slosh for launch vehicles. *SPIE Sensors and Sensor Integration*, 1480, 11–22.
- Abraham, R., Marsden, J. E., and Ratiu, T. (1988). Manifolds, tensor analysis and applications. Springer-Verlag, New York.
- Aneke, N. P. I., Nijmeijer, H., and de Jager, A. G. (2003). Tracking control of second-order chained form systems by cascaded backstepping. *International Journal of Robust and Nonlinear Control*, 13, 2, 95–115.
- Aneke, N. P. I. (2003). Control of underactuated mechanical systems. Ph.D. Dissertation, Eindhoven, The Netherlands.
- Astolfi, A. (1996). Discontinuous control of nonholonomic systems. *Systems and Control Letters*, 27, 37–45.
- Baillieul, J. (1993). Kinematically redundant robots with flexible components. *IEEE Control Systems Magazine*, 13, 15–21.
- Bandyopadhyay, B., Gandhi, P. S., and Kurode, S. (2009a). Sliding mode observer based sliding mode controller for slosh-free motion through PID scheme. *IEEE Transactions on Industrial Electronics*, 56, 3432–3442.
- Bandyopadhyay, B., Gandhi, P. S., and Kurode, S. (2009b). Sliding mode control for slosh-free motion-a class of underactuated system. *International Journal of Advanced Mechatronics Systems*, 1, 203–213.
- Bhat, S. P. and Bernstein, D. S. (2005). Geometric homogeneity with applications to finite-time stability. *Mathematics of Control, Signals, and Systems*, 17, 2, 101–127.

- Bianchini, R. M. and Stefani, G. (1993). Controllability along a trajectory: a variational approach. *SIAM Journal on Control and Optimization*, 31, 4, 900–927.
- Biswal, C., Bhattacharyya, S.K., and Sinha, P.K. (2003) Dynamic characteristics of liquid filled rectangular tank with baffles. *IE (I) Journal-CV*, 84, 145–148.
- Blackburn, T. R. and Vaughan, D. R. (1971). Application of linear optimal control and filtering theory to the Saturn V launch vehicle. *IEEE Transactions on Automatic Control*, 16, 6, 799–806.
- Bloch, A. M., Reyhanoglu, M., and McClamroch, N. H. (1992) Control and stabilization of nonholonomic dynamic systems. *IEEE Transactions on Automatic Control*, 37, 11, 1746–1757.
- Bloch, A. M. (2003). Nonholonomic mechanics and control. Springer, New York.
- Brockett, R. W. (1983). Asymptotic stability and feedback stabilization. Differential Geometric Control Theory, R. W. Brockett, R. S. Millman and H. J. Sussmann, eds., Birkhauser, Boston, 181–191.
- Bryson, A. E. (1994). *Control of spacecraft and aircraft*. Princeton University Press.
- Cho, S., McClamroch, N. H., and Reyhanoglu, M. (2000a). Dynamics of multibody vehicles and their formulation as nonlinear control systems. *Proceedings of American Control Conference*, 3908–3912.
- Cho, S., McClamroch, N. H., and Reyhanoglu, M. (2000b). Feedback control of a space vehicle with unactuated fuel slosh dynamics. *Proceedings of AIAA Guidance, Navigation, and Control Conference*, 354–359.
- Coron, J.-M. (1990). A necessary condition for feedback stabilization. *Systems and Control Letters*, 14, 227–232.
- Crampin, M. and Pirani, F. A. E. (1986). Applicable differential geometry. Lecture Notes Series, London Mathematical Society, Cambridge University Press, 59.
- Dodge, F. T. (2000). The new “Dynamic behavior of liquids in moving containers.” Southwest Research Institute, San Antonio, TX.
- Enright, P. J. and Wong, E. C. (1994). Propellant slosh models for the Cassini spacecraft. *Proceedings of AIAA/AAS Conference*, AIAA-94-3730-CP, 186–195.

- Feddema, J. T., Dohrmann, C. R., Parker, G. G., Robinett, R. D., Romero, V. J., and Schmitt, D. J. (1997). Control for slosh-free motion of an open container. *IEEE Control Systems Magazine*, 29–36.
- Freeman, P. (2012). Minimum jerk trajectory planning for trajectory constrained redundant robots. Ph.D. Dissertation, Washington University, Paper 689.
- Freudenberg, J. and Morton, B. (1992). Robust control of a booster vehicle using H^∞ and SSV techniques. *Proceedings of IEEE Conference on Decision and Control*, 2448–2453.
- Gandhi, P. S. and Duggal, A. (2009). Active stabilization of lateral and rotary slosh in cylindrical tanks. *Proceedings of IEEE International Conference on Industrial Technology*, 1–6.
- Godhavn, J. M. and Egeland, O. (1997). A Lyapunov approach to exponential stabilization of nonholonomic systems in power form. *Proceedings of IEEE Transactions on Automatic Control*, 42, 7, 1028–1032.
- Grundelius, M. and Bernhardsson, B. (1999). Control of liquid slosh in an industrial packaging machine. *Proceedings of IEEE International Conference on Control Applications*, 1654–1659.
- Grundelius, M. (2000). Iterative optimal control of liquid slosh in an industrial packaging machine. *Proceedings of the 39th IEEE Conference on Decision and Control*, 3427–3432.
- Hertz, H. R. (1894). Gessamelte werke, band III. Der prinzipien der mechanik in neuem Zusammenhange dargestellt. Barth, Leipzig.
- Hon, Y. (2002). Finite-time stabilization and stabilizability of a class of controllable systems. *Systems & Control Letters*, 46, 4, 231–236.
- Hubert, C. (2003). Behavior of spinning space vehicles with onboard liquids. Hubert Astronautics Technical Report B3007, NASA/KSC Contract NAS10-02016.
- Hubert, C. (2004). Design and flight performance of a system for rapid attitude maneuvers by a spinning vehicle. *Proceedings of the 27th Annual AAS Guidance and Control Conference*, AAS 04-078.

- Jarzebowska, E. (2002). On derivation of motion equations for systems with nonholonomic high-order program constraints. *Multibody System Dynamics*, 7, 3, 307–329.
- Jarzebowska, E. (2005). Dynamics modeling of nonholonomic mechanical systems: theory and applications. *Nonlinear Analysis*, 63, e185–e197.
- Jarzebowska, E. (2006). Control oriented dynamic formulation for robotic systems with program constraints. *Robotica*, 24, 61–73.
- Jiang, Z. P. and Nijmeijer, H. (1997). Tracking control of mobile robots: a case study in backstepping. *Automatica*, 33, 7, 1393–1399.
- Jiang, Z. P. and Nijmeijer, H. (1999). A recursive technique for tracking control of nonholonomic systems in chained form. *IEEE Transactions on Automatic Control*, 44, 2, 265–279.
- Jiang, Z. P., Lefeber A. A. J., and Nijmeijer, H. (2001). Saturated stabilization and tracking of a nonholonomic robot. *Systems and Control Letters*, 42, 327–332.
- H.K. Khalil, H. K. (2002). *Nonlinear systems*. Prentice-Hall, New Jersey, Third Edition.
- Kim, D. H. and Choi, J. W. (2000). Attitude controller design for a launch vehicle with fuel-slosh. *Proceedings of SICE*, 235–240.
- Kolmanovsky, I., Reyhanoglu, M., and McClamroch, N. H. (1996). Switched mode feedback control laws for nonholonomic systems in extended power form. *Systems and Control Letters*, 27, 1, 29–36.
- Krishnan, H., McClamroch, N. H., and Reyhanoglu, M. (1992). Attitude stabilization of a rigid spacecraft using gas jet actuators operating in a failure mode. *Proceedings of IEEE Conference on Decision and Control*, 1612–1617.
- Kryachkov, M., Polyakov, A., and Strygin, V. (2010). Finite-time stabilization of an integrator chain using only signs of the state variables. *Proceedings of the International Workshop on Variable Structure Systems*, VSS 2010, art. no. 5544675, 510–515.
- Laumond, J.-P. (1993). Controllability of a multibody mobile robot. *IEEE Transactions on Robotics and Automation*, 9, 6, 755–763.

- Lefeber, A. A. J. (2000). Tracking control of nonlinear mechanical systems. Ph.D. Dissertation, Enschede, The Netherlands.
- Levant, A. (2001). Universal Single-Input-Single-Output (SISO) sliding-mode controllers with finite-time convergence. *IEEE Transactions on Automatic Control*, 46, 9, 1447–1451.
- Mahindrakar, A. D., Banavar, R. N., and Reyhanoglu, M. (2005). Controllability and point-to-point control of 3-DOF planar horizontal underactuated manipulators. *International Journal of Control*, 78, 1–13.
- Murray, R. M. and Sastry, S. S. (1993). Nonholonomic motion planning: steering using sinusoids. *IEEE Transactions on Automatic Control*, 38, 5, 700–716.
- Nakamura, Y. and Mukherjee, R. (1991). Nonholonomic motion planning of space robots via a bi-directional approach. *IEEE Transactions on Robotics and Automation*, 7, 4, 500–514.
- Nielsen, J. (1935). Vorlesungen uber elementare mechanic. Verlag von J. Springer, Berlin.
- Perez, E. (2006). Vega user’s manual. Issue 3, Arianespace.
- Peterson, L. D., Crawley, E. F., and Hansman, R. J. (1989). Nonlinear fluid slosh coupled to the dynamics of a spacecraft. *AIAA Journal*, 27, 1230–1240.
- Pridgen, B., Bai, K., and Singhose, W. (2010). Slosh suppression by robust input shaping. *Proceedings of IEEE Conference on Decision and Control*, 2316–2321.
- Qi, N., Dong, K., Wang, X., and Li, Y. (2009). Spacecraft propellant sloshing suppression using input shaping techniques. *Proceedings of International Conference on Computer Modeling and Simulation*, 162–166.
- Nijmeijer, H. and van der Schaft, A. J. (1990). Nonlinear dynamical control systems. Springer-Verlag, New York.
- Reyhanoglu, M. and McClamroch, N. H. (1991) Controllability and stabilizability of planar multibody systems with angular momentum preserving control torques. *Proceedings of American Control Conference*, 1102–1107.
- Reyhanoglu, M. (1992) Control and stabilization of nonholonomic dynamic systems. Ph.D. Dissertation, The University of Michigan.

- Reyhanoglu, M. and Al-Regib, E. (1994) Nonholonomic motion planning for wheeled mobile systems using geometric phase. *Proceedings of IEEE International Symposium on Intelligent Control*, 135–140.
- Reyhanoglu, M., van der Schaft, A.J., McClamroch, N.H., and Kolmanovsky, I. (1996). Nonlinear control of a class of underactuated systems. *Proceedings of IEEE Conference on Decision and Control*, 1682–1687.
- Reyhanoglu, M., van der Schaft, A.J., McClamroch, N.H., and Kolmanovsky, I. (1999). Dynamics and control of a class of underactuated mechanical systems. *IEEE Transactions on Automatic Control*, 44, 9, 1663–1671.
- Reyhanoglu, M., Cho, S., and McClamroch, N.H. (2000). Discontinuous feedback control of a special class of underactuated mechanical systems. *International Journal of Robust and Nonlinear Control*, 10, 4, 265–281.
- Reyhanoglu, M. (2003). Maneuvering control problems for a spacecraft with unactuated fuel slosh dynamics. *Proceedings of IEEE Conference on Control Applications*, 695–699.
- Reyhanoglu, M. and Rubio Hervas, J. (2011a) Nonlinear control of a spacecraft with multiple fuel slosh modes. *Proceedings of IEEE Conference Decision and Control and European Control Conference*, 6192–6197.
- Reyhanoglu, M. and Rubio Hervas, J. (2011b) Nonlinear control of space vehicles with multi-mass fuel slosh dynamics. *Proceedings of International Conference Recent Advances in Space Technologies*, 247–252.
- Reyhanoglu, M. and Rubio Hervas, J. (2012a) Robotically controlled sloshing suppression in point-to-point liquid container transfer. *Journal of Vibration and Control*, DOI: 10.1177/1077546312456865, 1–8.
- Reyhanoglu, M. and Rubio Hervas, J. (2012b) Nonlinear dynamics and control of space vehicles with multiple fuel slosh modes. *IFAC Journal Control Engineering Practice*, 20, 912–918.
- Reyhanoglu, M. and Rubio Hervas, J. (2012c) Partial-state feedback control design for liquid container transfer with sloshing suppression. *Proceedings of IEEE Industrial Electronics Conference*, 2377–2381.

- Reyhanoglu, M. and Rubio Hervas, J. (2012d) Point-to-point liquid container transfer via a PPR robot with sloshing suppression. *Proceedings of IEEE American Control Conference*, 5490–5494.
- Reyhanoglu, M. and Rubio Hervas, J. (2013) Nonlinear modeling and control of slosh in liquid container transfer via a PPR robot. *Communications in Nonlinear Science and Numerical Simulation*, 18, 1481–1490.
- Rubio Hervas, J. and Reyhanoglu, M. (2012a) Thrust vector control of an upper-stage rocket with multiple fuel slosh modes. *Mathematical Problems in Engineering*, vol. 2012, article ID 848741, 18 pages.
- Rubio Hervas, J. and Reyhanoglu, M. (2012b) Control of a spacecraft with time-varying propellant slosh parameters. *Proceedings of International Conference on Control, Automation and Systems*, 1621–1626.
- Rubio Hervas, J. and Reyhanoglu, M. (2013a) Controllability and stabilizability of higher-order nonholonomic systems. To appear in *Proceedings of Asian Control Conference*.
- Rubio Hervas, J. and Reyhanoglu, M. (2013b) Nonlinear control of a class of systems with higher-order nonholonomic constraints. Submitted to *Nonlinear Analysis*.
- Rubio Hervas, J. and Reyhanoglu, M. (2013c) Modeling and control of systems with higher-order nonholonomic constraints. Submitted to *International Journal of Control*.
- Rubio Hervas, J., Reyhanoglu, M., and Kamran, N. N. (2013) Thrust-vector control of a three-axis stabilized spacecraft with fuel slosh dynamics. Submitted to *Acta Astronautica*.
- Rubio Hervas, J. and Reyhanoglu, M. (2013d) Nonlinear control of a third-order nonholonomic system. To appear in *Proceedings of International Conference on Control, Automation and Systems*.
- Rubio Hervas, J. and Reyhanoglu, M. (2013e) On the nonlinear modeling of systems with higher-order nonholonomic constraints. To appear in *Proceedings of International Conference on Control, Automation and Systems*.

- Rubio Hervas, J. and Reyhanoglu, M. (2013f) Nonlinear observer based control of slosh in liquid container transfer via a PPR Robot. To appear in *Proceedings of International Conference on Control, Automation and Systems*.
- Rubio Hervas, J. and Reyhanoglu, M. (2013g) Thrust-vector control of a three-axis stabilized spacecraft with fuel slosh dynamics. To appear in *Proceedings of International Conference on Control, Automation and Systems*.
- Samson, C. (1995) Control of chained systems application to path following and time-varying point-stabilization of mobile robots. *IEEE Transactions on Automatic Control*, 40, 1, 64–77.
- Shekhawat, A., Nickkawde, C., and Ananthkrishnan, N. (2006). Modeling and stability analysis of coupled slosh-vehicle dynamics in planar atmospheric flight. *44th AIAA Aerospace Sciences Meeting and Exhibit*, AIAA-2006-427.
- Sidi, M. J. (1997). *Spacecraft dynamics and control*. Cambridge Aerospace Series, Cambridge University Press.
- Sontag, E. D. (1990). Feedback stabilization of nonlinear systems. in M.A. Kaashoek et. al., editors, *Robust Control of Linear Systems and Nonlinear Control, Proceedings of the International Symposium MTNS-89*, Birkhauser, Boston, 61–81.
- Sordalen, O. J. and Egeland, O. (1995). Exponential stabilization of nonholonomic chained systems *IEEE Transactions on Automatic Control*, 40, 1, 35–49.
- Sussmann, H. J. and Jurdjevic, V. (1972). Controllability of nonlinear systems. *J. Differential Equations*, 12, 95–116.
- Sussmann, H. J. (1979). Subanalytic sets and feedback control. *J. Differential Equations*, 31, 31–52.
- Sussmann, H. J. (1987a). A general theorem on local controllability. *SIAM Journal on Control and Optimization*, 25, 1, 158–194.
- Sussmann, H. J. (1987b). Nonlinear controllability and optimal control. Monographs and Textbooks in Pure and Applied Mathematics, New York.
- Terashima, K. and Schmidt, G. (1994) Motion control of a cart-based container considering suppression of liquid oscillations. *Proceedings of IEEE International Symposium on Industrial Electronics*, 275–280.

- Tzenoff, J. (1924) Sur les equations du mouvement des systems mecanique non-holonomes. *Mat. Ann.*, 91.
- Venugopal, R. and Bernstein, D.S. (1996) State space modeling and active control of slosh. *Proceedings of IEEE International Conference on Control Applications*, 1072–1077.
- Walsh, G. C., Tilbury, D., Sastry, S., Murray, R., Laumond, J. P. (1994). Stabilization of trajectories for systems with nonholonomic constraints. *IEEE Transactions on Automatic Control*, 39, 1, 216–222.
- Walsh, G. C. and Bushnell, L. G. (1995). Stabilization of multiple input chained form control systems. *Systems and Control Letters*, 25, 227–234.
- Wie, B. (1998). *Space vehicle dynamics and control*. AIAA Education Series.
- Yano, K., Toda, T., and Terashima, K. (2001a). Sloshing suppression control of automatic pouring robot by hybrid shape approach. *Proceedings of IEEE Conference on Decision and Control*, 1328–1333.
- Yano, K., Higashikawa, S., and Terashima, K. (2001b). Liquid container transfer control on 3D transfer path by hybrid shaped approach. *Proceedings of IEEE International Conference on Control Applications*, 1168–1173.
- Yano, K. and Terashima, K. (2001) Robust liquid container transfer control for complete sloshing suppression. *IEEE Transactions on Control Systems Technology*, 9, 3, 483–493.
- Yano, K. and Terashima, K. (2005) Sloshing suppression control of liquid transfer systems considering a 3-D transfer path. *IEEE-ASME Transactions on Mechatronics*, 10, 2, 8–16.
- Zabczyk, J. (1989) Some comments on stabilizability. *Applied Mathematics and Optimization*, 19, 1–9.
- Ze-chun, S. and Feng-xiang M. (1987). On the new forms of the differential equations of the systems with higher-order nonholonomic constraints. *Applied Mathematics and Mechanics*, 8, 2, 189–196.